VOLUME 32 | SUPPLEMENT 2 | MARCH 2019

MODERN PATHOLOGY

USCAP 2019

ABSTRACTS

BONE AND SOFT TISSUE PATHOLOGY (37-99)

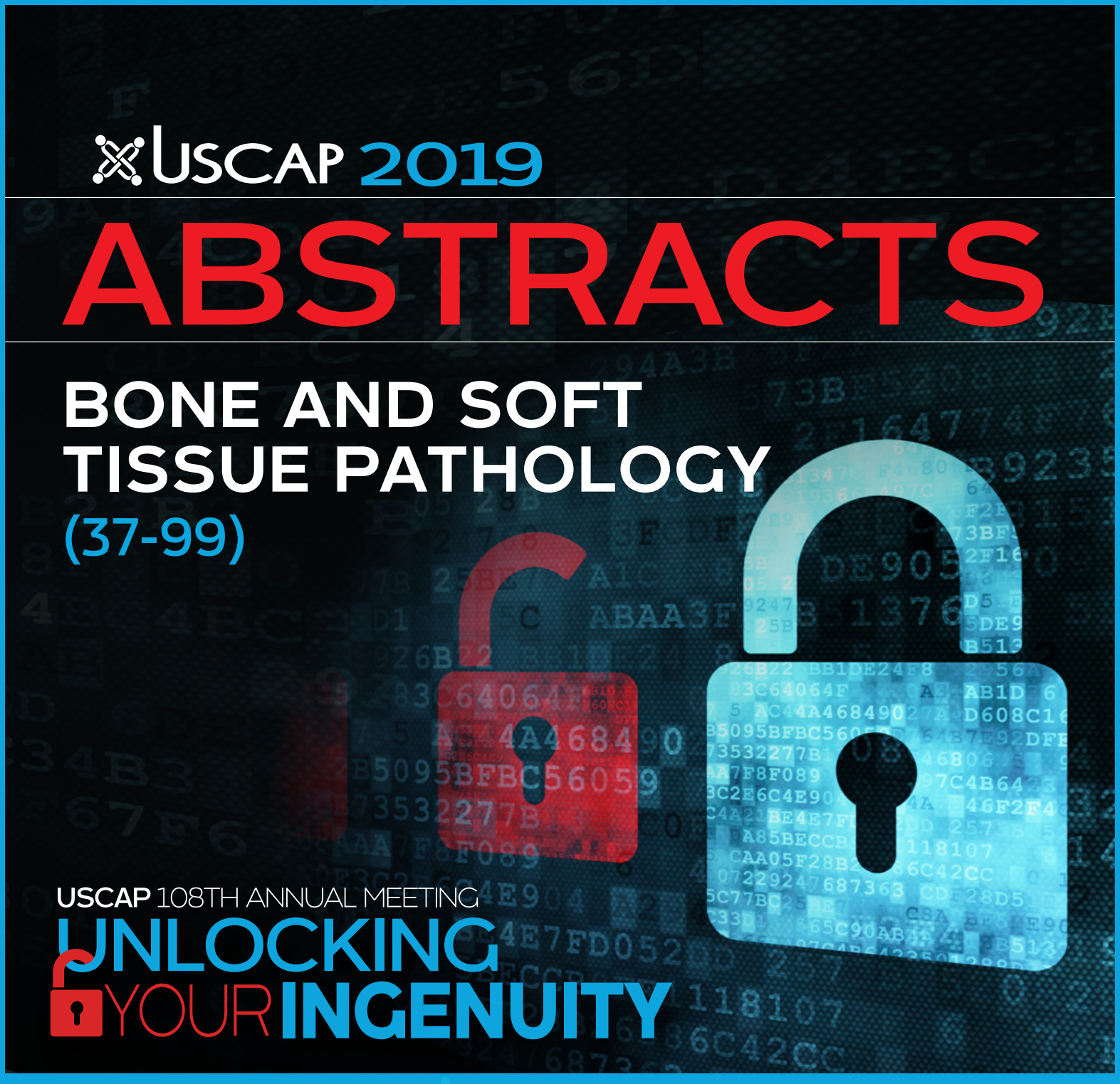

USCAP 108TH ANNUAL MEETING

UNLOCKING YOUR INGENUITY

MARCH 16-21, 2019

National Harbor, Maryland
Gaylord National Resort & Convention Center

Published by
SPRINGER NATURE
www.ModernPathology.org

USCAP Creating a Better Pathologist
AN OFFICIAL JOURNAL OF THE UNITED STATES AND CANADIAN ACADEMY OF PATHOLOGY

EDUCATION COMMITTEE

Jason L. Hornick, Chair
Rhonda K. Yantiss, Chair, Abstract Review Board and Assignment Committee
Laura W. Lamps, Chair, CME Subcommittee
Steven D. Billings, Interactive Microscopy Subcommittee
Shree G. Sharma, Informatics Subcommittee
Raja R. Seethala, Short Course Coordinator
Ilan Weinreb, Subcommittee for Unique Live Course Offerings
David B. Kaminsky (Ex-Officio)
Aleodor (Doru) Andea
Zubair Baloch
Olca Basturk
Gregory R. Bean, Pathologist-in-Training
Daniel J. Brat
Ashley M. Cimino-Mathews
James R. Cook
Sarah M. Dry
William C. Faquin
Carol F. Farver
Yuri Fedoriw
Meera R. Hameed
Michelle S. Hirsch
Lakshmi Priya Kunju
Anna Marie Mulligan
Rish Pai
Vinita Parkash
Anil Parwani
Deepa Patil
Kwun Wah Wen, Pathologist-in-Training

ABSTRACT REVIEW BOARD

Benjamin Adam
Michelle Afkhami
Narasimhan (Narsi) Agaram
Rouba Ali-Fehmi
Ghassan Allo
Isabel Alvarado-Cabrero
Christina Arnold
Rohit Bhargava
Justin Bishop
Jennifer Boland
Elena Brachtel
Marilyn Bui
Shelley Caltharp
Joanna Chan
Jennifer Chapman
Hui Chen
Yingbei Chen
Benjamin Chen
Rebecca Chernock
Beth Clark
James Conner
Alejandro Contreras
Claudiu Cotta
Timothy D'Alfonso
Farbod Darvishian
Jessica Davis
Heather Dawson
Elizabeth Demicco
Suzanne Dintzis
Michelle Downes
Daniel Dye
Andrew Evans
Michael Feely
Dennis Firchau
Larissa Furtado
Anthony Gill
Ryan Gill
Paula Ginter
Tamara Giorgadze
Raul Gonzalez
Purva Gopal
Anuradha Gopalan
Jennifer Gordetsky
Rondell Graham
Alejandro Gru
Nilesh Gupta
Mamta Gupta
Krisztina Hanley
Douglas Hartman
Yael Heher
Walter Henricks
John Higgins
Mai Hoang
Mojgan Hosseini
Aaron Huber
Peter Illei
Doina Ivan
Wei Jiang
Vickie Jo
Kirk Jones
Neerja Kambham
Chiah Sui (Sunny) Kao
Dipti Karamchandani
Darcy Kerr
Ashraf Khan
Rebecca King
Michael Kluk
Kristine Konopka
Gregor Krings
Asangi Kumarapeli
Alvaro Laga
Cheng-Han Lee
Zaibo Li
Haiyan Liu
Xiuli Liu
Yan-Chun Liu
Tamara Lotan
Anthony Magliocco
Kruti Maniar
Jonathan Marotti
Emily Mason
Jerri McLemore
Bruce McManus
David Meredith
Anne Mills
Neda Moatamed
Sara Monaco
Atis Muehlenbachs
Bita Naini
Dianna Ng
Tony Ng
Ericka Olgaard
Jacqueline Parai
Yan Peng
David Pisapia
Alexandros Polydorides
Sonam Prakash
Manju Prasad
Peter Pytel
Joseph Rabban
Stanley Radio
Emad Rakha
Preetha Ramalingam
Priya Rao
Robyn Reed
Michelle Reid
Natasha Rekhtman
Michael Rivera
Michael Roh
Andres Roma
Avi Rosenberg
Esther (Diana) Rossi
Peter Sadow
Safia Salaria
Steven Salvatore
Souzan Sanati
Sandro Santagata
Anjali Saqi
Frank Schneider
Jeanne Shen
Jiaqi Shi
Wun-Ju Shieh
Gabriel Sica
Deepika Sirohi
Kalliopi Siziopikou
Lauren Smith
Sara Szabo
Julie Teruya-Feldstein
Gaetano Thiene
Khin Thway
Rashmi Tondon
Jose Torrealba
Evi Vakiani
Christopher VandenBussche
Sonal Varma
Endi Wang
Christopher Weber
Olga Weinberg
Sara Wobker
Mina Xu
Shaofeng Yan
Anjana Yeldandi
Akihiko Yoshida
Gloria Young
Minghao Zhong
Yaolin Zhou
Hongfa Zhu
Debra Zynger

37 Primary gastric leiomyosarcoma: Clinicopathologic study of 11 cases

Abbas Agaimy[1], Michael Michal[2], Michal Michal[3], Brian Rubin[4]
[1]Erlangen, Germany, [2]Charles University and Bioptic Laboratory Ltd. Pilsen, Plzen, Czech Republic, [3]Biopticka Laborator SRO, Plzen, Czech Republic, [4]Cleveland Clinic, Cleveland, OH

Disclosures: Abbas Agaimy: None; Michael Michal: None; Michal Michal: None; Brian Rubin: None

Background: The vast majority of gastric mesenchymal tumors are gastrointestinal stromal tumors (GISTs). Primary gastric smooth muscle tumors are rare and most are benign paucicellular leiomyomas arising from the muscularis mucosae. Leiomyosarcoma are exceptionally rare in the stomach; none was included among 1765 GISTs reported from the AFIP files. Accordingly, only single case reports exist in the literature.

Design: The pathology files of our institutions including consultation files were searched for primary gastric leiomyosarcoma. Immunohistochemistry was performed to verify smooth muscle differentiation and exclude GISTs and other relevant entities. Primary origin was verified via review of clinical data.

Results: Eleven cases were retrieved (8 men and 3 women aged 52-82 years; median, 66). Of six cases with specified site, 5 originated in the proximal part (body/fundus/cardia) and one in the antrum. Tumor size ranged from 2.1-11.5 cm (mean, 6.6). One patient had a history of retinoblastoma. All tumors presented as intramural masses with frequent ulceration. Treatment was partial gastrectomy (9) and enucleation (2). Histologically, gastric leiomyosarcomas were similar to leiomyosarcomas of soft tissue and genital tract with uniform expression of smooth muscle markers while lacking reactivity with GIST markers (CD117, DOG1). Seven tumors were frankly malignant high-grade (5 grade 3 and 2 grade 2 according to the French grading system). Four tumors were grade 1 characterized by higher cellularity compared to conventional leiomyomas, low but unequivocal mitotic activity (2-4/10 hpf) and mild to moderate nuclear atypia. Limited follow-up was available for 3 patients and showed synchronous (2) and metachronous (1) liver metastasis.

Conclusions: This is the first case series on gastric leiomyosarcoma. Due to its extreme rarity, this aggressive neoplasm should be distinguished from the more frequently diagnosed gastric GIST. Diagnosis of genuine leiomyosarcoma requires clinical correlation to exclude metastasis from leiomyosarcoma of other sites and extension from intra-abdominal dedifferentiated liposarcoma which can have heterologous leiomyosarcomatous differentiation. We delineated a novel, low-grade variant affecting mainly the elderly. The biological behavior and the best terminology for this variant (low-grade variant of gastric leiomyosarcoma versus smooth muscle neoplasm of uncertain malignant potential) remain to be assessed in larger series.

38 GLI1-Amplified Soft Tissue Neoplasm: A Novel Entity Showing Morphologic Overlap with Tumors with GLI1 Gene Fusions

Narasimhan Agaram[1], Lei Zhang[1], Yun-Shao Sung[1], David Swanson[2], Brendan Dickson[3], Cristina Antonescu[1]
[1]Memorial Sloan Kettering Cancer Center, New York, NY, [2]Mount Sinai Hospital, Toronto, ON, [3]Mount Sinai Health System, Toronto, ON

Disclosures: Narasimhan Agaram: None; Lei Zhang: None; Yun-Shao Sung: None; David Swanson: None; Brendan Dickson: None; Cristina Antonescu: None

Background: *GLI1* gene fusions were first described in 'pericytomas with t(7;12) translocation' and subsequently found in other unrelated gastric tumors such as plexiform fibromyxoma and gastroblastoma. More recently, *GLI1* fusions involving *ACTB, MALAT1* and *PTCH1* genes were reported in a subset of soft tissue tumors with a characteristic monomorphic nested epithelioid morphology. We encountered a group of soft tissue tumors with a similar morphology but lacking *GLI1* gene fusions, and sought to investigate their genetic abnormalities for further molecular characterization.

Design: Archival and personal consultation material was searched for unclassified tumors with morphology reminiscent of tumors with *GLI1* fusions. Combined approach including RNA-sequencing, targeted exome sequencing and FISH methodologies was used to identify potential gene fusions and copy number abnormalities.

Results: We identified 7 patients (5 F, 2 M) with age range 4-54 years (median 26). Tumors were located in the thigh (2), shoulder, lung (2), back and elbow. Histologically, tumors revealed ovoid to epithelioid cells arranged in a nested-trabecular pattern, thin septa and delicate vascular network. Two cases showed areas of increased nuclear pleomorphism and focal fascicular spindle cell growth. Four tumors showed a low mitotic activity (2-5/10 HPFs) while remaining 3 had a high mitotic count (>15/10 HPFs). Necrosis was seen in the 3 tumors with increased mitotic activity and lymphovascular invasion in 1 case. No consistent immunoprofile was detected, with positivity for CD56 (5 cases), patchy S100 (4 cases), SMA (2 cases) and pan-CK (1 case). No *GLI1*-gene rearrangements were detected by FISH or by RNA-sequencing analysis (in 1 case). Instead, FISH showed *GLI1* (12q13.3) gene amplification in all 7 cases, with co-amplification of *CDK4*(12q14.1) in 6 (86%) and *MDM2* (12q15) in 5 (71%) cases. Targeted exome sequencing was performed in 3 cases, confirming the *GLI1*, *CDK4* and *MDM2* co-amplification.

Conclusions: We report what appears to be a novel entity characterized by *GLI1* gene amplifications, often associated with co-amplifications of C*DK4* and *MDM2* genes. Its distinctive morphology is highly reminiscent to the recently described soft tissue tumors with *GLI1* gene fusions and similarly display a non-specific immunoprofile. *GLI1* gene amplification might be an alternative mechanism of GLI1 oncogenic activation akin to *GLI1* related gene fusions. Its relationship to other *GLI1* rearranged tumor entities needs further investigation.

39 Cathepsin K: A Potential Association Between PEComas and Granulomatous Disease

Nada Al Qaysi[1], Michael Feely[1], Consuelo Soldevila-Pico[1], Jesse Kresak[1]
[1]University of Florida, Gainesville, FL

Disclosures: Nada Al Qaysi: None; Michael Feely: None; Consuelo Soldevila-Pico: None; Jesse Kresak: None

Background: Perivascular epithelioid cell tumors (PEComa) are rare mesenchymal neoplasms that express myomelanocytic markers, such as SMA, desmin, HMB-45, Melan-A and MITF, and often harbor genetic alterations in *MITF*, *TFE3*, or *TSC*genes. Cathepsin K, a cysteine protease, is strongly expressed by immunohistochemistry in PEComas, as Cathepsin K is upregulated by MITF and TFE3. Cathepsin K has also been associated with granuloma formation and animal models have found that inhibition of this protein blocks the development of sarcoidosis. The purpose of this study was to elucidate a potential correlation between PEComa and granuloma formation.

Design: Retrospective search of our pathology archives was performed from 2008-2018 to identify patients with resected PEComas as well as lymph node dissection. Clinicopathologic features were reviewed.

Results: A total of 10 cases were identified from 10 individual patients (Table 1). The patients consisted of 9 women and 1 man, ranging in age from 33-69 years. 20% of cases (2/10), and 50% of malignant cases (2/4), demonstrated non-caseating granuloma formation within the accompanying lymph nodes. The first case was a 52 year old female with a malignant PEComa of the cecum. This tumor was found to have strong expression of cathepsin K by immunohistochemistry. Extensive areas of non-caseating granulomas were identified within the terminal ileum and surrounding lymph nodes. The patient also had mediastinal lymphadenopathy which was found to be secondary to non-caseating granulomas and she was eventually clinically considered to have sarcoidosis. The second case was of a 57 year old female with a deep thigh mass accompanied by mediastinal lymphadenopathy, who was also eventually clinically considered to have sarcoidosis. The remaining 8 case demonstrated no evidence of granulomatous inflammation in the accompanying lymph nodes.

Case	Age/ Gender	Site of PEComa	PEComa malignancy status	Granulomatous inflammation
1	52/F	Cecum	Malignant	Yes – mediastinal nodes and terminal ileum
2	57/F	Uterus	Malignant	No
3	57/F	Thigh	Malignant	Yes – mediastinal nodes
4	46/F	Lung (LAM)	Benign	No
5	57/F	Kidney (AML)	Benign	No
6	45/F	Uterus	Uncertain malignant potential	No
7	33/F	Thigh (malignant)	Malignant	No
8	69/F	Kidney (AML)	Benign	No
9	57/M	Kidney (AML)	Benign	No
10	43/F	Kidney (AML)	Benign	No

Conclusions: Our results suggest there may be an association between malignant PEComa and granulomatous inflammation. As animal studies have linked cathepsin K and granuloma formation, we propose this protease as the possible link correlating these rare tumors to granuloma formation. The extreme rarity of idiopathic sarcoid in the small bowel lends support to an alternative etiology in one of our cases. Whether this is indeed 'sarcoidosis' or better regarded as 'tumor-associated granulomatous inflammation', and whether the differentiation is clinically relevant, requires additional cases with clinical or radiographic follow-up for review.

40 Copy Number Variations in Primary and Metastatic Synovial Sarcoma

Mercia Bezerra Gondim[1], Madhurima Kaushal[2], Tiffany Chen[1], Brooj Abro[3], Louis Dehner[2], John Pfeifer[3], Mai He[2]
[1]Barnes Jewish Hospital/Washington University, St. Louis, MO, [2]Washington University School of Medicine, St. Louis, MO, [3]Washington University, St. Louis, MO

Disclosures: Mercia Bezerra Gondim: None; Madhurima Kaushal: None; Tiffany Chen: None; Brooj Abro: None; Louis Dehner: None; John Pfeifer: None; Mai He: None

Background: Synovial sarcoma is a soft-tissue malignancy that often affects adolescents and young adults. Genetically it is characterized by driver translocation most involving one of the fusions SS18-SSX1 or SS18-SSX2. Prognosis of patients with recurrent or metastatic disease is generally poor. Biomarkers for metastasis are lacking, and most focusing on individual gene mutations. There are few studies on

other genomic alterations in synovial sarcoma. Our hypothesis is that since there is driver translocation, there are most likely few copy number variations (CNV) in synovial sarcoma. Current study investigated chromosomal alterations in primary synovial sarcoma and within metastasis.

Design: With IRB approval, cases of synovial sarcoma with fusion confirmed by cytogenetics were searched in the departmental archives for cases with material from both initial presentation and metastasis. Genomic DNA was extracted with FFPE blocks with tumor > 80% of tissue. Whole-exome sequencing (WES) was performed on the initial tumor and metastasis samples, with normal tissue control, with 25-30M read for normal and 45-50M read for tumor cells. CNV was determined by comparing the aligned number of reads per gene generated by WES in tumor with those in normal tissue control by cn.mops.

Results: We used 7 pairs of primary and metastatic synovial sarcoma cases for this study, including 5 female and 2 male, with age 13-89 years. Recurrent copy number variations were observed with the most common change as 8q24.3 gain in 6/7 (85.7%) primary tumors, which harbors genes associated with carcinogenesis, such *BOP1* known to be associated with colon cancer. Gain in 2q37.3 was seen in 4/7 (57.1%) primary tumor and the region harbors PD-1 gene (Programmed cell death-1) which is broadly expressed and gene product is involved in suppression of immune response towards tumor cells. Other commonly seen recurrent CNV include gains in 7q22.1, 12p13.31, 14q11.2 and some other regions. Differences in CNV were observed in 5 of 7 (71.4%) pairs between primary and metastatic, including 2q37.3.

Conclusions: We observed recurrent CNV in synovial sarcoma, where harbored genes involved in carcinogenesis, immune response and tumor progression. We also observed differences in CNV between primary and metastatic tumor. Alteration in 2q27.3 raises further question of how immune response is involved in carcinogenesis and tumor progression in synovial sarcoma, which can serve as potential predictor for checkpoint immunotherapy.

41 Succinate Dehydrogenase-Deficient Gastric Gist With An Additional KIT Mutation

Iva Brcic[1], Karl Kashofer[1], Bernadette Liegl-Atzwanger[1]
[1]Medical University of Graz, Graz, Austria

Disclosures: Iva Brcic: None; Karl Kashofer: None; Bernadette Liegl-Atzwanger: None

Background: In up to 85% of cases, gastrointestinal stromal tumors (GIST) harbour mutually exclusive mutations in *KIT* and *PDGFRA* gene. Among others, known as wild type GIST, succinate dehydrogenase (SDH)-deficient tumors develop due to genetic or epigenetic alterations in any of four SDH genes: *SDHA*, *SDHB*, *SDHC* or *SDHD* (or collectively *SDHX*). They respond poorly to standard targeted therapy.

Design: We describe a case of SDHB-deficient GIST with unique molecular findings detected by next-generation sequencing (NGS) using the Ion Torrent Ampliseq technology (MUG GIST panel) searching for mutations in the *KIT, PDGFRA, PDGFRB, K-RAS, N-RAS, H-RAS, BRAF, SDHA, SDHB, SDHC, SDHD, NF1, CDKN2A, TP53* and *RB1* gene. Sanger Sequencing confirmed results obtained by NGS and germ line mutation were excluded.

Results: A 50 years old patient presented with a 20 cm large gastric mass. On histology, the tumor showed a typical multinodular growth pattern with mixed epitheloid and spindle cell morphology. In addition, microcystic stromal changes and foci of pronounced nuclear atypia with hyperchromasia as well as high mitotic activity (15 mitoses per $5mm^2$) were present. Immunohistochemistry showed a multifocal expression of CD117 (KIT) and DOG-1. SDHB and SDHA stains showed loss of expression in some of the nodules, while others presented with an unusual weak patchy positivity. Molecular analysis revealed a point mutation in exon 5 of the *SDHA* (p.Q170L) gene (MAF 43%) and in addition a mutation in exon 11 of the *KIT* (p.D579del) gene (MAF 15%).

Conclusions: We present a unique case of SDH-deficient GIST with an unusual heterogeneous SDHA and SDHB immunohistochemical staining pattern and mutations detected in the *SDHA* and *KIT* gene, confirmed by 2 independent methods. We hypothesize that, based on the allele frequency of *SDHA*and *KIT* mutations, our tumor is best regarded as SDH-deficient GISTin which SDH loss is most likely the driver. Further one, the identified convincing *KIT* mutation in a small allele fraction raises the distinct possibility that the *KIT* mutation is a second event reflecting some type of clonal evolution. To the best of our knowledge this is the first case of a treatment naive GIST habouring a somatic *SDHA* as well as a *KIT* mutation. This case, together with another recently reported case with *SDHB and PDGFRA* D842Vmutations,challenges the dogma that oncogenic mutations in GIST are mutually exclusive. Expanded molecular testing in the era of NGS may be of diagnostic and therapeutic value.

42 Clinicopathologic and Genomic Features of EWSR1-PATZ1 Fusion "Sarcoma"

Julia Bridge[1], Marilyn Bui[2], Mihaela Druta[2], Evita Henderson Jackson[2], Konstantinos Linos[3], Michael Baker[3], Christine Walko[2], Janos Sumegi[4], Sherri Millis[5], Andrew Brohl[2]
[1]Nebraska Medicine, Omaha, NE, [2]Moffitt Cancer Center, Tampa, FL, [3]Dartmouth-Hitchcock Medical Center, Lebanon, NH, [4]TGen, Phoenix, AZ, [5]Phoenix, AZ

Disclosures: Julia Bridge: None; Marilyn Bui: None; Mihaela Druta: None; Evita Henderson Jackson: None; Konstantinos Linos: None; Michael Baker: None; Christine Walko: None; Janos Sumegi: None; Sherri Millis: *Employee*, Foundation Medicine; Andrew Brohl: None

Background: The identification of specific fusion transcripts has played a vital role in the classification of sarcomas. *EWSR1-PATZ1* is a rare fusion partnering that currently resides in the WHO undifferentiated sarcoma category. Descriptions of clinicopathologic features to include outcomes or treatment response data are limited or lacking.

Design: *EWSR1-PATZ1* fusions were detected in three "sarcomas" (Cases 1-3) from two institutions of the authors by a commercial NGS platform with subsequent RT-PCR and Sanger sequencing confirmation. Eight additional *EWSR1-PATZ1*cases (5 "sarcomas", 3 CNS tumors) were identified across all tumors sequenced on the same commercial platform. Retrospective chart review was performed for clinicopathologic details of Cases 1-3.

Results: At least 4/8 "sarcomas" arose in the chest wall. In all cases, exon 8 or 9 of *EWSR1* fused with *PATZ1* exon 5. Loss of *CDKN2A/B* was seen in 6 of the 11 cases including 2 of 3 "in-house" patients (Cases 1 and 2) who presented with metastatic disease but had experienced a >1 year latency period from initial symptomatic presentation to time of diagnosis. Moreover, *MDM2* amplification was also seen in Case 1. Despite initial modest response to conventional systemic chemotherapies, both patients succumbed to their disease within months. In contrast, Case 3 lacking *CDKN2A/B* loss remains disease free 1 yr following excision of her paravertebral neoplasm. Cases 2 and 3 exhibited somewhat similar histology (hypercellular/hypocellular areas composed of ovoid to round cells without notable mitotic activity) and both were S100 and GFAP positive (cytokeratin negative) raising the possibility of a myoepithelial tumor. However similar to previous description, the divergent morphology and immunoprofiles in the overall current series posed classification challenges.

Conclusions: The clinicopathologic and molecular profiling of *EWSR1-PATZ1* "sarcoma" suggest that this neoplasm may represent a distinct entity with a tendency to arise in the chest wall. In this series, comprehensive molecular testing revealed a number of secondary aberrations expected to contribute to oncogenesis. Most notably, *CDKN2A/B* loss was frequent, occurring in 5/8 (62.5%) "sarcomas" and 1/3 (33.3%) CNS tumors. *CDKN2A/B* loss is considered a common mechanism for cell cycle dysregulation and may have prognostic significance in *EWSR1-PATZ1* neoplasia.

43 Hematolymphoid Neoplasms Rarely Mimic Undifferentiated Pleomorphic Sarcoma of Soft Tissue

John Cannatella[1], Karthik Ganapathi[1], Andrew Horvai[1]
[1]University of California, San Francisco, San Francisco, CA

Disclosures: John Cannatella: None; Andrew Horvai: None

Background: Undifferentiated pleomorphic sarcoma (UPS) of soft tissue is a diagnosis reserved for pleomorphic malignancies that lack a specific histotype. Careful clinicopathologic review and novel ancillary studies over the past few decades have identified mesenchymal (myogenic, lipogenic etc.) and non-mesenchymal (carcinoma, melanoma) neoplasms in cases previously diagnosed as UPS; however, few studies have considered pleomorphic hematolymphoid neoplasms in UPS cases. We investigated what proportion, if any, of a large group of UPS cases may represent pleomorphic hematolymphoid malignancies, including anaplastic large cell lymphoma (ALCL), diffuse large B-cell lymphoma (DLBCL), histiocytic sarcoma (HS), myeloid sarcoma (MS), and follicular dendritic cell sarcoma (FDCS).

Design: Sixty-three soft tissue sarcomas, previously classified as UPS were incorporated into a tissue microarray (TMA). Tumors arising in discrete lymph nodes were excluded. The tumors were evaluated for expression of leukocyte, lymphoid, histiocytic, follicular dendritic and myeloid markers by immunohistochemistry (IHC) stains for CD30, CD20, CD4, CD34, MPO, CD68, CD21, CD23, PU.1 and LCA-C (CD43, CD20, CD79A, and CD45 cocktail). The staining intensity and quantity were scored only in the pleomorphic, malignant cells. Additional IHC stains were performed on whole sections of cases suspicious for hematolymphoid differentiation. Results were scored independently by experts in soft tissue pathology and hematopathology.

Results: Five of 63 cases (8%) were suggestive of HS on the TMA, but no immunophenotypic evidence of ALCL, DLBCL, MS or FDCS was observed. Whole sections of the 5 putative HS cases were focally positive for LCA-C (n=2), CD45 (n=2), CD163 (n=4), CD68 (n=3), lysozyme (n=3), and PU.1 (n=4). One case, presenting as a mediastinal mass (19 cm) involving the pleura in a 45-year-old man, was diagnosed as HS. In this case, the large malignant cells were diffusely positive for CD45, CD68 and PU.1. Nuclear staining for PU.1, a macrophage transcription factor, was more definitive than staining for cytoplasmic/membrane antigens when significant background inflammation was present.

Conclusions: Our results show that UPS cases are unlikely to represent mis-classified DLBCL, ALCL, MS, or FDCS. Thus, excluding these entities by IHC is not required to diagnose UPS. HS may rarely mimic UPS and immunostaining for PU.1 may be a useful in addition to CD45 and CD68 in difficult cases.

44 Comparison of Fluorescence In Situ Hybridization (FISH), immunohistochemistry (IHC) and Dual-ISH (DISH) in the Determination of MDM2/CDK4 amplification in liposarcoma and other adipocytic tumors

Wei Chen[1], Amad Awadallah[1], Margaret Lawless[1], Robin Elliott[2]
[1]University Hospitals Cleveland Medical Center, Cleveland, OH, [2]University Hospitals Cleveland Medical Center, Case Western Reserve University, Cleveland, OH

Disclosures: Wei Chen: None; Amad Awadallah: None; Robin Elliott: None

Background: The 12q13-15 gene locus, which spans MDM2 (mouse double minute 2) and CDK4 (cyclin-dependent kinase 4) is consistantly amplified in well-differentiated liposarcoma/atypical lipomatous tumor (WDLPS/ALT) and dedifferentiated liposarcoma (DDLPS). FISH for the MDM2 gene is recognized as the gold standard for confirmation of the diagnosis of WDLPS/ALT and DDLPS, however, it is a time-consuming and expensive assay. Detection of MDM2/CDK4 protein expression by immunohistochemistry (IHC) as a surrogate for FISH has been widely used. However, IHC is less sensitive (65%) and specific (89%) compared to FISH. An alternative to FISH is dual in situ hybridization (DISH), which can be performed using differentially labeled chromogenic probes targeting the MDM2 gene and the chromosome 12 centromere.

Our study compares the performance of IHC and DISH with FISH in cases of WDLPS/ALT, DDLPS, and other adipocytic tumors.

Design: Thiry-eight cases with known FISH results (19 positive and 19 negative cases) were selected, including WDLPS/ALT, DDLPS, other soft tissue tumors, and lipoma. DISH were performed with MDM2 and CEP12 probes (Ventana). IHC was performed with antibodies for MDM2 (clone 1F2, 1:15, EMD Millipore) and CDK4 (clone D9G3E, 1:400, Cell Signaling). The result were correlated with FISH data and diagnosis. Cohen's Kappa (k) analysis was used to exam the agreement for DISH and ISH with FISH.

Results: In the selected population, the mean age was 59.6 years (10-81 years) with a male-to-female ratio of 3.2:1. DISH results were obtained in 22 cases, with a sensitivity of 100% (9/9) and a specificity of 76.9% (10/13). There was a 86.3% (19/22) concordance between FISH and DISH (k=0.73, $p<0.01$).(Table 1) Three cases were DISH positive but FISH negative, including two cases diagnosed as lipoma with necrosis, and one case of ALT. IHC results were obtained in 36 cases. Compared with FISH, IHC for MDM2 has a 75.0% (27/36) concordance (k= 0.50; $p< 0.01$) with 50.0% sensitivity and 100.0% specificity; and IHC for CDK4 has a concordance of 66.7% (k=0.33; p=0.03), with 44.4% sensitivity and 88.9% specificity.(Table 1)

Table 1. Concordance of FISH and DISH/IHC.

		FISH			
		Positive	Negative	Total	k *
DISH					
	Positive	9	3	12	0.73
	Negative	0	10	10	
	Total	9	13	22	
IHC MDM2					
	Positive	9	0	9	0.50
	Negative	9	18	27	
	Total	18	18	36	
IHC CDK4					
	Positive	8	2	10	0.33
	Negative	10	16	26	
	Total	18	18	36	

* Cohen's kappa value is calculated compared with FISH

Conclusions: Our data show an excellent correlation (k>0.7) for FISH and DISH results in liposarcoma and benign soft tissue tumors; while IHC has lower sensitivity and agreement with the golden standard. With a high concordance with FISH, reduced reporting time, and lower cost, DISH may be a more practical option for many laboratories for the confirmation of WDLPS/ALT and DDLPS.

45 Are ALK Rearrangements Found in Smooth Muscle Tumors of the Gastrointestinal Tract?

Shefali Chopra[1], Alexander Lazar[2], Wei-Lien Billy Wang[2]
[1]University of Southern California, San Marino, CA, [2]The University of Texas MD Anderson Cancer Center, Houston, TX

Disclosures: Shefali Chopra: None; Alexander Lazar: None; Wei-Lien Billy Wang: None

Background: Leiomyomas are the most common smooth muscle tumors of the gastrointestinal (GI) tract, with esophagus being the most frequent site. Recently ALK rearrangement was described in two gastrointestinal leiomyomas (one esophageal and one jejunal). *ALK* rearrangements have also been described in uterine tumors which were originally classified as smooth muscle tumors in the female genital tract in few large series but later felt best re-classified as inflammatory myofibroblastic tumors. Patients with these tumors may benefit from crizotinib, a selective ALK inhibitor. We wanted to confirm whether GI leiomyomas harbored *ALK* rearrangements and the frequency of this event.

Design: Thirty smooth muscle tumors were archived from the pathology files of two institutions. Immunohistochemistry (IHC) for 25 cases was performed on whole sections using ALK1 clone 5A-4, Leica ready to use antibody, on Leica Bond III autostainer. Five cases were tested using ALK1, clone D5F3, on DAKO autostainer. *ALK* fluorescence in-situ hybridization (FISH) was performed on whole sections from 4 cases using the commercial DAKO/Agilent break apart probe for *ALK* FISH. Fifty representative nuclei were assessed and the cut off used was 10%.

Results: Thirteen of the tumors were located in the esophagus, nine were gastric, five were located in the colon, two were at the gastroesophageal junction and one was jejunal. Twenty-nine of these tumors were leiomyomas and there was a single gastric leiomyosarcoma. The tumor size ranged from 0.1 cm to 27 cm with the mean size being 2.6 cm. Nineteen of the patients were male and 11 were female. The median age of the patients was 66 years. Histology and immunohistochemical stains when present were re-reviewed in all cases. Ten of the cases had positive desmin stain with the negative CD117 or DOG1 supporting the diagnosis. Two additional cases had positive smooth muscle actin with negative CD117. ALK IHC was negative on all thirty cases, which was further validated by negative *ALK* FISH on 4 of the 30 cases. *ALK* FISH was performed on 3 leiomyomas and 1 leiomyosarcoma and all of the tumors on which FISH was performed were 4.5 cm or greater in size.

Conclusions: Despite initial studies to the contrary none of the smooth muscle tumors of the GI tract in our series harbored *ALK* rearrangements by IHC or FISH.Thus the frequency of this molecular derangement is apparently low and very few cases of smooth muscle tumors in the GI tract seem to share this feature with inflammatory myofibroblastic tumor.

46 Utility of H3F3A Expression in Atypical and Malignant Giant Cell Tumors of Bone

Christian Curcio[1], Davis Ingram[2], Khalida Wani[3], Samia Khan[3], Alexander Lazar[3], Wei-Lien Billy Wang[3]
[1]The University of Texas MD Anderson Cancer Center, Flemington, NJ, [2]Houston, TX, [3]The University of Texas MD Anderson Cancer Center, Houston, TX

Disclosures: Christian Curcio: None; Davis Ingram: None; Khalida Wani: None; Samia Khan: None; Alexander Lazar: None; Wei-Lien Billy Wang: None

Background: Giant cell tumor of bone (GCTB) is a benign but locally aggressive neoplasm. Unusual atypical variants and tumors with rare situation of malignant sarcomatous transformation can be challenging to diagnose. Recently, GCTBs have been found to harbor *H3F3A* gene mutations, resulting in a histone H3.3 variant where glycine is replaced by tryptophan at amino acid position 34 (G34W). This amino acid substitution can be detected using immunohistochemistry. While the utility of anti-histone H3.3 G34W in labeling benign GCTB is well-documented, whether this marker remains expressed in more challenging variants, including those with sarcomatous transformation, is less explored. A marker with the ability to identify a GCTB origin of a sarcoma would be of significant utility, particularly in instances where a sarcomatous component comprises most or all of a specimen, since identifying a GCTB lineage can have therapeutic implications. This study examines anti-histone H3.3 G34W labeling in malignant GCTBs, morphologically atypical GCTBs, and giant cell-rich osteosarcomas (GCROS), a potential histologic mimic of malignant GCTB.

Design: Retrospective pathology file review identified all malignant GCTBs, GCTBs with atypia insufficient for sarcomatous transformation, and GCROSs diagnosed at our high-volume institution from 2002 through 2018. All cases with available archived formalin-fixed, paraffin-embedded tumor sample were stained with anti-histone H3.3 G34W rabbit monoclonal antibody (ReMab Biosciences, Clone RM263, 1:200) using a Leica Bond III Autostainer (Leica Biosystems, Buffalo Grove, IL) and microscopically examined for patterns of labeling (positive defined as staining of any intensity with thresholds as follows: diffuse – 51-100%, patchy – 11-50%, focal – 1-10%).

Results: Twelve malignant GCTBs, six atypical GCTBs, and five GCROSs were tested. Of the malignant GCTBs, 5/12 (42%) demonstrated reactivity for anti-histone H3.3 G34W with at least focal staining present in the sarcomatous component. Staining patterns present in the sarcomatous components included focal (2), patchy (1), and diffuse (2). Of the atypical GCTBs, all six demonstrated reactivity with either patchy (2) or diffuse (4) staining, and of the GCROSs, none were reactive.

Conclusions: Immunohistochemical study with anti-H3.3 G34W can be useful in the diagnosis of atypical GCTB variants. However, malignant GCTB can lose reactivity for anti-histone H3.3 G34W in sarcomatous areas limiting its sensitivity for these tumors.

47 PHH3 Immunohistochemistry in Distinguishing Cellular and Dedifferentiated Liposarcoma on Biopsy

Christian Curcio[1], David Wang[2], Davis Ingram[3], Khalida Wani[4], Samia Khan[4], Alexander Lazar[4], Wei-Lien Billy Wang[4]
[1]The University of Texas MD Anderson Cancer Center, Flemington, NJ, [2]Hummelstown, PA, [3]Houston, TX, [4]The University of Texas MD Anderson Cancer Center, Houston, TX

Disclosures: Christian Curcio: None; David Wang: None; Davis Ingram: None; Khalida Wani: None; Samia Khan: None; Alexander Lazar: None; Wei-Lien Billy Wang: None

Background: In 2007, HL Evans published data indicating that the cellular form of atypical lipomatous tumor (ALT) clinically behaves similarly to conventional ALT. Cellular ALT was defined as an ALT containing a non-lipogenic component with a mitotic rate of <5/10 high-power fields (hpf) and cellularity less than traditional dedifferentiated liposarcoma (DDLPS). Given that cellular ALT and DDLPS can have overlapping features and mitoses are not always easily appreciated on core biopsies due to their fibrotic nature, distinguishing these entities on core biopsy can be challenging. Correct diagnosis is crucial as therapy may differ significantly. Immunohistochemical study for phosphohistone H3 (pHH3) is a useful, specific marker for identifying mitoses. This study examines the utility of pHH3 immunohistochemistry in distinguishing cellular ALT from DDLPS on core biopsy.

Design: Retrospective pathology file review identified all needle core biopsies diagnosed as cellular ALT at our high-volume institution from 2002 through 2018 that also had a subsequent surgical resection specimen. All biopsy specimens with available archived formalin-fixed, paraffin-embedded tumor sample were stained with anti-pHH3 rabbit monoclonal antibody (BioCare Medical, Clone BC37, 1:100) using a Leica Bond III Autostainer (Leica Biosystems, Buffalo Grove, IL) and microscopically examined to quantify staining nuclei per 10 hpf (area assessed of ~2.2 mm^2).

Results: Seventeen biopsy samples were assessed. Nine (53%) had subsequent resection diagnoses of ALT without dedifferentiation; the remaining eight (47%) had subsequent resection diagnoses of DDLPS. All biopsy samples had H&E-based mitotic counts of 0-4/10 hpf (mean: 0.8/10 hpf, median: 0/10 hpf). Biopsy samples with subsequent resection diagnoses of ALT without dedifferentiation had pHH3 counts of 1-10/10 hpf (mean: 4.9/10 hpf, median: 5/10 hpf). Biopsy samples with subsequent resection diagnoses of DDLPS had pHH3 counts of 9-56/10 hpf (mean: 21/10 hpf, median: 18/10 hpf).

Conclusions: Mitotic figures can be difficult to appreciate in core biopsies of non-lipogenic components of ALT, which can sometimes lead to underdiagnosis of DDLPS. Immunohistochemical study with anti-pHH3 can be a useful adjunct in assessing mitoses in these cases. Given that the original mitotic cut-off was established on resection specimens by H&E, the mitotic cut-off for a diagnosis of DDLPS using pHH3 may need to be adjusted to account for increased sensitivity using this assay.

48 USP6 Gene Rearrangements with Novel Fusion Partners in a Subset of So-Called "Cellular Fibroma of Tendon Sheath"

John Gross[1], Jose Mantilla[1], Yajuan Liu[1], Benjamin Hoch[2], Robert Ricciotti[1]
[1]University of Washington, Seattle, WA, [2]University of New Mexico, Albuquerque, NM

Disclosures: John Gross: None; Jose Mantilla: None; Yajuan Liu: None; Benjamin Hoch: None; Robert Ricciotti: None

Background: Fibroma of tendon sheath (FTS) is a benign (myo)fibroblastic neoplasm that arises from tenosynovial tissues. Histologically, FTS is typically well-circumscribed, paucicellular, and composed of bland spindle cells within a collagenous matrix. A cellular variant (CFTS), showing morphologic overlap with nodular fasciitis (NF), has been described and previously shown to harbor *USP6* translocations in a subset of cases, further suggesting a relationship to NF. In this study, we analyze 12 cases of CFTS using targeted anchored PCR/next-generation sequencing (NGS) to evaluate for *USP6* rearrangements and identify gene fusion partners.

Design: With prior IRB approval, we searched our institutional pathology archives to identify tumors classified as FTS and reviewed slides for all cases to search for those morphologic features of CFTS. All cases of CFTS were subjected to total nucleic acid extraction for targeted anchored PCR/NGS. Clinical, pathologic and demographic characteristics were recorded.

Results: We identified 39 tumors classified as FTS of which 14 showed features of CFTS including increased cellularity and NF-like growth pattern as well as some showing focally enlarged cells with epithelioid features (extensive in one tumor), vague palisading, and rare giant cells. CFTS affected 9 males and 5 females with a mean patient age of 43 yrs (range 28-73 yrs) and occurred in the hands/fingers (n=10), wrist (n=1), ankle (n=1), elbow (n=1), and over the tibia (n=1). Mean tumor size was 1.9 cm (range 1.0-4.3 cm). We were able to obtain nucleic acids of adequate quality for molecular testing from 12 cases. Gene fusions were identified in 6 (50%) tumors, all of which involved *USP6*. Fusion partners were identified in these 6 cases and included *PKM*, *RCC1*, *ASPN, COL1A1*, *COL3A1*, and *MYH9*, each found in one case.

Conclusions: A subset of CFTS harbor *USP6* rearrangement and highly variable fusion partners. To our knowledge, this is the first report to identify fusion partners of *USP6* in CFTS including novel partners *PKM* which was found in one tumor with unusual epithelioid features and palisading growth, RCC1, and *ASPN.* We also identified partners previously reported in NF. While these findings suggest that some lesions classified as CFTS may represent tenosynovial examples of NF, we identified a subset with morphologic features quite distinct from nodular fasciitis and harboring novel fusion partners, likely representing a tumor distinct from NF.

49 Expanding the immunophenotypic spectrum of malignant gastrointestinal neuroectodermal tumor

John Gross[1], Jose Mantilla[1], Yajuan Liu[1], Camtu Truong[1], Robert Ricciotti[1]
[1]University of Washington, Seattle, WA

Disclosures: John Gross: None; Jose Mantilla: None; Yajuan Liu: None; Camtu Truong: None; Robert Ricciotti: None

Background: Malignant gastrointestinal neuroectodermal tumor (GNET) (AKA clear cell sarcoma-like tumor of the gastrointestinal tract) is a rare, aggressive neoplasm that typically shows evidence of neuroectodermal differentiation and harbors *EWSR1* rearrangement with either *CREB1* or *ATF1* fusion partners. Immunohistochemically, it expresses S100 and SOX10, often diffusely, and lacks HMB45 and Melan-A. Due to its rarity, however, additional studies are needed to further refine the characterization of GNET and identify potential diagnostic pitfalls. Here we describe the characteristics of 4 GNETs, including immunoreactivity for DOG1, reported as negative in previous studies, and beta-catenin, both of which resulted in initial misdiagnosis.

Design: With prior IRB approval, we identified 4 cases of GNET in our institutional pathology archives. Histologic slides, immunostains, and PCR/FISH studies were reviewed to confirm the diagnosis. All cases were stained with antibodies against DOG1, CD117, S100, SOX10, CD34 and beta-catenin. Anchored PCR/NGS (AMP/NGS) was performed on 3 tumors to identify fusion genes. Clinical and demographic information was recorded.

Results: Morphologic features in all 4 cases were consistent with GNET. Tumors affected 3 females and 1 male and involved small bowel (N=2), stomach (N=1), and retroperitoneum (N=1). The mean patient age was 44 yrs (range 37-48). RT-PCR identified an *EWSR1-CREB1* fusion transcript in 1 case. FISH studies showed *EWSR1* rearrangement (split signals) in 3 cases for which AMP/NGS was performed and identified an *ATF1* fusion partner in 2 cases. No fusion partner was identified for 1 case. Immunostaining results are summarized in [**Table 1].** Immunoreactivity for DOG1 and beta-catenin each contributed to initial misdiagnoses of epithelioid GIST and solid pseudopapillary tumor (SPPT), respectively.

Case	Fusion	SOX10	S100	CD34	CD117	DOG1	Beta-catenin
1	EWSR1-CREB1	Diffuse	Diffuse	(-)	(-)	(-)	Variable cytoplasmic
2	ND. FISH only	(-)	(-)	(-)	(-)	Incomplete membrane	Cytoplasmic + focal nuclear
3	EWSR1-ATF1	Diffuse	Patchy	(-)	(-)	(-)	Weak membrane
4	EWSR1-ATF1	Diffuse	Diffuse	(-)	(-)	Incomplete membrane	Cytoplasmic + focal nuclear

Conclusions: In the 4 GNETs evaluated, we demonstrate that the extent of S100 and SOX10 expression may be variable and even absent. DOG1 and beta-catenin reactivity, as well as some morphologic overlap, may lead to confusion with epithelioid GIST and/or SPPT. These findings expand the described immunophenotype of GNET and highlight potential diagnostic pitfalls.

50 Extraskeletal Osteosarcoma of the Breast: A Single Institution's Experience with 7 cases and Tips to Avoid Misdiagnosis

John Gross[1], Suzanne Dintzis[2], Robert Ricciotti[1]
[1]University of Washington, Seattle, WA, [2]Mercer Island, WA

Disclosures: John Gross: None; Suzanne Dintzis: None; Robert Ricciotti: None

Background: Extraskeletal osteosarcoma (ESOS) is a rare and highly aggressive sarcoma most commonly affecting adults in the deep soft tissues of the extremities. A prior history of radiation has been reported in 10% of cases. Radiologically, ESOS often presents as an ill-defined, large, mineralized soft tissue mass. By definition, a primary bone origin must be excluded, malignant cells must produce osteoid or bone, and an epithelial component must be absent. Histologically identical to its skeletal counterpart, this diagnosis is often challenging due to its variable clinical presentation, more common mimics (i.e. metaplastic carcinoma, OS in a phyllodes tumor and myositis ossificans) and limited tissue on biopsies. Immunohistochemistry with SATB2 may help identify osteoblastic differentiation. The true incidence of breast ESOS is difficult to assess as older studies may have included epithelial malignancies, however, we believe fewer than 100 pure breast

ESOS have been reported. Herein, we discuss our experience with 7 cases to improve our understanding of this disease and help avoid misdiagnosis.

Design: With prior IRB approval, we searched our institutional pathology archives for primary breast ESOS. Histologic slides were re-reviewed and demographic, clinical, radiologic and pathologic characteristics as well as pertinent clinical follow up were evaluated from all patients.

Results: 7 cases of breast ESOS were identified with an average age of 69 yrs (46-88). 4 cases were previously misdiagnosed as metaplastic carcinoma (N=3) and aneurysmal bone cyst (ABC) of soft tissue (N=1). 2 patients reported a prior history of local radiation; both occurring 11 years prior. The average tumor size was 5.1 cm (3.4-6.5). Histology was osteoblastic (N=3), mixed osteoblastic/chondroblastic (N=3) and telangiectatic (N=1) **[Figure 1]**. The average time to follow up was 2.3 yrs (0.2-4). 6 patients received adjuvant chemotherapy; 1 had palliative radiation. 4 patients are alive; 2 currently NED and 2 with metastatic disease. 3 patients have died from their disease.

Case	Age	Misdiagnosis	Prior Radiation	Size (cm)	Histology	Clinical F/U
1	69	Yes - ABC of soft tissue	Yes 11 yrs prior	5.0	Telangiectatic	Alive; 4 yrs; adjuvant chemo, 4 local recurrences; current liver metastases
2	73	Yes - metaplastic carcinoma	No	3.4	Osteoblastic	Deceased; 3 yrs; adjuvant chemo; diffuse metastases
3	55	No	Yes 11 yrs prior	5.5	Osteoblastic	Alive; 4 yrs; adjuvant chemo; local recurrence resected; currently NED
4	46	No	No	6.5	Mixed; osteoblastic + chondroblastic	Deceased; 3 yrs; adjuvant chemo; lung metastases
5	88	No	No	5.2	Mixed; osteoblastic + chondroblastic	Deceased; 1 year; palliative radiation; lung, bone metastases
6	84	Yes- metaplastic carcinoma	No	6.2	Mixed; osteoblastic + chondroblastic	Alive; 2 months; adjuvant chemo; NED
7	69	Yes- metaplastic carcinoma	No	4.2	Osteoblastic	Alive; 1 year, adjuvant chemo; currently >20 lung metastases

Figure 1 - 50

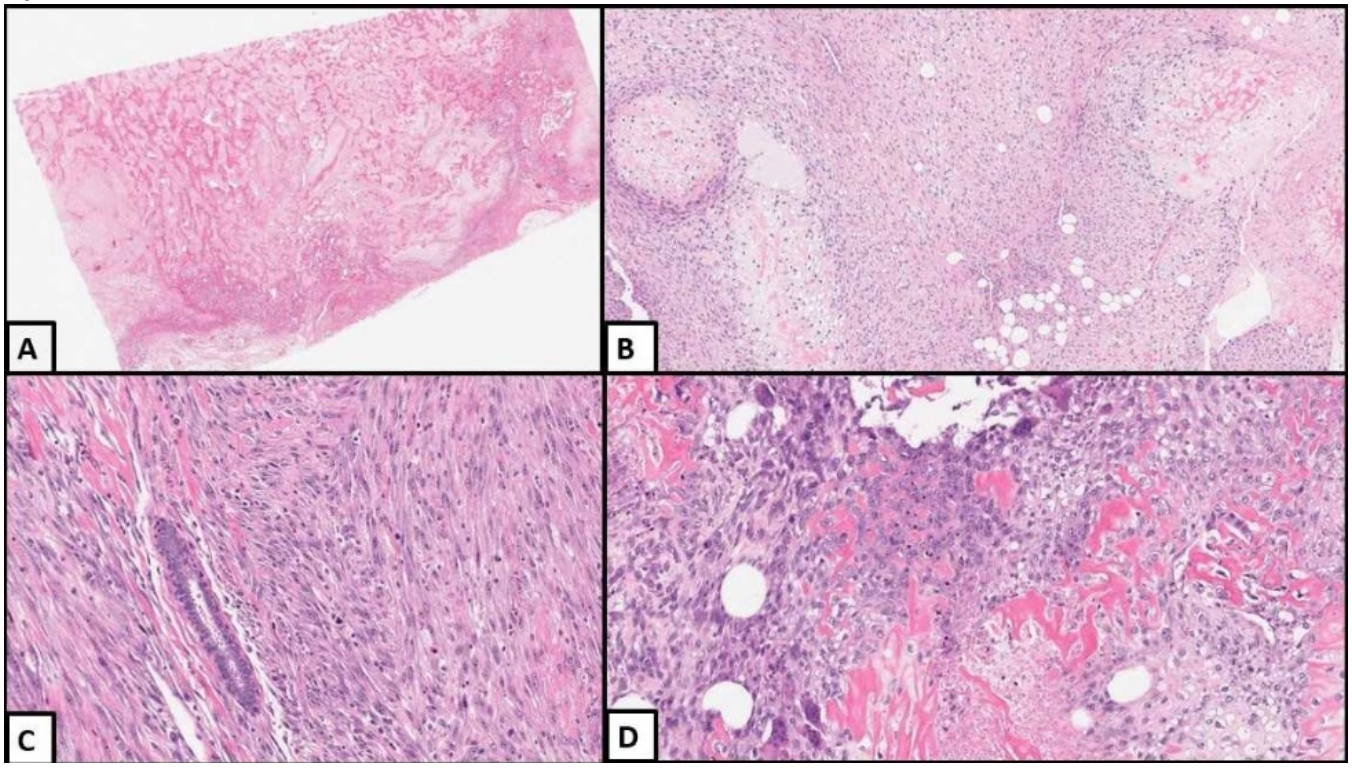

Conclusions: While rare, it is critical to distinguish primary breast ESOS from its mimics as the treatment and prognosis are radically different. Primary breast ESOS cannot have an epithelial component and may contain only focal osteoid, especially on small biopsies. SATB2 IHC can help identify osteoblastic differentiation. Finally, clinical and radiologic information must be considered as a high index of suspicion is necessary to avoid misdiagnosis.

51 Beyond Triton: Malignant Peripheral Nerve Sheath Tumor with Complete Heterologous Rhabdomyoblastic Differentiation Mimicking Spindle Cell Rhabdomyosarcoma

Jason Hornick[1], Gunnlaugur Petur Nielsen[2]
[1]Brigham and Women's Hospital, Harvard Medical School, Boston, MA, [2]Massachusetts General Hospital, Boston, MA

Disclosures: Jason Hornick: *Consultant*, Eli Lilly; *Consultant*, Epizyme; Gunnlaugur Petur Nielsen: None

Background: Spindle cell rhabdomyosarcoma (RMS) is an aggressive sarcoma type with a predilection for the head and neck and frequent transactivating *MYOD1* mutations. Malignant peripheral nerve sheath tumors (MPNST) show heterologous (most often rhabdomyoblastic) differentiation in 10% of cases; such tumors have been referred to as malignant Triton tumors. MPNST harbors inactivating mutations in *SUZ12* or *EED*, resulting in PRC2 dysfunction and loss of histone H3 lysine 27 trimethylation (H3K27me3), most often seen in sporadic or radiation-associated, high-grade tumors; immunohistochemistry (IHC) for H3K27me3 is a useful diagnostic marker. We recently encountered a tumor showing H3K27me3 loss but with otherwise typical features of spindle cell RMS. The purpose of this study was to evaluate H3K27me3 in spindle cell RMS and further investigate the putative spindle cell RMS with loss of H3K27me3.

Design: IHC for H3K27me3 (clone C36B11) was performed on 25 cases of spindle cell RMS. H3K27me3 loss was defined as a complete absence of nuclear staining in tumor cells. Targeted sequencing of all exonic and selected intronic regions of ~450 genes was performed on the tumor with H3K27me3 loss using hybrid capture with a custom probe set and massively parallel (next-generation) sequencing (NGS).

Results: Of the 25 patients, 15 were male and 10 were female with a median age of 34 yrs (range 6 wks – 77 yrs). Tumors involved head and neck (N=15); trunk wall (N=4); extremities/limb girdles (N=3); and other sites (N=3). All tumors showed diffuse staining for desmin and extensive expression of myogenin and/or MyoD1. Only 1 case (4%) showed loss of H3K27me3: a 15-cm deep-seated groin mass in a 76-year-old female with no history or signs of type 1 neurofibromatosis. The resected tumor showed diffuse hypercellularity with a fascicular architecture, marked nuclear atypia, eosinophilic cytoplasm, and a high mitotic rate (see Fig. 1); rhabdomyoblasts were not apparent. By IHC, the tumor showed diffuse staining for desmin, myogenin, and MyoD1, whereas S100 protein and SOX10 were negative. NGS revealed 2-copy deletion of *NF1*, *CDKN2A*, and *SUZ12*, and a *TP53* mutation with loss of 17p, findings characteristic of MPNST. The patient rapidly developed bilateral lung metastases.

Figure 1 - 51

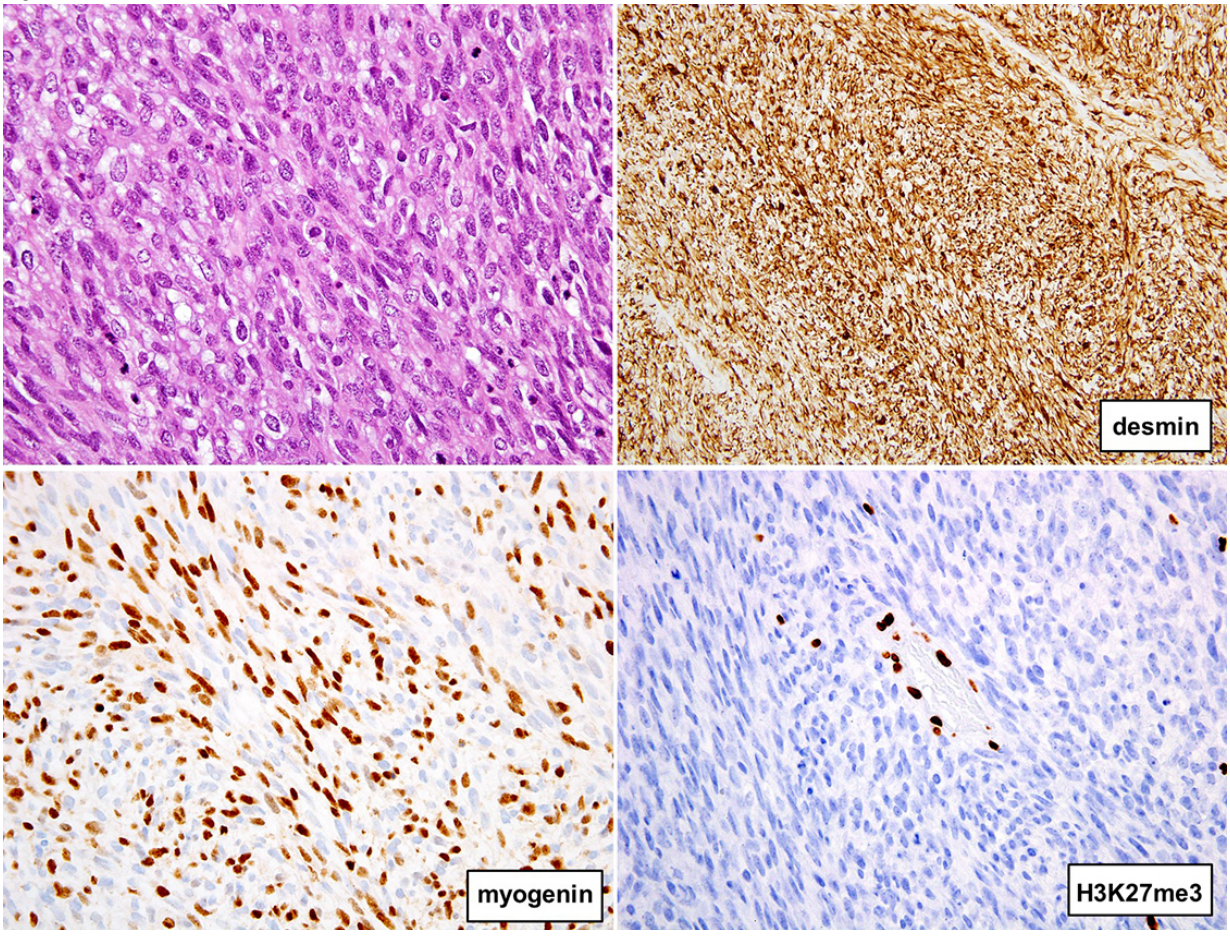

Conclusions: MPNST may occasionally show complete heterologous rhabdomyoblastic differentiation without histologic evidence of residual conventional MPNST, closely mimicking spindle cell RMS. IHC for H3K27me3 reliably distinguishes MPNST from spindle cell RMS.

52 Strong desmin positivity along with weak CD117 positivity in GISTs (Gastrointestinal Stromal Tumors): Potential pitfall in diagnosis on needle core biopsies and cell block specimens

Ahmad Ibrahim[1], Shefali Chopra[2]
[1]University of Southern California, Los Angeles, CA, [2]University of Southern California, San Marino, CA

Disclosures: Ahmad Ibrahim: None; Shefali Chopra: None

Background: GISTs are the most common mesenchymal tumors of the gastrointestinal tract. Diagnosis of GIST relies on CD117 immunohistochemical staining. Approximately 95% of GISTs are immunoreactive for CD117, most show strong and diffuse cytoplasmic staining for CD117 with a small minority of GISTs exhibiting a dot-like or membranous staining pattern. Rare desmin positivity has been reported in GISTS. DOG1 detects 30-40% of KIT-negative GISTs, but a small percentage of smooth muscle tumors have also been reported to be DOG1 positive.

Design: All biopsies/ cell block material with a diagnosis of gastrointestinal stromal tumor from 2015 to 2018 were retrieved and reviewed along with the immunohistochemical stains and genotyping report where available. The demographic data, site, size and type of procedure (biopsy versus fine needle aspiration with cell block) was recorded. Desmin (clone DE-R-11), SMA (Clone ASM-1), DOG1 (clone K9) were ready to use Leica antibodies. The CD117 (clone YR145) was used in dilution 1:100 and is a cell marque antibody. Scoring of desmin, smooth muscle actin (SMA), CD117 and DOG1 was done and quantified on a 3-tier scale based on the intensity and percentage positive cells.1+ was defined as <20% of the tumor cells positive with weak intensity, 2+ as 20-75% tumor cells positive with strong intensity and 3+ as strong diffuse (>75%) positive.

Results: A total of 35 cases were identified. Out of these 17 cases had no desmin immunostain but CD117 was strongly positive in all these cases. Of the 18 cases where desmin was performed it was negative in 13 cases. Six (33%) of GISTs showed desmin positivity. There were 3 cases with strong 2-3+ desmin positive along with 1+ CD117 positive. SMA on two of these cases was also 3+. DOG1 was strong diffuse in all of these cases. Genotyping was performed in 2 of the 3 cases and one case had KIT exon 11 mutation and the second case mutation in PDGFRa exon 18. Results are summarized in Table1. All 3 cases with strong desmin positivity along with weak CD117 positivity were located in the stomach, and the size of these tumors ranged from 0.5 to 1.5 cm.

Case No.	Desmin	Actin	DOG1	CD117	Genotyping	Site	Size
1	2+	1+	3+	3+	N/A	Gastric	2.0 cm
2	1+	1+	3+	3+	N/A	Gastric	4.5 cm
3	1+	1+	3+	2+	N/A	Gastric	3.1 cm
4	2+	N/A	3+	1+	N/A	Gastric	0.5 cm
5	3+	3+	3+	1+	KIT mutation in exon 11	Gastric	1.5 cm
6	2+	3+	3+	1+	PDGFRa exon 18 mutation	Gastric	0.7 cm

Table1: Immunoprofile and genotyping results on the desmin positive GISTS

Figure 1 - 52

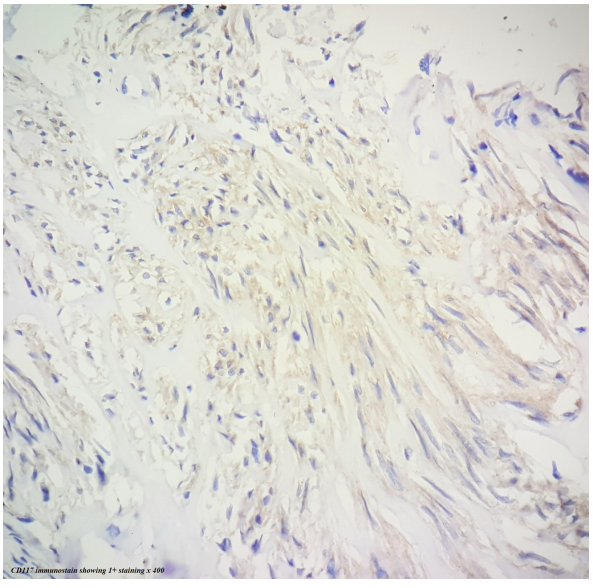

Figure 2 - 52

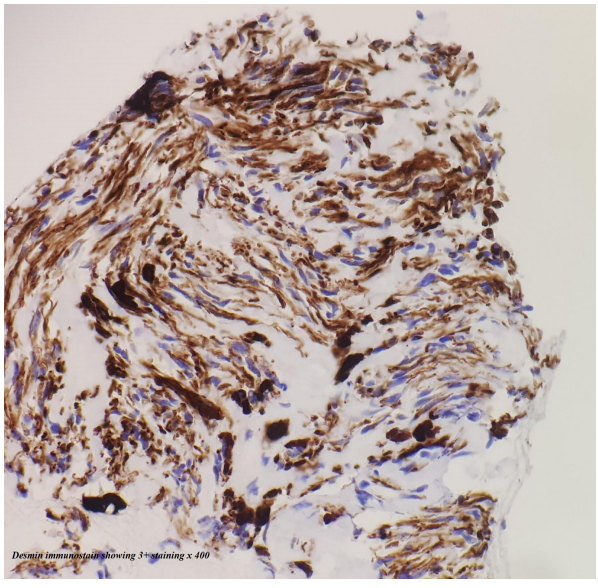

Conclusions: There is a small percentage of GISTS which can have strong desmin positivity (4/35). Strong desmin positivity along with weak CD117 positivity (3/35) can be a pitfall in diagnosis especially on needle core biopsies and cell block material. DOG1 immunostain as well as genotyping can help in definitive diagnosis. Strong desmin positivity can be seen in both KIT and PDGFRA mutated GISTs.

53 Myxoinflammatory Fibroblastic Pseudotumor of Perinephric Type; A Clinicopathologic Analysis of 13 Cases

Nooshin Karamzadeh Dashti[1], Andrew Folpe[1]
[1]Mayo Clinic, Rochester, MN

Disclosures: Nooshin Karamzadeh Dashti: None; Andrew Folpe: None

Background: In 2009, Tanas et al reported 12 unusual, renal cell carcinoma-associated pseudotumors of the perinephric fat, mimicking well-differentiated liposarcoma (WDL) (Mod Pathol 2009; 22: 1196). No subsequent studies of this entity exist. We report 13 similar lesions, termed “myxoinflammatory fibroblastic pseudotumor of perinephric type” (MIFPT), arising in patients with and without associated renal neoplasia, with the goal of increasing awareness of this distinctive pseudoneoplastic lesion.

Design: Slides and blocks from 13 perinephric masses were retrieved from our archives. Immunohistochemistry for IgG/IgG4 and FISH for *MDM2* amplification was performed. Clinical information was obtained from medical charts and referring pathologists.

Results: Cases occurred in 11M and 2F ranging from 43-84 years of age (median 63 years). Diagnostic procedures included core biopsy (n=4), perinephric/periureteral mass resection (n=3) and nephrectomy (n=6). Twelve patients presented with perinephric masses (size range 2-28cm) and one with bilateral periureteral "thickening". Four were bilateral or multiple. Underlying renal disease included diabetes mellitus (n=5), end-stage kidney (n=3), chronic pyelonephritis (n=1), and contralateral renal cell carcinoma (n=1). Four patients were not known to have renal disease. Submitting diagnoses included: WDL (n=8); angiomyolipoma, spindle cell lipoma, myxoid neoplasm, low grade sarcoma, IgG4-disease, fibromatosis, aggressive angiomyxoma and "reactive". Histologically, the tumors consisted of an admixture of mature fat, myxoid stroma, bland spindled to stellate cells and a variably intense mixed inflammatory cell infiltrate. Hyperchromatic stromal cells were absent. IgG4+ plasma cells were focally increased in one case (hot spot 30%) which otherwise lacked morphologic features of IgG4-disease; 10 other tested cases were negative. FISH for MDM2 amplification was negative in all 13 cases. Clinical follow-up (10 patients; range 1-120 months; median 29 months) showed absent or stable disease in 8 patients; 2 died of unrelated causes. Three cases were too recent for meaningful follow up.

Conclusions: MIFPT is a distinctive pseudoneoplasm of the perinephric fat occurring in association with neoplastic and non-neoplastic renal disease. Careful morphologic evaluation and ancillary testing for MDM2 amplification should allow its confident distinction from WDL. The etiology of MIFPT is obscure, but it does not appear to represent a manifestation of IgG4-disease.

54 MDM2 Amplification Status and Its Diagnostic Utility In Myxofibrosarcoma: A Clinicopathologic Analysis of 21 Cases

Nooshin Karamzadeh Dashti[1], Darlene Knutson[1], Sara Kloft-Nelson[1], Patricia Greipp[1], Karen Fritchie[1]
[1]Mayo Clinic, Rochester, MN

Disclosures: Nooshin Karamzadeh Dashti: None; Darlene Knutson: None; Sara Kloft-Nelson: None; Patricia Greipp: None; Karen Fritchie: None

Background: Myxofibrosarcomas (MFS) classically present as slowly enlarging superficial masses in elderly patients. These tumors fail to exhibit a distinct immunophenotype and often harbor a complex karyotype. Dedifferentiated liposarcoma (DL) with myxoid features can mimic MFS, especially deep-seated lesions that arise in the extremity. Distinction may be difficult on core biopsy when a definitive well-differentiated liposarcomatous component cannot be identified. Furthermore, infiltration of MFS into surrounding fat may mimic the atypical hyperchromatic stromal cells characteristic of well-differentiated liposarcoma. The vast majority (~ 90%) of DL show *MDM2* amplification, whereas limited data exists as to the *MDM2*status of MFS. We sought to explore the rate of *MDM2* amplification in cases of classic MFS to determine its utility in this diagnostic setting

Design: Our archives were searched for resection specimens diagnosed as MFS. Only superficial lesions arising above the fascia were included, while cases with neoadjuvant treatment were excluded. All available slides were reviewed to confirm the presence of classic morphologic features of MFS. FISH for *MDM2* amplification was performed on a representative section from each case.

Results: 21 resection (16 primary; 5 recurrence) specimens of MFS were identified (M=11, F=10; 44-85 years; median: 71 years). The tumors (1.1-11 cm; median 3.8 cm) occurred in lower extremity (n=11), upper extremity (n=7) and trunk (n=2). All cases contained an infiltrative population of atypical cells embedded in a myxoid stroma with coarse curvilinear blood vessels. 3 cases were classified as the epithelioid variant. The mitotic rate ranged from 0 to 73 per 10 HPFs (median 11), and 10 (of 21) cases had necrosis. FNCLCC grading was as follows: grade 1: n=7, grade 2: n=4, grade 3: n=10. *MDM2* amplification was identified in 2 (of 21; 9.5%) cases. Follow up available on 17 cases (range 1-96 months; median 18.5 months) revealed 6 patients with local recurrence. One patient died of disease. One of the patients with an *MDM2* amplified tumor experienced recurrence and died of unrelated causes, while the second was alive without disease 24 months after diagnosis.

Conclusions: The rate of *MDM2* amplification in MFS appears to be low (9.5%), suggesting that FISH for *MDM2* may be a useful diagnostic tool in distinguishing MFS from cases of myxoid DL, especially on core biopsy material. Further studies are necessary to determine if amplification status adds prognostic value.

55 Plexiform Fibrohistiocytic Tumor: A Clinicopathological and Immunohistochemical Study of 41 Tumors

Nooshin Karamzadeh Dashti[1], Abbas Agaimy[2], Andrew Folpe[1]
[1]Mayo Clinic, Rochester, MN, [2]Erlangen, Germany

Disclosures: Nooshin Karamzadeh Dashti: None; Abbas Agaimy: None; Andrew Folpe: None

Background: Plexiform fibrohistiocytic tumor (PFHT) usually occurs in the superficial soft tissues of young patients and typically shows bimorphic histology, with fascicles of fibroblastic spindled cells and nodules composed of mononuclear cells and osteoclasts. The mononuclear cells of PFHT are assumed to represent histiocytes, largely based on CD68 expression. However, CD68 is not lineage-specific, and expression of other histiocytic markers such as HLA-DR or lysozyme is absent. Anecdotally, we have observed these mononuclear cell nodules to contain a mixture of cell types, including osteoclasts (positive for CD11c and CD4, but not CD163), true histiocytes (positive for CD163, CD11c and CD4) and a "null" cell population lacking expression of all histiocyte-related antigens. We studied the clinicopathological and immunohistochemical features of a large cohort of PFHTs in order to better understand their behavior and lineage.

Design: Slides and blocks from 41 PFHTs were retrieved. Immunohistochemistry for CD11c and CD163 was performed. Clinical information including patient follow-up was obtained.

Results: PFHT occurred in 27 females and 13 males aged 8months to 55 years (median 15.5 years). One patient with neurofibromatosis type-1 had two tumors. Sites included: upper extremity (n=19), lower extremity (n=13), trunk (n=5) and head/neck (n=4). Tumor size ranged from 0.4-6.1cm (median 1.5 cm, average: 1.7 cm). Morphology was biphasic (n=33) and fibroblastic (n=8). Unusual features included nuclear atypia (n=4), ossification (n=1) and marked inflammation (n=1). IHC (27 cases) showed subsets of mononuclear cells to express CD163 and CD11c; all cases contained mononuclear cells negative for both markers. Follow-up (20 cases; range 3-120 months; median 54 months) showed 5 local recurrences and no metastases. One patient died of an unrelated cause; all others were alive without disease.

Conclusions: Although PFHT has traditionally been thought of as a true "fibrohistiocytic" neoplasm, composed of both neoplastic histiocytes and fibroblasts, our results suggest the presence of another cell population within the histiocytic nodules. We hypothesize that this represents the true neoplastic population, with recruitment of CD163/CD11c-positive histiocytes and osteoclasts. On-going molecular genetic studies should help to clarify the nature of these "null" cells.

56 Fibro-Adipose Vascular Anomaly (FAVA): A Clinico-Pathologic Study of a Recently Described Entity

Hatim Khoja[1], Tariq Al-Zaid[1], Ayman Aboujoukh[1], Ayman Aldeheshi[1]
[1]King Faisal Specialist Hospital and Research Center, Riyadh, Saudi Arabia

Disclosures: Hatim Khoja: None; Tariq Al-Zaid: None; Ayman Aboujoukh: None; Ayman Aldeheshi: None

Background: Fibro-adipose vascular anomaly (FAVA) is a recently described clinical-radiological-pathological entity that is considered a mesenchymal malformation with predilection to the skeletal muscle of lower extremity especially the calf. Clinically, it is commonly associated with intense pain and sometimes joint contractures. Histologically, it is composed of dense fibrous tissue with nerve entrapment, adipose tissue that infiltrates skeletal muscle, lymphoplasmacytic aggregates, and venous malformation. Its main differential diagnosis is intramuscular hemangioma

Design: All patients diagnosed with FAVA or have radiological suspicion of FAVA were collected from our archival material. 16 specimens from 12 patients were identified including 10 core biopsies and 6 excisions. Histopathologic features were evaluated by two soft tissue pathologists.

Results: Patients' age ranged from 14 to 31 years (median: 23). There were 8 females and 4 males. Intense pain was the main presenting symptom in all patients. Two patients presented with limping, due to shortening of Achilles tendon in one of them. The calf muscles were involved in (7/12; 58.3%), thigh in (3/12; 25%), buttock in (1/12; 8.3%), and para vertebral muscles in (1/12; 8.3%). Histologically, dense fibrosis, lymphoplasmacytic aggregates, and large thick-walled veins were present in the majority of patients (11/12; 92%). Fat infiltration into skeletal muscle and thin- walled cavernous vascular spaces were present in (10/12; 83%). Entrapment of vessels and nerves by fibrosis was noted in (10/12; 83.3%) and (6/12; 50%); respectively. Metaplastic bone formation was noted in (5/12; 41.6%).

Conclusions: FAVA is a distinct entity localized mainly to the calf muscles of adolescence and young adults. Intense pain is a common initial presenting symptom. Dense fibrosis with entrapment of vessels and nerves, fat infiltration into skeletal muscle, venous malformation, and lymphoplasmacytic aggregates are the main characteristic histological features. Because it may require different management approaches; it is important to distinguish FAVA from other vascular lesions with overlapping histologic features e.g. intramuscular hemangioma.

57 Novel and Established EWSR1 Gene Fusions Identified in a 5-Year Cohort by Next Generation Sequencing and Fluorescence In-Situ Hybridization

Melissa Krystel-Whittemore[1], Martin Taylor[2], Jochen Lennerz[3], Long Le[1], Dora Dias-Santagata[1], John Iafrate[1], Vikram Deshpande[1], Ivan Chebib[3], Gunnlaugur Petur Nielsen[1], Valentina Nardi[1]
[1]Massachusetts General Hospital, Boston, MA, [2]Boston, MA, [3]Massachusetts General Hospital, Harvard Medical School, Boston, MA

Disclosures: Melissa Krystel-Whittemore: None; Martin Taylor: None; Jochen Lennerz: None
Long Le: *Consultant*, ArcherDx; *Major Shareholder*, ArcherDx; Dora Dias-Santagata: None; John Iafrate: *Major Shareholder*, ArcherDx; *Consultant*, Roche; *Grant or Research Support*, Pfizer; *Grant or Research Support*, Sanofi; Vikram Deshpande: None; Ivan Chebib: None; Gunnlaugur Petur Nielsen: None; Valentina Nardi: None

Background: *EWSR1* rearrangements occur in a wide variety of clinically and pathologically diverse sarcomas as well as in non-mesenchymal tumors. *EWSR1* can rearrange with different transcription factors in phenotypically identical tumors or conversely can rearrange with the same genes in morphologically and behaviorally different tumors. Our study set out to examine the *EWSR1* fusions identified at our institution over a 5-year period, their association with specific entities, and detection of novel partners and associations.

Design: 64 consecutive cases with *EWSR1* gene fusions in tumors diagnosed between 2013 and 2018 at our institution were included in this study. Fusions were identified by either break-apart fluorescence in-situ hybridization (FISH), our clinical next generation sequencing (NGS) RNA-based assay for fusion transcript detection, or both. The fusion assay (Solid Fusion Assay version 1 and 2, and Sarcoma Fusion Assay), performed off formalin-fixed paraffin embedded tumor specimens, is based on Anchored Multiplex PCR (AMP) to enrich for the targets of interest which are then sequenced on an Illumina MiSeq or Next-Seq instrument. A laboratory-developed algorithm is used for fusion transcript detection and annotation.

Results: 32 *EWSR1* fusions were identified solely by FISH testing. 25 cases had concurrent FISH and fusion assay performed. Of these 25 cases, 21 cases were positive by both assays for an *EWSR1* gene fusion, and 4 cases were discordant (3 were FISH+ and NGS-, and 1 case was NGS+, but FISH-). 7 cases had only NGS assay performed, showing an *EWSR1* gene fusion. Of the 3 FISH+NGS- cases, one was a lung adenocarcinoma, most likely a false positive FISH result, as the tumor had numerous copy number changes. The other two cases were likely false negative fusion results due to either lack of *EWSR1* primers for a complex or unusual rearrangement, or poor tumor RNA quality. The one NGS+ and FISH- case had a complex rearrangement involving three genes (*EWSR1-RBFOX2-ERG*) in a Ewing sarcoma. A novel fusion, *EWSR1/TCF7L2,* was detected in a colon adenocarcinoma. Although *TCF7L2* fusions have been identified in colorectal carcinoma, fusions have not been previously associated with *EWSR1*. In five cases, detection of a specific partner had an impact on the histological diagnosis, two of which directly impacted patient management. [Table 1]

Table 1. *EWSR1* fusions identified by NGS Fusion Assay with FISH concordance.

Study number	Left Partner Gene	Break point 1	Right Partner Gene	Break point 2	Diagnosis	*EWSR1* FISH
1	EWSR1	Exon 12	ATF1	Exon 3	Hyalinizing clear cell carcinoma of the salivary gland	NA
2	EWSR1	Exon 8	ATF1	Exon 4	Hyalinizing clear cell carcinoma	C
3	EWSR1	Exon 8	CREB1	Exon 7	Angiomatoid fibrous histiocytoma	C
4	EWSR1	Exon 8	CREB1	Exon7	Angiomatoid fibrous histiocytoma	C
5	EWSR1	Exon 7	CREB1	Exon7	Angiomatoid fibrous histiocytoma	C
6	EWSR1	Exon 8	CREB1	Exon 7	Angiomatoid fibrous histiocytoma	C
7	EWSR1	Exon 8	CREB1	Exon 7	Angiomatoid fibrous histiocytoma	C
8	EWSR1	Exon 8	CREB3L1	Exon 5	Sclerosing epithelioid fibrosarcoma	C
9	EWSR1		ERG/RBFOX2		Malignant round cell and epithelioid neoplasm with clear cell features most consistent with sarcoma in the Ewing family*	D**
10	ERG	Exon 9	EWSR1	Exon 8	Ewing sarcoma	NA
11	EWSR1	Exon 8	FLI1	Exon 3	Adamantinoma-like Ewing sarcoma (AES)*	C
12	EWSR1	Exon 8	FLI1	Exon 3	High-grade Ewing sarcoma	C
13	EWSR1	Exon 8	FLI1	Exon 4	Ewing sarcoma	NA
14	EWSR1	Exon 7	FLI1	Exon 6	Ewing sarcoma	C
15	EWSR1	Exon 7	FLI1	Exon 7	Ewing sarcoma	NA
16	EWSR1	Exon 7	FLI1	Exon 6	Ewing sarcoma	NA
17	EWSR1	Exon 7	FLI1	Exon 6	Ewing sarcoma	C
18	EWSR1	Exon 7	FLI1	Exon 5	Ewing sarcoma	C
19	EWSR1	Exon 8	FLI1	Exon 3	Ewing sarcoma	C
20	EWSR1	Exon 7	NFATC2	Exon 3	Malignant myoepithelioma	C
21	EWSR1	Exon 13	NR4A3	Exon 4	Extraskeletal myxoid chondrosarcoma	C
22	EWSR1	Exon 9	PATZ1	Exon 1	EWSR1-PATZ1 spindle and round cell sarcoma*	C
23	EWSR1	Exon 9	PATZ1	Exon 1	EWSR1-PATZ1 spindle and round cell sarcoma*	C
24	EWSR1	Exon 9	PATZ1	Exon 1	Pleomorphic xanthoastrocytoma	C
25	EWSR1	Exon 9	PBX3	Exon 5	Malignant myoepithelioma	NA
26	EWSR1	Exon12	TCF7L2	Exon 5	Colon adenocarcinoma	C
27	EWSR1	Exon 7	TFEB	Intron 4	Translocation associated renal cell carcinoma	NA
28	EWSR1	Exon 7	WT1	Exon 8	Desmoplastic small round cell tumor*	C
29	EWSR1	Exon 11	WT1	Exon 8	Desmoplastic small round cell tumor	C

C=concordant; D=discordant; NA=not available

* = detection of a specific partner had impact on histologic diagnosis

** = False negative FISH result, which was most likely due to the complex EWSR1 rearrangement detected by NGS (a 3-way fusion between EWSR1, ERG and RBFOX2). This was confirmed by RT-PCR with primers for EWSR1 and ERG.

Conclusions: *EWSR1* break-apart FISH and a targeted AMP-based fusion assay complement each other in detecting known and novel *EWSR1* rearrangements.

58 PRRX1-NCOA1 Gene Fusions In A Series Of Fibroblastic Mesenchymal Neoplasms

Maribel Lacambra[1], Ka-Fai To[1], Kwok-Chuen Wong[2], David Swanson[3], Ilan Weinreb[4], Brendan Dickson[5]
[1]The Chinese University of Hong Kong, Shatin, Hong Kong SAR, [2]Orthopaedic Oncology, Prince of Wales Hospital, Shatin, Hong Kong SAR, [3]Mount Sinai Hospital, Toronto, ON, [4]University Health Network, Toronto, ON, [5]Mount Sinai Health System, Toronto, ON

Disclosures: Maribel Lacambra: None; Ka-Fai To: None; Kwok-Chuen Wong: None; David Swanson: None; Ilan Weinreb: None; Brendan Dickson: None

Background: Angiofibroma of soft tissue is a mesenchymal neoplasm characterized by bland spindle cells set within abundant myxoid-collagenous extracellular matrix, and containing a prominent delicate and thin-walled vasculature. Recently, most cases were found to harbor *NCOA2* rearrangement, with common fusion partners including *AHRR* and *GTF2I*. Herein, we describe a series of unique fibroblastic mesenchymal tumous containing novel *PRRX1-NCOA1* gene fusions.

Design: Retrospective archival reviews were performed at two reference centers – in which targeted RNA-sequencing is routinely used in the diagnosis of bone and soft tissue tumors – for mesenchymal tumors containing *PRRX1-NCOA1* gene fusions. Tumors bearing the fusion gene were reviewed to compare their clinical and pathologic details. The fusion results were independently validated by fluorescence *in situ* hybridization and/or reverse transcriptase-polymerase chain reaction.

Results: Three patients with *PRRX1-NCOA1* gene fusions were identified. The mean age was 44 years (range: 33-55); there were 2 females and 1 male. Two tumors occurred in the neck, and one in the thigh. The average size was 7 cm (range: 3-14 cm). Morphologically somewhat heterogeneous, each of the tumors was vaguely lobulated, and variably cellular. They were comprised of haphazardly arranged spindle-stellate cells with inconspicuous cytoplasm. The nuclei were ovoid and monomorphic; mitotic activity was not conspicuous. Occasional epithelioid cells were interspersed; there was no significant pleomorphism. Each of the tumors contained abundant collagenous-to-myxoid stroma; however, none of the cases contained the prominent thin-walled and branching vasculature. The immunohistochemical findings were non-specific. Two cases were positive for bcl-2, and all were negative for CD34, SMA, S100, EMA, and keratins.

Conclusions: This study establishes a fibroblastic neoplasm characterized by a recurrent *PRXX1-NCOA1* gene fusion. *PRXX1* is a transcription co-activator, with diverse roles including regulating mesenchymal cell fate. The cytologic features in each case was reminiscent of angiofibroma of soft tissue, although all lacked the vasculature prototypic of this entity. While it is possible that fibroblastic neoplasms with *PRXX1-NCOA1* fusions fall on the morphologic and genetic spectrum of angiofibroma of soft tissue, the possibility these may represent a distinct entity cannot be entirely excluded.

59 Conventional Chondrosarcoma with Focal Clear Cell Change: a Clinicopathological and Molecular Analysis

Suk Wai Lam[1], Arjen Cleven[2], Judith Bovee[1], Albert Suurmeijer[3]
[1]Leiden University Medical Center, Leiden, Netherlands, [2]LUMC, Leiden, Netherlands, [3]University Medical Center Groningen, Groningen, Netherlands

Disclosures: Suk Wai Lam: None; Arjen Cleven: None; Judith Bovee: None; Albert Suurmeijer: None

Background: Clear cell chondrosarcoma are known to occasionally contain small areas of (low-grade) conventional chondrosarcoma. However, the opposite phenomenon has not been described yet. In our bone tumor consultation practice we identified five cases of conventional chondrosarcoma alongside areas of clear cell chondrosarcoma. Our main was to report on their histopathological characterization, and to investigate whether these hybrid lesions should be considered a collision tumor, a conventional chondrosarcoma with clear cell change, or clear cell chondrosarcoma with extensive areas of conventional chondrosarcoma.

Design: Histopathological features of both components were characterized. Since ~50% of conventional chondrosarcomas harbor *IDH1* or *IDH2* mutations, the tumors were subjected to mutation analysis for *IDH*, with either Next-generation sequencing (NGS) or Sanger sequencing. In presence of an *IDH* mutation, molecular analysis of *IDH* in the clear cell component followed. Furthermore, as ~7% of clear cell chondrosarcomas have a *H3F3B* mutation, the mutation status of the clear cell component was evaluated, either with NGS or immunohistochemistry.

Results: All five chondrosarcomas consisted predominantly of areas with conventional chondrosarcoma. Different grades were encountered (grade I (n=1), grade II (n=2), and grade III (n=2)). Up to 5% of the tumor consisted of classical features of clear cell chondrosarcoma. A gradual merge between both components was observed. Molecular analysis of conventional chondrosarcoma components revealed in two cases an *IDH1* c.395G>T, p.(Arg132Leu) mutation, and in one case an *IDH 1* c.394C>T, p.(Arg132Cys) mutation. Two cases were *IDH* wild-type. In addition, identical *IDH1* mutations were present in the microdissected clear cell areas of all *IDH* mutant cases (100%). None of the clear cell components harbored *H3F3B* mutations. High grade tumors had an aggressive course, as three patients died of the disease.

Conclusions: Clear cell chondrosarcoma alongside conventional chondrosarcoma is a rarely encountered phenomenon that can puzzle the bone tumor pathologist. Since we identified identical *IDH* mutations in both components and lack of *H3F3B* mutations, and these tumors behaved as would be expected based on the grade, these lesions should be considered conventional chondrosarcoma, with clear cell change. Pathologists should be aware of its existence to avoid confusion with clear cell chondrosarcoma, dedifferentiated chondosarcoma, or chondroblastic osteosarcoma.

60 Utility of FOS and FOSB Immunohistochemistry in Osteoid Osteoma and Osteoblastoma

Suk Wai Lam[1], Arjen Cleven[2], Inge I.H.Briaire-de Bruijn[1], Judith Bovee[1]
[1]Leiden University Medical Center, Leiden, Netherlands, [2]LUMC, Leiden, Netherlands

Disclosures: Suk Wai Lam: None; Arjen Cleven: None; Inge I.H.Briaire-de Bruijn: None; Judith Bovee: None

Background: Osteoid osteoma and osteoblastoma are common benign bone forming tumors. Recently, mainly *FOS* (87%) and to a lesser extent (3%) *FOSB* rearrangements were identified as a recurrent genetic alteration in these tumors. The aim of this study was to evaluate the immunohistochemical expression of FOS and FOSB in these tumors in comparison to other bone forming and giant cell containing tumors of bone.

Design: We performed FOS and FOSB immunohistochemistry on whole-tissue sections from osteoid osteoma (n=23), osteoblastoma (n=23) and osteoblastoma-like osteosarcoma (n=3). Proliferative bone lesions (subungual exostosis (n=3), bizarre parosteal osteochondromatous proliferation (BPOP)(n=5) and myositis ossificans (n=3)) and reactive callus formation (n=3) were also included. Furthermore, immunoreactivity of FOS and FOSB in giant cell tumor of bone (n=74), aneurysmal bone cyst (n=6), chondromyxoid fibroma (n=20), osteosarcoma (n=79), chondroblastoma (n=17), and clear cell chondrosarcoma (n=20) was assessed using tissue micro arrays (TMAs). Positivity was defined as strong nuclear staining in >50% of tumor cells and slides were scored by two observers independently.

Results: Positivity of FOS was observed in all osteoid osteomas (22/22), in 59% of the osteoblastomas (13/22), and in one cases with reactive callus formation (1/3). No osteoblastoma-like osteosarcoma was positive (0/3). Of note, moderate staining in >50% of the cells was seen in 45% of the proliferative bone lesions (3/5 BPOP, 1/3 subungual exostosis and 1/3 myositis ossificans). Evaluation of 179 samples on TMAs revealed one positive osteosarcoma. All other tumors did not show strong and diffuse staining, but rather showed a variable staining pattern. Nine % (2/23) of osteoblastomas were FOSB positive, while no osteoid osteoma (0/22) or osteoblastoma-like osteosarcoma (0/3) was. However, five proliferative bone lesions (4/5 BPOP and 1/3 myositis ossificans) were positive. None of the other 164 samples on TMAs were positive.

Conclusions: Strong and diffuse expression of FOS seems to characterize osteoid osteoma (100%) and a subset of osteoblastomas (55%), while a small percentage (9%) of osteoblastomas strongly expressed FOSB. However, staining in other tumors is variable with extensive FOS and FOSB expression in proliferative bone lesions.This suggests that expression of FOS and FOSB is also upregulated in metaplastic bone in the absence of rearrangements, which can be a pitfall. Further FISH analysis is essential and currently ongoing.

61 Pathology Assessment of Hip Arthroplasty Specimens: An important quality assurance procedure

Lester Layfield[1], Julia Crim[1], Robert Schmidt[2]
[1]University of Missouri, Columbia, MO, [2]Salt Lake City, UT

Disclosures: Lester Layfield: None; Julia Crim: None

Background: The decision to perform hip arthroplasty utilizes both radiographic and clinical findings. Radiologists assess the degree of osteoarthritis (OA) and document other significant findings. Studies have reported frequency of unsuspected findings in arthroplasty specimens but we are unaware of a prior study correlating radiographic (XR) and pathologic (PA) assessment of degree of OA present.

Design: 492 consecutive hip arthroplasties performed between January 2015 and June 2018 with radiographs performed less than 6 months prior to surgery and had subsequent histologic study were reviewed. PA grading used a modified OARSI system. XR/PA agreement was calculated by Cohen's kappa. Findings unrecognized radiographically but recorded pathologically were noted.

Results: 21 cases of osteomyelitis (OM) were diagnosed radiographically or pathologically. Nine discrepancies occurred including 5 false negative RG cases, 3 possible OM by XR (one negative on PA and 2 PA positive) and one false positive on XR but negative by PA and follow-up. Pathology recognized 1 enchondroma and 1 B-cell neoplasm missed on radiographs. One enchondroma was misdiagnosed on radiographs (as PVNS vs. synovial chondromatosis). Twenty-five cases of avascular necrosis were seen pathologically but not radiographically. 35 cases of avascular necrosis were seen on radiograph but not by pathology.

Osteoarthritis was graded on both radiology and pathology from 0-3. The majority of cases (62%) were grade 3. Pathologists and radiologists had perfect agreement in 73% of cases. Weighted agreement was 92% and expected agreement was 78%. There was no statistically significant difference in proportion of cases upgraded or downgraded by pathologists (p=0.34).

Conclusions: Pathologic review of hip arthroplasty specimens revealed 9 significant lesions not recognized radiographically. There were significant discrepancies between radiology and pathology in diagnosis of avascular necrosis. Radiology and pathology showed high levels of correlation for the presence and severity of OA. Radiology is a highly accurate method for assessing the presence and degree of OA preoperatively.

62 A Re-Appraisal of Parosteal Osteosarcoma with Emphasis on Histopathologic Diagnosis: A Single Tertiary Institutional Experience

George Mao[1], Thomas Scharschmidt[2], O. Hans Iwenofu[3]
[1]Columbus, OH, [2]The Ohio State University Wexner Medical Center, Columbus, Ohio, [3]The Ohio State University, Columbus, OH

Disclosures: George Mao: None; O. Hans Iwenofu: None

Background: Parosteal osteosarcoma (POS) is a rare low-grade surface osteosarcoma (OS) characterized by bland hypocellular spindle cell proliferation admixed with anastomosing bone trabeculae. The bone may be woven or cancellous and is disposed in streaming array with pagetoid appearance. The deceptively banal nature may suggest other benign fibro-osseous entities. Prompted by a recent case of an extremely well differentiated calcified mass in the humerus of a young male, with a presumptive clinical diagnosis of a heterotopic ossification, we decided to perform a retrospective review of all cases of POS over a 20 year period with emphasis on re-appraisal of histopathologic features.

Design: All cases with the diagnosis of POS at OSUWMC from 1992 to 2018 were reviewed. Radiographs when available was reviewed. Each specimen was assessed for the following: anastomosing and streaming bony trabeculae (ASBT), pagetoid bone features (PBF), spindle-cell fibroblastic proliferation (SFP), cartilaginous differentiation, cytologic atypia, degree of cellularity and MDM2/CDK4 expression by IHC or FISH.

Results: 22 cases (biopsies/resections) of POS belonging to 12 patients (6 males, 6 females; mean age 21) were reviewed. All patients presented with large exophytic bony masses. The sites of involvement included femur (n=13), humerus (6), tibia (2), ulna (1). 2 patients also had foci of dedifferentiated POS. ASBP, PBF and SFP were present in all cases. 16 cases (73%) contained cartilaginous components, ranging from focal to prominent. 6 (27%) showed minimal atypia, 15 (68%) showed mild to moderate atypia, and 1 case showed severe atypia. 9 (41%) showed low cellularity, 12 (55%) showed moderate cellularity, and 1 case showed high cellularity; cellularity highly correlated with cytologic atypia (r=0.77). 6 of 6 cases had either MDM2 immunoreactivity or amplification. 2 of 3 cases showed CDK4 positivity. Importantly, 3 cases were initially misdiagnosed; 2 cases (similar to the index case) diagnosed as fibro-osseous lesion and 1 case diagnosed as chrondroblastic OS.

Conclusions: POS remains a diagnostic challenge, with an initial misdiagnosis rate of 14%. Prototypic histopathologic features are highly variable, posing a diagnostic challenge particularly in the context of limited biopsy materials. A holistic approach including maintaining a high index of suspicion, radiographic features, careful attention to histopathologic features and confirmatory ancillary testing with FISH-MDM2 will facilitate the diagnosis.

63 Histone H3 K27 Dimethyl Loss is a Specific Marker for MPNST, and Distinguishes True PRC2 Loss from Isolated H3 K27 Trimethyl Loss

Dylan Marchione[1], Amanda Lisby[1], Angela Viaene[2], Mariarita Santi[3], MacLean Nasrallah[1], Erik Williams[4], Ana Larque Daza[5], Ivan Chebib[6], Benjamin Garcia[1], John Wojcik[1]
[1]University of Pennsylvania, Philadelphia, PA, [2]Bryn Mawr, PA, [3]Philadelphia, PA, [4]Boston, MA, [5]Hospital Clinic of Barcelona, Barcelona, Spain, [6]Massachusetts General Hospital, Harvard Medical School, Boston, MA

Disclosures: Dylan Marchione: None; Amanda Lisby: None; Angela Viaene: None; Mariarita Santi: None; MacLean Nasrallah: None; Erik Williams: None; Ana Larque Daza: None; Ivan Chebib: None; Benjamin Garcia: None; John Wojcik: None

Background: Malignant peripheral nerve sheath tumors (MPNST) have loss of function of the polycomb repressive complex 2 (PRC2), causing a global loss of histone H3 lysine 27 trimethylation (H3K27me3). H3K27me3 loss was initially thought to be a sensitive and specific marker for MPNST, but recent reports have identified H3K27me3 loss in other tumors, including H3K27M mutant glioma, Merkel cell carcinoma and a subset of ependymomas. More problematically, researchers have reported that some melanomas and synovial sarcomas show H3K27me3 loss. Since these tumors are in the differential diagnosis of MPNST, H3K27me3 may be insufficient to reliably distinguish between MPNST and histologic mimics. Motivated by our mass spectrometry analysis of histone post-translational modifications in MPNST, which revealed global loss of H3K27 dimethylation (H3K27me2) in addition to H3K27me3, we set out to determine whether loss of H3K27me2 was more specific for MPNST and PRC2 loss.

Design: We conducted immunohistochemical staining for H3K27me2 and H3K27me3 on tissue blocks and microarrays for the following tumor types, reported to have varying degrees of K27me3 loss in prior studies: MPNST (76), Ependymoma (43), Melanoma (40), Synovial

Sarcoma (25), Merkel cell carcinoma (10), K27M glioma (2). Staining was scored from 0-3+ for intensity. Only cases scoring 0 counted as negative. We used mass spectrometry to semi-quantitatively measure histone modifications in a subset of cases (22 total tumors).

Results: H3 K27me3 loss was identified in MPNST (26/76) as well as K27M gliomas (2/2), Merkel cell carcinomas (9/10), ependymomas (21/43) and melanomas (5/40). All synovial sarcomas showed at least partially retained H3K27me3, though staining was of variable intensity. Only MPNST had global H3K27me2 loss (25/76 total cases; Figure 1), indicating ~100% specificity in the study cohort. Moreover, H3K27me2 loss was concordant with H3 K27me3 loss in 25/26 cases. Thus, greater specificity does not come at the cost of greatly reduced sensitivity. H3K27me2 IHC was also more intense in positive cases, with significantly fewer samples scoring 1+ ($p<0.001$, Fisher's exact test; Figure 2), suggesting greater ease of interpretation. Mass spectrometry validated the qualitative IHC results, and demonstrated that global K27me2 loss was limited to MPNST.

Figure 1 - 63

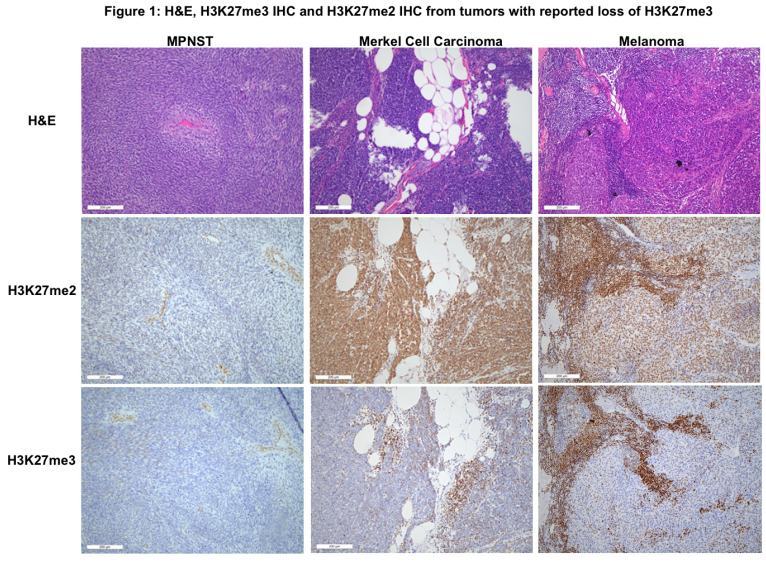

Figure 2 - 63

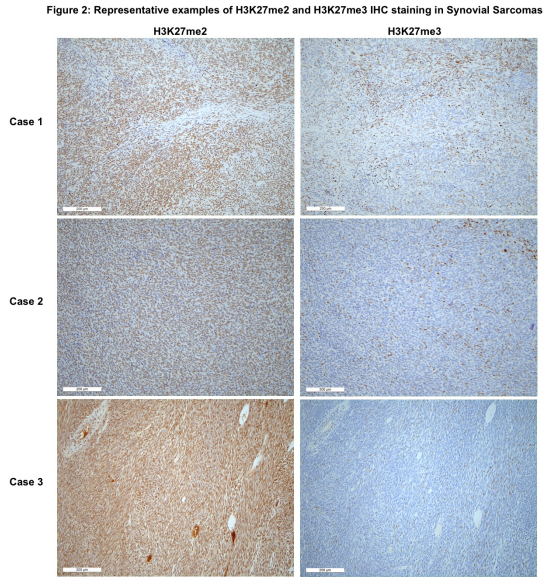

Conclusions: H3K27me2 loss is specific for MPNST and is not seen in other tumors with H3K27me3 loss. It may thus discriminate PRC2 loss from distinct mechanisms of K27me3 dysregulation.

64 Histiocytic Sarcoma: A Case Series with Molecular Analysis by Targeted Next-Generation Sequencing

Lucas Massoth[1], Danielle Kurant[2], Valentina Nardi[3], Vikram Deshpande[3], Abner Louissaint[3], Lawrence Zukerberg[4]
[1]Boston, MA, [2]Brigham and Women's Hospital, Boston, MA, [3]Massachusetts General Hospital, Boston, MA, [4]Auburndale, MA

Disclosures: Lucas Massoth: None; Danielle Kurant: None; Valentina Nardi: None; Vikram Deshpande: None; Abner Louissaint: None; Lawrence Zukerberg: None

Background: Histiocytic sarcoma (HS) is a rare neoplasm with morphologic and immunophenotypic features of mature histiocytes. These tumors exhibit aggressive behavior and carry a poor prognosis. HS belongs to a heterogeneous group of histiocytic neoplasms that show constitutional MAP kinase pathway activation. Prior genetic profiling of HS has primarily identified BRAF alterations including BRAFV600E.

Design: Ten cases of HS were identified based on morphologic features and immunohistochemistry. We performed targeted next-generation sequencing (NGS) on three cases.

Results: The ten patients had an average age of 64 years at time of diagnosis, and 50% were female. Three patients had a history of prior hematologic malignancy. Of patients with follow-up data available, six were dead of disease with an average survival time of 12.3 months. Two patients were alive without recurrence at >5 years. Both had small, localized tumors (tonsil, shoulder).

Common histomorphologic features included enlarged, irregular nuclei and abundant pink cytoplasm. Tumors ranged from an epithelioid to sarcomatoid appearance. All cases were CD68+, while 5/8 were CD163+ and 3/4 were PU.1+. No staining was observed for CD1a, langerin, or dendritic cell markers.

NGS findings included mutations in KIT, KRAS, CREBBP, STAT3, TNFAIP3, and DNMT3A (see table).

Case	NGS mutations	Mutation type
1	KIT (p.His802Tyr)	missense
2	CREBBP (c.3982+1G>A)	splice donor variant
3	KRAS (p.Gly13Asp)	missense
	STAT3 (p.Ile439Asn)	missense
	TNFAIP3 (p.Asn776_Gly777insAsp)	insertion
	DNMT3A (p.Pro162Leu)	missense

Conclusions: HS is an aggressive neoplasm with poor prognosis, but smaller tumors at peripheral sites appear more amenable to treatment. KIT mutations, not previously identified in HS, represent an actionable target for therapy. KRAS mutations have been reported in other histiocytic neoplasms, particularly Rosai-Dorfman disease. Our findings support a more diverse view on the genetic profile of HS, and the possibility of targeted therapy based on patient genomics in some cases.

65 Clinical and Pathologic Characterization of Radiation-Associated Sarcomas

Abbye McEwen[1], Robert Ricciotti[1], Jose Mantilla[1]
[1]*University of Washington, Seattle, WA*

Disclosures: Abbye McEwen: None; Robert Ricciotti: None; Jose Mantilla: None

Background: Radiation therapy is one of the cornerstones of cancer treatment. However, a minority of patients (<1%) are reported to develop secondary malignancies, with sarcomas being the most common histologic type. Due to their rarity, characterization of radiation-associated sarcoma has been limited to primarily case studies and few case series.

Design: In this study, we aim to retrospectively evaluate the clinical and pathologic characteristics of radiation-associated sarcoma at our institution, a high-volume tertiary care center with a comprehensive cancer center. Our pathology laboratory information system was searched for the terms "radiation-associated sarcoma," "radiation-induced sarcoma," and "post-radiation sarcoma." The cases obtained were screened using the following criteria: 1) History of radiation in the same anatomic location, 2) latency interval > 2 years, and 3) histologic diagnosis of sarcoma, distinct from the previous neoplasm.

Results: A total of 73 cases meeting these criteria were identified (67 sarcoma/6 most consistent with sarcoma). These patients included a near equal number of males and females with a mean age of 57 years (range 7-87). The mean latency period between radiation therapy and diagnosis of secondary sarcoma was 13.7 years (range 3-41). [Table 1]. 19% of patients were reported to have at least one additional malignancy.

Most cases (30/67; 45%) demonstrated no specific line of differentiation. Other common subtypes showed osseous, myofibroblast, and smooth muscle differentiation. [Table 2] 67% of cases had a reported histologic grade. Of these cases, the majority were high grade (71%).

The most common sites of secondary sarcoma were chest and trunk (32%), pelvis (21%), and head and neck (15%). The majority of primary neoplasms were carcinomas (64%), including primaries from breast (39%), head and neck (17%), and prostate (11%). [Tables 3 and 4]. Recurrence and metastasis were each reported in 11/73 (15%) patients.

Table 1: Patient Characteristics (N=73)

Age	Mean	Standard Deviation	Median	Range
Mean Age (years)	56.8	19.2	57	7 to 87
Mean Latency Interval (years)	13.7	8.6	11	3 to 41
Gender	Male	Female		
	35	38		

Table 2: Histologic Characteristics (N=67*)

Differentiation	Number of Cases	Percent
Undifferentiated	30	44.8
Bone	11	16.4
Myofibroblastic	10	14.9
Smooth Muscle	8	11.9
Nerve Sheath	4	6.0
Vascular	2	3.0
Skeletal Muscle	2	3.0

*Not including the 6 cases diagnosed as consistent with sarcoma.

Table 3: Sarcoma Location (N=72*)

Site of Sarcoma	Number of Cases	Percent
Chest/trunk	23	31.9
Pelvis/ genital urinary	15	20.8
Head/neck	11	15.3
Skull	7	9.7
Lower extremity	6	8.3
Brain	3	4.2
Spinal/paraspinal	3	4.2
Upper extremity	3	4.2
Other Visceral	1	1.4

*Not including 1 case with unreported location.

Table 4: Original Neoplasm (N=72*)

Primary Neoplasm	Number of Cases	Percent
Carcinoma	46	63.9
Glioneuronal	9	12.5
Sarcoma	8	11.1
Hematologic	6	8.3
Benign Soft Tissue	3	4.2

*Not including 1 case with unreported primary neoplasm.

Table 4: Location of Primary Carcinoma (N=46)

Carcinoma	Number of Cases	Percent
Breast	18	39.1
Head and neck	8	17.4
Prostate	5	10.9
Colorectal	4	8.7
Cervix	3	6.5
Cutaneous	2	4.3
Anal	1	2.2
Endometrial	1	2.2
Esophagus	1	2.2
Lung	1	2.2
Penis	1	2.2
Ovary	1	2.2

Conclusions: Here we describe one of the largest single-institution retrospective studies of radiation associated sarcoma. We show that the majority of these lesions consist of high-grade sarcomas, with the most common type being undifferentiated sarcomas. Prognosis was generally unfavorable, with a high rate of recurrence and metastatic disease. Further studies to understand the risk factors leading to the development of these neoplasms, as well as potential treatment strategies, are necessary.

66 Inflammatory Leiomyosarcoma: Immunohistochemical study of 8 cases with Long-term Follow-up

Michael Michal[1], Brian Rubin[2], Saul Suster[3], Kvetoslava Michalova[4], Petr Steiner[5], Petr Grossmann[6], Marian Svajdler[6], Denisa Kacerovska[7], Ladislav Hadravsky[8], Michal Michal[6]
[1]Charles University and Bioptic Laboratory Ltd. Pilsen, Plzen, Czech Republic, [2]Cleveland Clinic, Cleveland, OH, [3]Medical College of Wisconsin, Milwaukee, WI, [4]Plzen, Czech Republic, [5]Biopticka Laborator SRO, Pilsen, Czech Republic, [6]Biopticka Laborator SRO, Plzen, Czech Republic, [7]Bioptical Laboratory SVO, Pilsen, Czech Republic, [8]Charles University, Prague, Czech Republic

Disclosures: Michael Michal: None; Brian Rubin: None; Saul Suster: None; Kvetoslava Michalova: None; Petr Steiner: None; Petr Grossmann: None; Marian Svajdler: None; Denisa Kacerovska: None; Ladislav Hadravsky: None
Michal Michal: None

Background: Inflammatory leiomyosarcoma (ILMS) is an exceedingly rare soft tissue tumor that usually follows an indolent clinical course, but long-term follow-up studies confirming this clinical behavior are lacking. Recent publications primarily focused on its genetic profile characterized by a near haploidization. ILMS has a very broad differential diagnosis, and since a karyotypic analysis is not technically feasible for most laboratories, morphology and immunohistochemistry (IHC) are the mainstay for classification. However, the IHC features of ILMS, particularly concerning more recently introduced markers such as PAX-7, MDM2 or ALK-1, are unknown.

Design: Eight archival cases of ILMS collected from 3 institutions were stained by a broad IHC panel which contained desmin, smooth muscle actin (SMA), muscle specific actin (MSA), caldesmon, MyoD1, MYF-4 myogenin, myoglobin, PAX-7, MDM2, CDK4, ALK-1, CD21, CD35, CD34, S100, and AE1-3. Intraabdominal tumors were also stained for CD117 and DOG-1 during the initial work-up. All cases were also analyzed by MDM2 FISH. An attempt to perform SNP-array was made but was unsuccessful due to the poor quality of archival tissue. Follow-up data were collected for 6/8 patients.

Results: The clinical details including location are listed in the Table. Patients were 4 men and 4 women, aged 32-75 years (mean: 39). The average tumor size was 7.1 cm (mean:8.5; 2.6-10). Follow-up of 6 patients with an average length of 14.2 years (mean: 16; 3-22 yrs) revealed 1 recurrence and 2 metastases. One patient with an omental tumor that metastasized to the peritoneum and to the pelvic ligaments is free of disease 7 years after surgery and chemotherapy. A second patient underwent surgical treatment of the initial retroperitoneal tumor and had been well for 9 years. He then developed 9 metachronous metastases (8/9 to subcutaneous sites) over the span of 3 years. He is now alive with disease. FISH and IHC results of markers expressed by ILMS are summarized in the Table. The remaining markers were negative in all cases.

Case	1	2	3	4	5	6	7	8
Age/sex	75/F	35/F	40/M	36/M	38/M	66/M	32/F	54/F
Location	Scalp	Omentum	NA	Scapula	Back	Retroperitoneum	Calf	Groin
Size (cm)	10x3.5x1.5	4x4x1	NA	9x7x11	8x5x3.5	9.2 in diam.	2.6x1.8x1.1	NA
Follow-up (length in yrs)	Recurrence (3)	Intraabdominal MTS in the following year (7)	NR (22)	NR (21)	NR (20)	9 MTS occurring 9 years after initial treatment (12)	NA	NA
Desmin	+++	+	+++	+++	+++	+	-	+++
SMA	+	-	-	-	-	+++	+	-
MSA	+++	+	++	+	-	+++	+	NA
Caldesmon	+++	+++	+	++	-	+++	-	-
MyoD1	+++	-	++	+	-	+	-	-
MDM2	-	+	-	-	-	-	NA	-
MDM2 FISH	NA	-	NA	-	NA	-	NA	NA
+ (1-33% of positive cells); ++ (34-66%); +++ (67-100%), NR- no recurrence; MTS – metastases; NA – not analyzable								

Conclusions: Compared to conventional LMS, ILMS has a more indolent behavior. Although metastases may occur, particularly from intraabdominal lesions, 2 patients with metastases are still alive, 3 and 7 years after metastasis. IHC analysis confirmed a myoid phenotype with occasional expression of MyoD1. However, other rhabdomyosarcoma markers, as well as markers of other differential diagnostic entities are negative.

67 Synovial Metaplasia: A Distinct Type of Tissue Repair Induced by a Specific Form of Injury. A Study of 100 cases

Michael Michal[1], Dmitry Kazakov[2], Kvetoslava Michalova[3], Michal Michal[4]
[1]Charles University and Bioptic Laboratory Ltd. Pilsen, Plzen, Czech Republic, [2]Biopticka Laborator SRO, Pilsen, Czech Republic, [3]Plzen, Czech Republic, [4]Biopticka Laborator SRO, Plzen, Czech Republic

Disclosures: Michael Michal: None; Dmitry Kazakov: None; Kvetoslava Michalova: None; Michal Michal: None

Background: Synovial metaplasia (SM) is a change most commonly seen in the tissues surrounding breast prostheses but has also been reported in many other cutaneous or soft tissue sites, usually following a trauma, surgical/orthopedic procedures or implantation of other kinds of foreign materials. Since all available data come from case reports or small case series, it might appear that SM is a rare finding. However, in our experience, SM is a relatively common phenomenon, and the inciting factors are often unknown.

Design: One hundred cases exhibiting SM were collected and studied with a primary focus on the associated conditions. Based on this parameter, cases were divided into primary (idiopathic) and secondary SM. The pathological and clinical diagnosis was recorded for each lesion. Then, we carefully reviewed all cases of primary SM in order to characterize its typical morphological appearance. Regarding the secondary SM, all cases were further subdivided with regard to the associated pathology.

Results: There were 51 females and 49 males, aged 6-80 years (average:47.3). Overall, 46 cases of primary SM were identified. The most commonly affected anatomical sites are listed in the Table. Morphologically, it typically consisted of synovium-lined cyst of various size surrounded by fibrous tissue with abundant neoformed vessels (Figure). In 3 cases (foot 2x, spine 1x), the lesion showed both clinical and morphological signs of aggressive local growth with erosion of the surrounding skeleton, to the point that a malignant tumor was clinically and radiologically suspected. The conditions associated with secondary SM are also listed in the Table.

PRIMARY SM: most commonly affected sites	Number of cases
Hands and feet	19x
Lower extremity (except feet)	12x
Upper extremity (except hands)	6x
The rest (including unexpected sites such as ear, penis, vulva)	9x
SECONDARY SM: most commonly associated conditions	Number of cases (typical examples)
Neoplasms	13x (various forms of lipomas 7x)
Non-neoplastic lesions	17x (rheumatoid nodules, deep granuloma annulare)
Trauma and iatrogenic factors	24x (breast prosthesis 9x, following tumor extirpation 3x, physical trauma 3x)

Figure 1 - 67

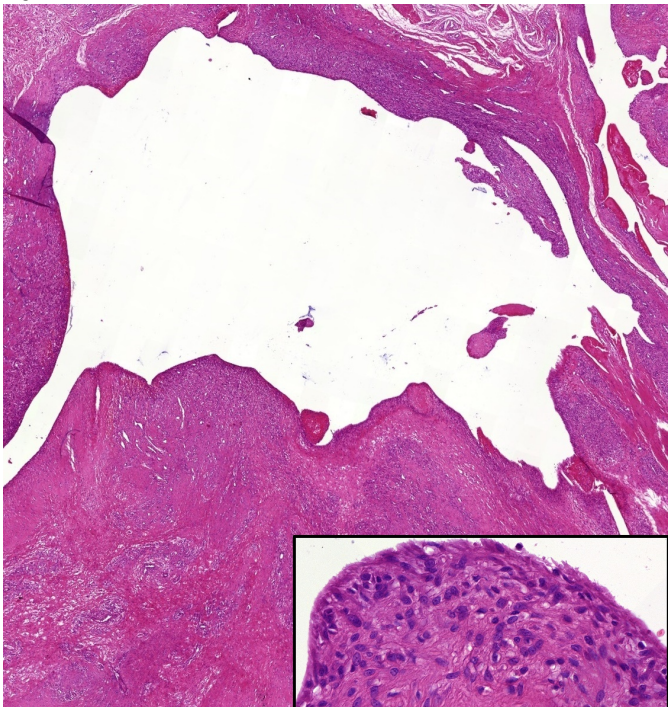

Conclusions: Our study confirms the frequent co-occurrence of secondary SM with various kinds of traumatic or iatrogenic lesions, and also shows its relatively common presence in neoplastic and non-neoplastic disorders. Most importantly, it shows that SM may frequently develop without an evident inciting cause. Although we cannot exclude a local extension of normal synovium in some cases of primary SM, we believe most cases are caused by a minor subclinical trauma. The major factor in both types of SM is the continuous friction which hampers normal healing and further stimulates fibroblastic processes. Irrespective of the cause, primary SM is a mass-forming lesion that causes a diagnostic dilemma, both histologically and clinically. In rare cases, it may show an aggressive growth with a destruction of the surrounding tissues, clinically simulating a malignancy.

68 Spindle cell predominant trichodiscoma or spindle cell lipoma with adnexal induction? A study of 25 cases, revealing a subset of cases with RB-1 heterozygous deletion in the spindle cell stroma

Kvetoslava Michalova[1], Heinz Kutzner[2], Petr Steiner[3], Ladislav Hadravsky[4], Michael Michal[5], Michal Michal[6], Dmitry Kazakov[3]
[1]Plzen, Czech Republic, [2]Dermatopathologie Friedrichshafen, Friedrichshafen, Germany, [3]Biopticka Laborator SRO, Pilsen, Czech Republic, [4]Charles University, Prague, Czech Republic, [5]Charles University and Bioptic Laboratory Ltd. Pilsen, Plzen, Czech Republic, [6]Biopticka Laborator SRO, Plzen, Czech Republic

Disclosures: Kvetoslava Michalova: None; Heinz Kutzner: None; Petr Steiner: None; Ladislav Hadravsky: None; Michael Michal: None; Michal Michal: None; Dmitry Kazakov: None

Background: In our routine and consultative pathology practices, we have noticed that a relatively high proportion of spindle cell predominant trichodiscomas demonstrate a remarkable stromal admixture of adipose tissue which along with spindle cells, prominent collagen bundles and myxoid change closely resembles spindle cell lipoma (SCL).

Design: In order to clarify their possible relationship to SCL, 25 cases of trichodiscoma and fibrofolliculoma with stromal “lipomatous metaplasia” were collected and examined using immunohistochemical stains (CD34 and Retinoblastoma-1 (RB-1) protein) and FISH (*RB-1* deletion).

Results: The patients ranged in age from 35 to 81 years (median 64). The male to female ratio was almost equal (14:11). All tumors with a known location were situated on the face with a special predilection for the nose. All cases were sporadic, with all patients having a single lesion and showing no clinical features of Birt-Hogg-Dubé syndrome. No case with available follow-up presented with a recurrence or an otherwise aggressive clinical course. Spindle cell stroma was immunohistochemically positive for CD34 in 16/20 cases, 18/19 cases showed loss of RB-1 staining in lesional spindle cells. FISH analysis detected *RB-1* heterozygous gene deletion in 6/20 cases.

Conclusions: We conclude that in spite of the spindle cell lipoma-like appearance of the investigated cases, the majority of them supposedly represent genuine spindle cell predominant trichodiscomas with adipose tissue admixture. However, there was a subset of

histopathologically indistinguishable cases with proved *RB-1* deletion which likely represent spindle cell lipoma with trichodiscoma/fibrofolliculoma-like epithelial/adnexal induction rather than spindle cell predominant variant of trichodiscoma.

69 Epithelioid Fibrous Histiocytoma with an Unusual Morphology and Novel ALK Gene Fusions: AP3D1-ALK and COL1A2-ALK

Kvetoslava Michalova[1], Dmitry Kazakov[2], Michal Michal[3], Michael Michal[4]
[1]Plzen, Czech Republic, [2]Biopticka Laborator SRO, Pilsen, Czech Republic, [3]Biopticka Laborator SRO, Plzen, Czech Republic, [4]Charles University and Bioptic Laboratory Ltd. Pilsen, Plzen, Czech Republic

Disclosures: Kvetoslava Michalova: None; Dmitry Kazakov: None; Michal Michal: None; Michael Michal: None

Background: Epithelioid fibrous histiocytoma (EFH) is a distinctive cutaneous neoplasm with a relatively variable morphological picture. Recently, it has been shown that it is molecularly characterized by *ALK* gene fusions. *ALK* is a promiscuous gene with potential to pair with numerous other genes; to date, 10 different fusion partners of *ALK* have been reported only in EFH. The aim of this study was to introduce two novel *ALK* gene fusions and further demonstrate the histological variability of EFH, by reporting an unusual variant with patterned sclerosis.

Design: Two cases of ALK-immunopositive EFHs were assessed for ALK gene rearrangements using a next generation sequencing based assay (FusionPlex Sarcoma Kit, ArcherDx); the detected *ALK* gene rearrangements were further confirmed by FISH.

Results: The main clinicopathological, immunohistochemical and molecular biologic features are summarized in the Table. Both patients were elderly and presented with a solitary lesion on the lower extremity. Histologically, Case 1 showed a proliferation of deeply eosinophilic spindled cells with a prominent sclerosis and storiform/whirling pattern of growth (Figure 1). These zones alternated with hypocellular and myxoid areas which contained scarce epithelioid cells (Figure 2). Case 2 had a more conventional appearance characterized by a predominantly epithelioid population of cells arranged in a vaguely storiform/whirling pattern. Both cases were immunohistochemically positive for ALK and TFE3 and negative for S100, CD34, SMA, desmin, EMA and Glut1. Case 1 was negative for MUC4 and Claudin 1 (not performed in Case 2). Both investigated cases manifested *ALK* gene rearrangements, namely *AP3D1-ALK* (Case 1) and *COL1A2-ALK* (Case 2).

Table. Summary of clinical and pathological features

	Case 1	Case 2
Sex/Age (years)	F/63	M/62
Location	left thigh	left fibula
Size (cm)	2x1.4x1.2	2x1.5x0.7
Gross appearrance	polypoid	polypoid
Predominant cell type	spindled	epithelioid
Predominant stroma type	myxoid hyalinized	hyalinized
IHC ALK	focal and moderate +	diffuse and strong +
Gene fusion	AP3D1-ALK	COL1A-ALK

Figure 1 - 69

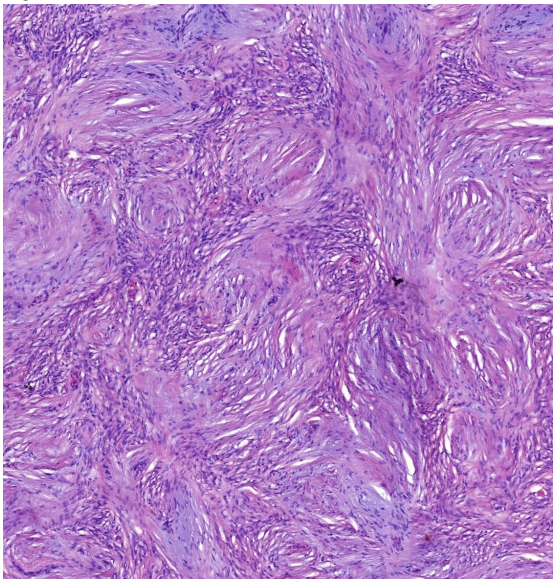

Figure 2 - 69

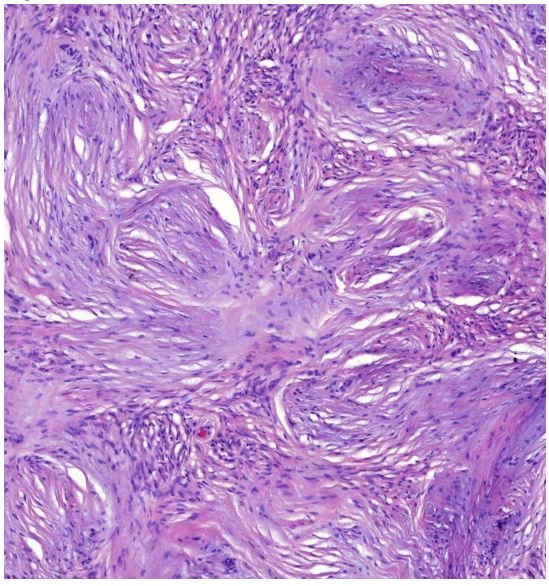

Conclusions: This study introduced two *ALK* gene fusions which have not been previously reported in EFH and extends its histopathologic spectrum, describing the striking sclerosing stroma and storiform/whirling architecture. The awareness of this morphological variant is important since it entertains a wide and slightly different differential diagnosis, which particularly encompasses sarcomas such as low-grade fibromyxoid sarcoma or dermatofibrosarcoma protuberans but also a non-neoplastic lesions such as erythema elevatum diutinum. The consistent ALK expression and continually expanding scale of *ALK* gene rearrangements provide a useful tool to distinguish EFH from its histologic mimics.

70 Expression of HSP70 and VEGF as Potential Markers of Angiogenesis in Dedifferentiated Chondrosarcomas

Virginia Miller[1], Ivy John[2], Karen Schoedel[3]
[1]University of Pittsburgh Medical Center Presbyterian Shadyside, Pittsburgh, PA, [2]University of Pittsburgh Medical Center, Pittsburgh, PA, [3]UPMC-Presbyterian Hospital, Pittsburgh, PA

Disclosures: Virginia Miller: None; Ivy John: None; Karen Schoedel: None

Background: Dedifferentiated chondrosarcomas are aggressive neoplasms with poor outcome. Angiogenesis plays an important role in tumor progression. Several factors influence this process including VEGF and heat-shock proteins. In an effort to elucidate the role of angiogenesis factors in dedifferentiated chondrosarcomas, a cohort of dedifferentiated chondrosarcomas was evaluated for immunohistochemical expression of VEGF and HSP70.

Design: 376 chondrosarcomas were identified from 1997 to 2018 in the institutional archives. A subset of 29 dedifferentiated chondrosarcomas was derived and tissue microarrays were constructed to include both well differentiated and dedifferentiated components. Antibodies against HSP70 and VEGF were applied with appropriate controls using standard methods. Expression of HSP70 was tabulated as nuclear and/or cytoplasmic, intensity (0, 1+, 2+, 3+) and diffuse/ focal staining. Expression of VEGF was evaluated for intensity and diffuse/focal cytoplasmic staining. Results were analyzed by the student t-test.

Results: There were 11 females and 18 males and the most frequent site of involvement was the extremity. VEGF expression was present in both well differentiated and dedifferentiated components. HSP70 demonstrated increased cytoplasmic expression in the dedifferentiated component as compared to the well differentiated areas, p=.001.

Conclusions: Dedifferentiated chondrosarcomas express both VEGF and HSP70. Although VEGF does not show a difference in expression between low grade and dedifferentiated components, HSP70 demonstrates increased expression in the dedifferentiated component. This result appears to be associated with dedifferentiation in these tumors. Both VEGF and HSP70 may play roles in angiogenesis in dedifferentiated chondrosarcomas.

71 Diffuse and Strong Nuclear Localization of Autophagy Marker p62/SQSTM1 Supports the Diagnosis of Desmoid-type Fibromatosis

Toru Motoi[1], Masumi Ogawa[1], Fumie Kakizaki[1], Tomotake Okuma[1], Ikuma Kato[2], Rin Yamada[3], Akiko Tonooka[4], Shin-ichiro Horiguchi[1], Akihiko Yoshida[5], Tsunekazu Hishima[1]
[1]Tokyo Metropolitan Cancer and Infectious Diseases Center Komagome Hospital, Bunkyo-ku, Japan, [2]Yokohama City University Graduate School of Medicine, Yokohama, Japan, [3]Tokyo Metropolitan Cancer and Infectious Diseases Center Komagome Hospital, Honkomagome, Japan, [4]Tokyo Metropolitan Cancer and Infectious Diseases Center Komagome Hospital, Bunkyo-ku, Tokyo, Japan, [5]National Cancer Center Hospital, Tokyo, Japan

Disclosures: Toru Motoi: None; Masumi Ogawa: None; Fumie Kakizaki: None; Tomotake Okuma: None; Ikuma Kato: None; Rin Yamada: None; Akiko Tonooka: None; Shin-ichiro Horiguchi: None; Akihiko Yoshida: None; Tsunekazu Hishima: None

Background: Desmoid-type fibromatosis (DF) is a fibroblastic/myofibroblastic tumor, whose diagnosis could be problematic. Although immunohistochemical detection of nuclear ?-catenin mainly caused by CTNNB1 mutation has been applied for diagnostic workup, the utility can be limited by imperfect sensitivity and specificity. In searching for new diagnostic markers of DF, we explored the use of autophagy markers p62/SQSTM1 and LC3b, based on the known tight association between autophagy and WNT/?-catenin pathway in several tumors.

Design: FFPE samples of 35 DFs were subjected to immunohistochemistry using anti-?-catenin, -p62 and -LC3b antibodies. As controls, a total of 52 tumors were also stained, including 31 fibroblastic/myofibroblastic tumors (12 malignant, 5 intermediate, and 12 benign), 3 cases each of undifferentiated pleomorphic sarcoma, benign fibrous histiocytoma, spindle cell lipoma, intramuscular myxoma, and 1 deep angiomyxoma. The immunoreactivity in the cytoplasm and nucleus was separately evaluated and scored as 2+ when ?50% of cells showed strong reactivity; 1+ when 10-50% of cells showed strong reactivity or ?10% of cells showed a few tiny dots (puncta) for p62 and LC3b; or 0 when <10% of cells showed positivity with any staining pattern. The percentage of reactive cells were calculated in DF by estimating 100 nuclei in a hot spot of each tumor for nuclear ?-catenin and p62.

Results: Strong and diffuse (2+) nuclear positivity of p62 was observed in 28 of 35 DFs (80%), whereas it was present in 6 of 52 non-DFs (12%). When 10% cut-off (1+ and 2+) was adopted, nuclear ?-catenin was positive in 29 of 35 DFSs (83%) and 4 of 52 non-DFs (8%). In distinguishing DFs from non-DFs, nuclear p62 and ?-catenin staining showed comparable sensitivity and specificity statistics. The average percentage of immunopositive cells were higher (63%) for nuclear p62 than nuclear ?-catenin (34%) in DFs. Furthermore, p62 identified 4 DFs that were negative for nuclear ?-catenin. By combined use of these 2 markers, all but 2 DFs were positive for either marker. On the other hand, no significant diagnostic value was found in cytoplasmic p62, ?-catenin, and LC3b expression.

Conclusions: p62 immunohistochemistry is applicable to the diagnosis of DF by its readily recognizable diffuse and strong nuclear positivity. p62 further identifies nuclear-?-catenin-negative DFs which may potentially harbor activated WNT pathway. Nuclear localization of p62 in DF may implicate tumor specific suppression of autophagy.

72 Novel Pathologic-Scoring for Charcot Arthropathy, with Intraneural Observations

Ben Murie[1], Julie Fanburg-Smith[2], Jesse Landon King[3], Donald Flemming[3], Michael Aynardi[3]
[1]Penn State Health Milton S. Hershey Medical Center, Palmyra, PA, [2]Penn State Health Milton S. Hershey Medical Center, McLean, VA, [3]Penn State Health Milton S. Hershey Medical Center, Hershey, PA

Disclosures: Ben Murie: None; Julie Fanburg-Smith: None; Jesse Landon King: None; Donald Flemming: None; Michael Aynardi: *Speaker*, Arthrex

Background: Charcot arthropathy is a destructive joint disorder in patients with longstanding neuropathy, commonly related to Type II diabetes (DM2). The diagnosis is historically classified via the radiologic Eichenholtz staging system (E-score). The purpose of this study is to examine histopathologic features and develop a correlative pathologic score for Charcot.

Design: Patients undergoing lower limb surgery with a clinical diagnosis of midfoot-ankle Charcot were included. Clinical data, radiology, E-score (1-3), and surgical pathology specimens were reviewed, to evaluate skin, adipose, vessel, skeletal muscle, nerve, bone, and bone fragments embedded in synovium. Charcot pathology-score 1 (CPSI) = large bone fragments ($\geq$ half 40x hpf objective) without host histiocytic response. CPSII = mixed large and small bone fragments with/without host histiocytic response, CPSIII = small to minute spicules to almost complete resorption/absence of bone fragments with prominent histiocytic/reactive response, were scored by the authors.

Results: There were 41 patients, 31 M: 10 F, mean age 60.3, median age 61, (range 28-83) years. Clinical risk factors for Charcot included DM2 and longstanding neuropathy. Elevated HbA1C, E-Score, preoperative American Society of Anesthesia score, and Charlson comorbidity index were predictors of amputation. Majority of pathologic specimens examined had superficial ischemic ulceration, dermal fibrosis, cellulitis, medial hypertrophy, atherosclerosis, skeletal muscle atrophy, and nerve hypertrophy with intraneural edema and perineural fibrosis. Osteomyelitis was present in >50%. P-scores CPSI = 6%, CPSII = 44%, CPSIII = 50% correlate with E-scores in 98% of

cases, without interobserver variability. Minor difference from E-score to P-score (2%) was due to sampling. Novel neuropathy change includes observation of intraneural vasculopathy, in all evaluable nerves.

Conclusions: CPS is reliable and reproducible and can be performed with adequate synovial sampling. Charcot progresses from large bone fragments in synovium, to mixed size with histiocytic response, and final small/resorbed fragments with marked host response/fibrosis. Intraneural vasculopathy likely plays a role in Charcot. Charcot P-score correlates with clinicoradiologic E-score.

73 Pathogenetic Implications of Early Growth Response 1 in Ewing Sarcoma

Byeong-Joo Noh[1], Woon-Won Jung[2], Hyun-Sook Kim[2], Yong-Koo Park[3]
[1]Gangneung Asan Hospital, Gangneung-si, Korea, Republic of South Korea, [2]College of Health Science, Cheongju University, Cheongju, Korea, Republic of South Korea, [3]Kyung Hee University, Seoul, Korea, Republic of South Korea

Disclosures: Byeong-Joo Noh: None; Yong-Koo Park: None

Background: Ewing sarcoma (ES) is the second most common primary malignant bone tumor, mainly occurs in children and adolescents, and has an overwhelming mortality. Despite extensive studies, few effective oncogenic signals have been described. Therefore, it is crucial to exploit novel pathognomonic factors and targetable biomarkers for ES patients. Based on previous studies, we speculate that insulin-like growth factor 1 receptor (IGF1R), which is upregulated by early growth response 1 (EGR1), may play a pivotal role in strengthening the downward transmission of IGF1 cascades. Therefore, in this study, we concentrated on determining the pathogenetic contribution of EGR1 in diverse ES cells. This report is the first to study the pathogenic role of EGR1 in ES.

Design: ES cells were cultured and transfected with Stealth RNAi human EGR1 small interfering RNA (siRNA) or negative control. Cell proliferation and invasion potential were measured. mRNA and protein expression of EGR1, IGF1R, and EWS-FLI1 also were assessed.

Results: Cell proliferation and invasive potential decreased significantly in EGR1 siRNA-transfected ES cells. mRNA (Fig. 1) and protein expression for EGR1, IGF1R, and EWS-FLI1 were also significantly reduced in all EGR1 siRNA-transfected cells (SK-ES-1, RD-ES, and HS863.T).

Figure 1 - 73

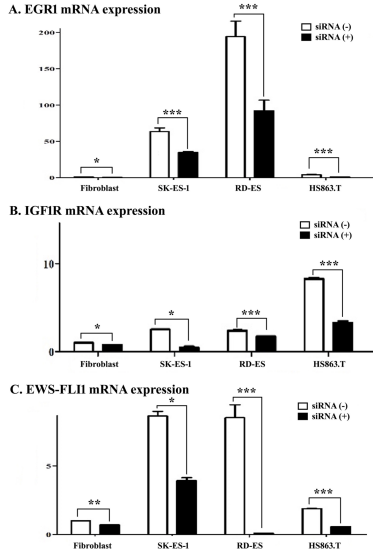

Figure 2 - 73

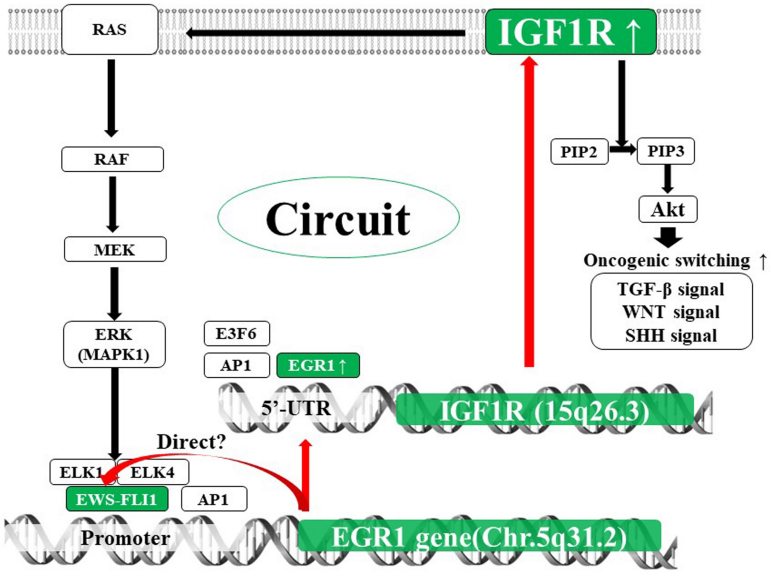

Conclusions: EGR1 upregulated IGF1R expression and enhanced the expression of the oncogenic fusion protein EWS-FLI1. The EWS-FLI1/EGR1/IGF1R cascade combined with the previously reported pathways can form a single circuit, implicating positive feedback for tumorigenesis in ES (Fig. 2). Therefore, EGR1 inhibitors are expected to be useful for the treatment of ES by preventing oncogenic IGF1/IGF1R expression.

74 Sinonasal Glomangiopericytoma: A Clinicopathologic, Immunohistochemical, and Molecular Study

Farres Obeidin[1], Borislav Alexiev[1]
[1]*Northwestern Memorial Hospital, Chicago, IL*

Disclosures: Farres Obeidin: None; Borislav Alexiev: None

Background: Sinonasal glomangiopericytoma (SNGP) is a rare neoplasm arising in the nasal cavity and paranasal sinuses. Initially described as a variant of hemangiopericytoma due to the presence of prominent vasculature seen in other soft tissue hemangiopericytoma, immunohistochemical studies have demonstrated a perivascular myoid differentiation. The diagnosis of SNGP may be diagnostically challenging due to a large number of potential morphological and immunohistochemical mimics in this location, including solitary fibrous tumor, synovial sarcoma, myopericytoma, glomus tumor, and biphenotypic sinonasal sarcoma.

Design: In the present study, we sought to characterize the histological and molecular features of six cases of SNGP found in prior surgical pathology records over a 15-year period. The average age at diagnosis was 48.5 years (range: 31-78 years), and the male-to-female ratio was 1:1. All cases were stained for SMA, ?-catenin, CD34, CD99, cyclin D1, desmin, AE1/AE3, SOX10, and TLE1. Molecular analysis for *CTNNB1* amplifications and *SS18-SSX* translocations were performed.

Results: Imaging studies in all six cases demonstrated avidly enhancing, lobulated soft tissue masses in the nasal cavity, extending into the sinuses and nasopharynx. Histologically, the tumors were unencapsulated and composed of a proliferation of closely packed, bland, and uniform spindle cells growing deep to an intact surface respiratory epithelium. The cells were separated by a distinctive vascular network ranging from capillaries to large vascular spaces. All cases demonstrated perivascular myoid differentiation by immunohistochemistry. Additionally, TLE1 was positive in all cases which has not previously reported (Table 1). Targeted sequencing revealed recurrent *CTNNB1* missense mutations in all cases tested while no tested cases harbored *SS18* translocations.

Table 1. Immunohistochemical findings

Case	1	2	3	4	5	6
SMA	+	+	+	+	+	+
?-catenin	+	+	+	+	F+	+
CD34	+	F+	F+	F+	-	F+
CD99	+	+	+	+	+	+
Cyclin D1	+	+	+	+	+	F+
TLE1	+	+	+	+	+	+
Desmin	-	-	-	-	-	-
AE1/AE3	-	-	-	-	-	-
SOX10	-	-	-	-	-	-
S100	-	-	-	-	-	-
STAT6	-	-	-	-	-	-
- (negative, <10%); F+ (focal positive, 10 – 25%); + (diffuse positive, >25%)						

Conclusions: We found that TLE1 is nonspecific in this differential as all cases of SNGP were positive. However, while no single marker resolves immunohistochemical overlap between sinonasal glomangiopericytoma and its histologic mimics, an extended immunohistochemical panel that includes ?-catenin, cyclin D1, STAT6, smooth muscle actin, pan-cytokeratin cocktails, S100, and SOX10 helps to support the diagnosis of sinonasal glomangiopericytoma without the need for molecular studies.

75 Radiation associated sarcomas demonstrate H3K27me3 loss

Gauri Panse[1], Ingram Ingram[2], Samia Khan[2], Khalida Wani[2], Alexander Lazar[2], Wei-Lien Billy Wang[2]
[1]*Yale University, New Haven, CT,* [2]*The University of Texas MD Anderson Cancer Center, Houston, TX*

Disclosures: Gauri Panse: None; Ingram Ingram: None; Samia Khan: None; Khalida Wani: None; Alexander Lazar: None; Wei-Lien Billy Wang: None

Background: Loss of histone H3 K27 trimethylation (H3K27me3) nuclear expression, due to mutations in *SUZ12* or *EED* (components of the polycomb repressive complex 2 or PRC2), has been observed in malignant peripheral nerve sheath tumors (MPNST), including most cases that were radiation-induced. A smaller proportion of radiation associated undifferentiated pleomorphic sarcomas (UPS) also show H3K27me3 loss. The aim of this study was to evaluate the immunohistochemical expression of H3K27me3 in a large, single institutional series of radiation associated sarcomas (RAS) of various subtypes, and to determine its prevalence and clinicopathologic significance.

Design: Slides from a clinically annotated tissue microarray comprising of specimens from patients with RAS were stained with H3K27me3 antibody (Cell Signaling Technology, clone C36B1, 1:200). Loss of expression was defined as less than 5% labeling within the nuclei of tumor cells in the presence of positive internal control.

Results: The cohort included 46 cases of RAS (29 UPS, 9 angiosarcomas, 6 MPNST and 2 osteosarcomas). The patients ranged from 31-82 years (mean 61 years), including 20 males and 26 females. The sites of involvement included head & neck (n=5), trunk (n=30) and extremities (n=11). H3K27me3 loss was observed in 17/46 (37%) cases, and was most frequent in MPNST (6/6 cases), but loss was also seen in subsets of UPS (6/29 cases), angiosarcoma (4/9), and osteosarcoma (1/2). Among radiation associated UPS, there was no significant association between H3K27me3 loss and gender, site or overall survival (p>0.05).

Conclusions: Loss of H3K27me3 expression was observed in 37% cases of RAS in our series. H3K27me3 has limited diagnostic utility in the setting of RAS, as RAS of various subtypes demonstrate loss of expression. Loss of H3K27me3 did not show significant association with clinical outcome in radiation associated UPS.

76 Pericytoma with t(7;12) and ACTB-GLI1 Fusion Involving the Musculoskeletal System and Ovary: A Report of Three Cases

Andre Pinto[1], Darcy Kerr[2], Breelyn Wilky[3], Matthew Schlumbrecht[4], Cristina Antonescu[5], Andrew Rosenberg[4]
[1]University of Miami, Miami Beach, FL, [2]Dartmouth-Hitchcock Medical Center and Geisel School of Medicine at Dartmouth, Hanover, NH, [3]University of Miami Sylvester Comprehensive Cancer Center, Miami, FL, [4]University of Miami Miller School of Medicine, Miami, FL, [5]Memorial Sloan Kettering Cancer Center, New York, NY

Disclosures: Andre Pinto: None; Darcy Kerr: None; Breelyn Wilky: None; Matthew Schlumbrecht: None; Cristina Antonescu: None; Andrew Rosenberg: None

Background: The entity “pericytoma with t(7;12)” is a rare perivascular myoid neoplasm that is classified within the family of myopericytic tumors. It shows distinctive morphological features and demonstrates t(7;12)(p22;q13) translocation with resultant *ACTB-GLI1* fusion. Thus far, only 7 cases have been reported in the literature, and biologically the tumor tends to behave in a benign fashion.

Design: We prospectively identified 3 cases of pericytoma involving the musculoskeletal system and ovary. The main histopathologic features, immunohistochemical and molecular results were reviewed.

Results: The tumors arose in female adults (41, 57 and 66 years-old) and involved the proximal tibia and adjacent soft tissues, pelvis (ischio-rectal region) and ovary. All tumors were composed of ovoid-to-spindle cells, frequently perivascular in distribution, with alternating areas of hypo and hypercellularity. The cells showed scant cytoplasm, vesicular chromatin and small nucleoli. Many delicate, branching blood vessels were seen. The case that occurred in the tibia showed histologic features of malignancy (necrosis, lymphovascular invasion and increased mitotic activity). This tumor was locally aggressive but no metastatic disease was found. The other two tumors were well circumscribed and lacked aggressive histological features. By immunohistochemistry, all tumors stained for SMA and CD99 (patchy), with variable staining for desmin (1/3), S-100 (1/3), EMA (2/3) and pan-keratin (1/3). Two cases (2/3) harbored the *ACTB-GLI1* gene fusion detected by next generation sequencing, while the pelvic tumor had a non-informative result. The patient with tibial tumor had surgical resection and received chemotherapy, having no evidence of disease (NED) after 9 months; the patient with pericytoma involving the ovary has NED 8 months post-surgery. No information was available on the patient with the pelvic tumor.

Conclusions: This study expands the number of cases of this exceedingly rare mesenchymal neoplasm. Pathological features suggestive of its diagnosis include the presence of vascular-rich stroma, alternating cellularity and positivity for SMA by immunohistochemistry. Histologic features of malignancy, although less common, do not exclude the diagnosis. To date, no tumor has been reported to metastasize, and very few have exhibited malignant histological features. Additional cases and longer follow up are needed to better understand its biological potential.

77 Primary Solitary Fibrous Tumors of Bone: A Monocentric Retrospective Analysis of 22 Patients

Alberto Righi[1], Marco Gambarotti[2], Marta Sbaraglia[3], Piero Picci[1], Angelo Dei Tos[4]
[1]Rizzoli Institute, Bologna, Italy, [2]Bologna, Italy, [3]Treviso, Italy, [4]University of Padua, Treviso, Italy

Disclosures: Alberto Righi: None; Marco Gambarotti: None; Marta Sbaraglia: None; Piero Picci: None; Angelo Dei Tos: None

Background: Primary solitary fibrous tumor (SFT) of the bone is exceedingly rare with only few cases described in the literature.

Design: To investigate the clinical relevance of criteria of malignancy developed for SFT of soft tissues, we reviewed all cases of primary bone solitary fibrous tumor treated at our institution. All cases were assessed morphologically immunohistochemically (CD34 and STAT6) and molecularly (*NAB2-STAT6* gene rearrangements by RT-PCR). Survival analysis was carried out using log-rank tests.

Results: Twenty-two cases of primary SFTs of bone were retrieved. Age ranged from 8 to 84 years (median: 50 years), with a slight female prevalence (12 female and 10 male). Most lesions were located in the axial skeleton (4 sacrum, 4 pubis, 2 scapula and 1 lumbar vertebra), followed by the lower extremities (5 femur and 3 tibia) and upper extremities (4 humerus). Radiologically, all cases were all lytic, with areas of sclerosis in 2 cases. Mean tumor size was 10.4 cm (range, 5-20 cm). Nineteen patients underwent segmental resection or amputation

with wide/radical margins in 15, intralesional margins in 3 and with marginal margins in one patient. In 3 patients only a biopsy was done, followed by radiation therapy. Thirteen cases showed more than 4 mitotic figures/10 HPF and were associated with high cellularity, cytologic atypia and foci of necrosis. CD34 and STAT6 immunopositivity was observed in 91% and in 95% of cases respectively. RT-PCR analysis was feasible in only two cases that confirmed the presence of *NAB2-STAT6* chimeric transcripts. Five and 10-year disease-free rates were 59% and 28%, respectively. Twelve out of 22 patients died of disease with multiple distant metastasis with a mean of 60 months from diagnosis; 3 patients died of other diseases; one patient was alive with multicentric diseases and the remaining 6 patients were disease-free at last follow-up (mean 255 months). Statistical analysis showed no correlation between disease free-survival and overall survival and all the clinicopathological parameters evaluated (age, gender, tumor size, tumor site, presence of necrosis, pleomorphism, mitosis, margin status and stage).

Conclusions: Criteria of malignancy devised for SFT of soft tissues failed to predict outcome in primary SFT of bone. Aggressive behavior seems to be independent from mitotic count or any other clinical and morphologic feature.

78 Epithelioid hemangioma of bone: clinicopathologic, immunohistochemical, and molecular analysis of 38 cases

Alberto Righi[1], Marta Sbaraglia[2], Costantino Errani[3], Marco Gambarotti[4], Stefania Benini[4], Piero Picci[1], Angelo Dei Tos[5]
[1]Rizzoli Institute, Bologna, Italy, [2]Treviso, Italy, [3]IRCCS Rizzoli Orthopaedic Institute, Bologna, Italy, [4]Bologna, Italy, [5]University of Padua, Treviso, Italy

Disclosures: Alberto Righi: None; Marta Sbaraglia: None; Costantino Errani: None; Marco Gambarotti: None; Stefania Benini: None; Piero Picci: None; Angelo Dei Tos: None

Background: Epithelioid hemangioma of bone remains controversial because of its rarity, unusual morphologic features, and unpredictable clinical behavior.

Design: We investigated the clinical behavior of epithelioid hemangioma of bone in patients diagnosed at a single Institution between 1978 and 2016.

Results: Thirty-eight primary epithelioid hemangioma of bone were retrieved. Males outnumbered females 23 to 15. Age ranged from 12 to 84 years (mean: 39 years). Most tumors occurred in the extremities followed by the trunk. Fifteen patients presented multifocal involvement, restricted to regional location in all but one patient. The mean size of the bone lesions was 4.5 cm (range, 1.4-11 cm). According to morphological, immunohistochemical and molecular features, 30 classic variants and 8 cellular variants of epithelioid hemangioma were recognized. Morphologically, all classic epithelioid hemangiomas showed insignificant cytologic atypia, with focal tumor necrosis detected in three cases. Mitotic rate was less than 2 mitoses/10 HPF in all but two cases. Immunohistochemically, all classic epithelioid hemangiomas were FOSB negative. Conversely, 8 cases (defined as cellular epithelioid hemangiomas based on the presence of solid areas composed of endothelial cells featuring mild to moderate nuclear atypia) exhibited strong nuclear expression of FOSB. Absence of *FOS* gene rearrangement was observed 4 cases where the material was feasible for FISH analysis. All these 38 cases were immunohistochemically negative for CAMTA1 and TFE3. Nineteen patients were treated with intralesional curettage, 13 patients underwent segmental resection with wide margins, and in 5 patients only biopsy of the tumor was performed, followed by radiation therapy or embolization. At follow-up (mean 10 years, range 1-26 years), 4 patients (2 with conventional variant and two with cellular variant) had a local recurrence at 12, 28, 48 and 120 months respectively, but none of patients had a fatal outcome.

Conclusions: Primary epithelioid hemangioma of bone appears as a vascular neoplasm that despite multifocal involvement pursues a benign clinical course. The presence of cellular areas does not seem to affect prognosis.

79 Intimal Sarcoma: a Clinicopathologic and Molecular Analysis of 20 Cases

Marta Sbaraglia[1], Elena Bellan[2], Lucia Zanatta[2], Angelo Dei Tos[3]
[1]Treviso, Italy, [2]University of Padua School of Medicine, Treviso, Italy, [3]University of Padua, Treviso, Italy

Disclosures: Marta Sbaraglia: None; Elena Bellan: None; Lucia Zanatta: None; Angelo Dei Tos: None

Background: Intimal Sarcoma represents a group of exceedingly rare sarcomas accounting for less than 1% of all mesenchymal malignancies. They arise from the subendothelial layer of large systemic arteries, heart and only occasionally from large veins, often showing an endoluminal growth. Amplification of *MDM2*, *PDGFRa* and other tyrosine kinase encoding genes has bene reported in a subset of cases.

Design: All cases diagnosed at our institution as intimal sarcoma between 2008 and 2018 were retrieved. All cases were evaluated morphologically and immunostained for MDM2, smooth muscle actin, myogenin, desmin, h-caldesmon, CD31 and ERG. *MDM2* gene amplification was analyzed by FISH.

Results: Twenty cases were identified. Patients ranged in age from 21 to 81 years old (mean 57). Male to female ratio was 1.5:1. Eleven cases arose from the left atrium, 8 from the pulmonary artery and 1 from the superior vena cava. Thromboembolism and atrial myxoma were the most common initial clinical diagnoses. Invasion of surrounding soft tissue was observed in 3 cases. Morphologically, all but two tumors were composed of atypical spindle cells with multifocal pleomorphism associated with epithelioid areas. Two cases showed high-grade pleomorphic morphology. Mitotic index ranged from 5 to 55 mitoses/2 mm^2. Nine out of 20 cases featured areas of necrosis. A prominent hemangiopericytoma-like vascular pattern was observed in 3 cases. Three cases featured osteochondrogenic differentiation that in one case was also associated with rhabdomyoblastic differentiation, highlighted by myogenin immunopositivity. All cases were negative for CD31 and ERG. Smooth muscle actin was present in half of cases, desmin focally in 15% of cases whereas h-caldesmon was negative. One lesion, composed of cytologically bland spindle cells, relapsed rapidly showing progression to high-grade pleomorphic morphology. MDM2 overexpression was observed in 14 cases, 1 was negative and in 5 was not available. *MDM2* gene amplification was present in all cases overexpressing MDM2. Cerebral and soft tissue metastases were seen in 3 cases. Overall survival ranged between 10 and 40 months (mean 18 months).

Conclusions: 1. Intimal sarcoma represents an exceedingly rare, extremely aggressive mesenchymal malignancy. 2. Heterologous differentiation occurs in 15% of cases. 3. MDM2 gene amplification occurs in a high proportion of cases and represents a potential target for molecular therapy.

80 Recurrent SMARCB1 Inactivation in Epithelioid Malignant Peripheral Nerve Sheath Tumors

Inga-Marie Schaefer[1], Fei Dong[1], Elizabeth Garcia[1], Christopher Fletcher[1], Vickie Jo[2]
[1]Brigham and Women's Hospital, Boston, MA, [2]Brigham and Women's Hospital, Harvard Medical School, Boston, MA

Disclosures: Inga-Marie Schaefer: None; Fei Dong: None; Elizabeth Garcia: None; Christopher Fletcher: None; Vickie Jo: None

Background: Epithelioid malignant peripheral nerve sheath tumors (EMPNST) are a rare variant of MPNST, with distinctive features of diffuse S100 positivity, frequent SMARCB1 loss by immunohistochemistry (IHC), and rare association with NF-1. Some cases arise in a pre-existing epithelioid schwannoma (ESCW), which may also show SMARCB1 loss in 40% of cases. While miRNA-mediated *SMARCB1* silencing has been reported in EMPNST, little is known about the genomic landscape. The aim of this study was to use targeted next-generation sequencing (NGS) to identify recurrent genomic alterations in EMPNST and a subset of ESCW, specifically those targeting the *SMARCB1* tumor suppressor locus at 22q11.23.

Design: 17 EMPNST diagnosed from 2007-2018 were retrieved from consultation and surgical pathology files; 13 had SMARCB1 loss and 4 retained SMARCB1 by IHC (clone 25/BAF47, BD Biosciences). 5 ESCW with SMARCB1 loss were also selected. DNA extracted from FFPE tissue was examined by targeted NGS, interrogating the exonic sequences of 447 cancer-associated genes and 191 introns across 60 genes.

Results: NGS identified *SMARCB1* genomic inactiation in 12/17 (71%) EMPNST and in all 5 (100%) ESCW, correlating with SMARCB1 IHC loss (Table 1). SMARCB1 IHC status and *SMARCB1* alterations were concordant in 16/17 EMPNST. *SMARCB1* inactivation occurred through homozygous deletion (N=8), nonsense (N=7), frameshift (N=2), or splice site (N=2) mutations. 2 EMPNST each harbored 2 concurrent mutations. Chromosome 2q gain was the second most common aberration following 22q deletions, and occurred in 9/17 (53%) EMPNST (including 8 with SMARCB1 loss) and 1/5 (20%) ESCW. *CDKN2A* genomic inactivation was found in 5/17 (29%) EMPNST (including 2 with SMARCB1 loss) and 1/5 (20%) ESCW. Among *SMARCB1* wild-type EMPNST, inactivating mutations of *NF1* and *NF2* were present in 1 case each; 1 case was *BRAF*-mutant and reclassified as melanoma. No cases had *SUZ12 or EED* mutations. EMPNST showed a higher mean number of mutations (5.1 vs 3.8 mutations/Mb) and chromosomal alterations (5.1 vs 1.8) compared with ESCW.

Table 1. SMARCB1 protein expression and genomic correlates in EMPNST and ESCW.

Tumor (N)	SMARCB1 IHC (N)	*SMARCB1* genomic (N)
Epithelioid MPNST (17)	Lost (13)	Homozygous deletion (6) Nonsense mutation (5) Splice site mutation (2) Frameshift mutation (1) None (1)
	Retained (4)	None (4)
Epithelioid schwannoma (5)	Lost (5)	Homozygous deletion (2) Nonsense mutation (2) Frameshift mutation (1)

Conclusions: We identified *SMARCB1* genomic inactivation in 71% of EMPNST and in all 5 ESCW selected, credentialing loss of *SMARCB1* tumor suppressor function as a key oncogenic event in these distinctive lesions. IHC loss of SMARCB1 correlates with *SMARCB1* genomic inactivation (sensitivity 100%; specificity 80%). *SMARCB1* wild-type EMPNST harbor different driver events.

81 Molecular Characteristics of Poorly Differentiated Chordoma

Angela Shih[1], Ivan Chebib[2], Vikram Deshpande[1], Brendan Dickson[3], John Iafrate[1], Gunnlaugur Petur Nielsen[1]
[1]Massachusetts General Hospital, Boston, MA, [2]Massachusetts General Hospital, Harvard Medical School, Boston, MA, [3]Mount Sinai Health System, Toronto, ON

Disclosures: Angela Shih: None; Ivan Chebib: None; Vikram Deshpande: None; Brendan Dickson: None; John Iafrate: *Major Shareholder*, ArcherDx; Gunnlaugur Petur Nielsen: None

Background: Chordoma is a rare malignant tumor of bone with a very high morbidity and mortality. Recently, a subset of tumors with absent INI1 expression, called poorly differentiated chordoma, has been described in pediatric populations with a particularly aggressive clinical course. This study aims to characterize the molecular features of poorly differentiated chordoma.

Design: A total of four cases with a diagnosis of poorly differentiated chordoma were identified with sufficient tissue for molecular analysis. Of these, three cases were sent for array CGH, two cases were sent for SNaPshot, and two cases were sent for RNA-Seq to further characterize molecular abnormalities in these tumors in comparison to conventional chordoma subtypes.

Results: Array CGH of three cases showed that two cases had chromosome 22q loss, but only one of these two cases included deletion of SMARCB1. Two cases also had chromosome 9p loss, including CDKN2A at the edge of the deletion. Only one of the cases showed a complex pattern with chromosomal gains and losses involving twelve chromosomes, similar to the pattern seen in conventional chordoma. Snapshot identified an Rb1 mutation at low allelic fraction in two cases tested. RNA-Seq identified no disease defining gene fusion events.

Conclusions: Pediatric poorly differentiated chordoma has a variably complex chromosomal abnormalities, occasionally with deletions involving SMARCB1 and chromosome 9p as well as Rb1 mutations. No defining translocation could be identified. Based on the molecular findings in this limited number of cases, a subset may represent a distinct type of tumor that does not appear to be genetically related to conventional chordoma. Recognition of this subtype is important because these malignancies should be treated aggressively with multimodality therapy. Further insight into the underlying genetics and biology of these tumors may suggest possible future targeted therapies.

82 Application of NGS in Molecular Pathology for Sarcoma Diagnosis

Irit Solar[1], Lital Tybloom Eliasov[1], Ruth Tzabari[1], Hanoch Goldshmidt[1], Osnat Sher[2]
[1]Tel Aviv Medical Center, Tel Aviv, Israel, [2]Sourasky Medical Center, Tel Aviv, Israel

Disclosures: Irit Solar: None; Hanoch Goldshmidt: None

Background: Sarcomas are malignant mesenchymal tumors arising from soft tissues and bones. Diagnosis of sarcomas can be challenging for pathologists due to the wide diversity of sarcoma subtypes, histologic heterogeneity, morphologic similarities, small core

needle biopsies used for initial diagnosis and limited specificity of certain immunhistochemical staining. Many sarcomas are associated with specific chromosomal translocations, which result in fusion genes encoding chimeric transcription factors or chimeric protein kinases that deregulate transcription and alter signaling pathways, respectively. These fusion genes are used as diagnostic biomarkers for supporting an accurate sarcoma diagnosis. Current standard molecular diagnostic methods for identifying gene fusions include FISH and RT-PCR. Targeted NGS panels are increasingly used for gene fusion identification in FFPE tissues, providing a high throughput technique and a comprehensive supportive tool for sarcoma diagnosis.

Design: We evaluated the utility of two targeted NGS panels for gene fusion identification in FFPE tissues of bone and soft tumors. We tested the capture hybridization-based sequencing panel (Trusight RNA Fusion Panel, Illumina) and the amplicon-based sequencing panel - the Anchored Multiplex PCR (AMP) (Archer FusionPlex Sarcoma kit). 34 excision and core biopsy FFPE specimens of bone and soft sarcoma tumors that were previously demonstrated to be fusion positive by FISH or RT-PCR, were examined by the targeted NGS.

Results: As demonstrated in the figures/table, 91% and 88% concordance with previously tested molecular techniques were detected, using the AMP-based technology and the hybrid capture-based technology, respectively. Both techniques enables identification

.No	Diagnosis	Alternative Test RT-PCR/FISH/Other	Trusight RNA Fusion, Illumina	FusionPlex Sarcoma, Archer
1	Ewing Sarcoma	EWSR1-FLI1	EWSR1-FLI1	EWSR1-FLI1
2	Ewing Sarcoma	EWSR1-FLI1	EWSR1-FLI1	EWSR1-FLI1
3	Ewing Sarcoma	EWSR1-FLI1	EWSR1-FLI1	EWSR1-FLI1
4	Ewing Sarcoma	EWSR1-FLI1	EWSR1-FLI1	EWSR1-FLI1
5	Ewing Sarcoma	EWSR1-FLI1	EWSR1-FLI1	EWSR1-FLI1
6	Ewing Sarcoma	EWSR1-FLI1	EWSR1-FLI1	EWSR1-FLI1
7	Ewing Sarcoma	EWSR1-FLI1	EWSR1-FLI1	EWSR1-FLI1
8	Synovial Sarcoma	SS18-SSX	SS18-SSX	SS18-SSX
9	Synovial Sarcoma	SS18-SSX	SS18-SSX	SS18-SSX
10	Synovial Sarcoma	SS18-SSX	SS18-SSX	SS18-SSX
11	Synovial Sarcoma	SS18-SSX	SS18-SSX	SS18-SSX
12	Synovial Sarcoma	SS18-SSX	SS18-SSX	SS18-SSX
13	Synovial Sarcoma	SS18-SSX	SS18-SSX	SS18-SSX
14	Alveolar Rhabdomyosarcoma	PAX3-FOXO1	PAX3-FOXO1	PAX3-FOXO1
15	Alveolar Rhabdomyosarcoma	PAX3-FOXO1	PAX3-FOXO1	PAX7-FOXO1
16	Myxoid Liposarcoma	FUS-DDIT3	FUS-DDIT3	FUS-DDIT3
17	Myxoid Liposarcoma	FUS-DDIT3	FUS-DDIT3	FUS-DDIT3
18	Myxoid Liposarcoma	FUS-DDIT3	FUS-DDIT3	FUS-DDIT3
19	Myxoid Liposarcoma	FUS-DDIT3	FUS-DDIT3	FUS-DDIT3
20	Myxoid Liposarcoma	FUS-DDIT3	FUS-DDIT3	FUS-DDIT3
21	Myxoid Liposarcoma	FUS-DDIT3	FUS-DDIT3	EWSR1-DDIT3
22	Solitary Fibrous Tumor	NAB2-STAT6	NAB2-STAT6	NAB2-STAT6
23	Dermatofibrosarcoma Protuberans	COL1A1-PDGFB	COL1A1-PDGFB	COL1A1-PDGFB
24	Extraskeletal Myxoid Chondrosarcoma	EWSR1-NR4A3	EWSR1-NR4A3	EWSR1-NR4A3
25	Angiomatoid Fibrous Histiocytoma	EWSR1-CREB1	EWSR1-CREB1	EWSR1-CREB1
26	Angiomatoid Fibrous Histiocytoma	EWSR1-ATF1	EWSR1-ATF1	EWSR1-ATF1
27	Low Grade Fibromyxoide Sarcoma	FUS-CREB3L2	FUS-CREB3L2	FUS-CREB3L2
28	Infantile Fibrosarcoma	ETV6-NTRK3	ETV6-NTRK3	ETV6-NTRK3
29	Alveolar Rhabdomyosarcoma	PAX3-FOXO1	Not Detected	Not Detected
30	Low Grade fibromyxoide Sarcoma	FUS-CREB3L2		Not Detected
31	Undifferentiated round cell sarcoma	CIC-DUX4	Not Detected	CIC-DUX4
32	Undifferentiated round cell sarcoma	CIC-DUX4	Not Detected	CIC-DUX4
33	Undifferentiated round cell sarcoma	CIC-DUX4		Not Detected
34	Myxoid Liposarcoma	FUS-DDIT3	Not Detected	FUS-DDIT3

of gene fusion whether or not the fusion partner is known and the detection of novel fusions. The turnaround time of the Archer test is shorter, its analysis is more interactive and it reflects unique reads, by using Unique Molecular Identifiers.

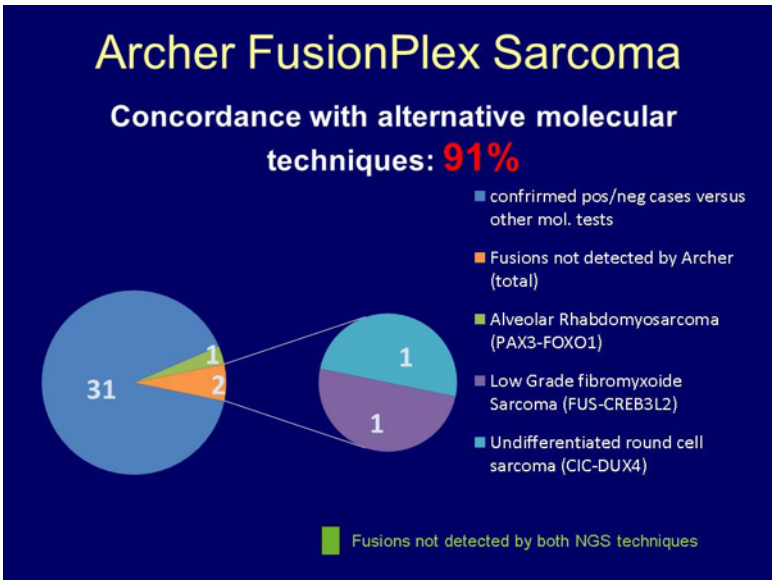

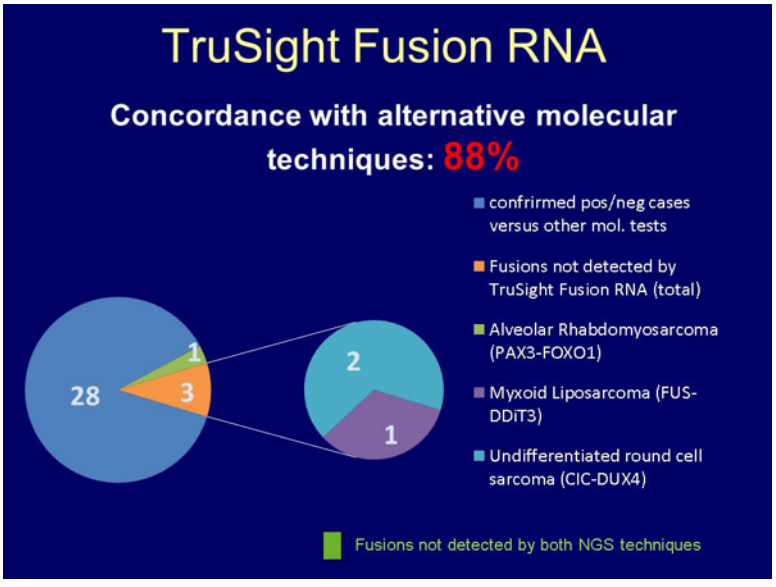

Conclusions: A variety of gene fusions from FFPE tissues of bone and soft tumors were successfully detected using both targeted NGS panels, with similar high sensitivity. We believe that the actual sensitivity is higher, since most of the false negative samples were of low RNA quality. Gene fusions were detected from both core needle and resection specimens. Targeted NGS panels for the detection of gene fusions in FFPE tissues provide a sensitive comprehensive tool for molecular diagnosis of bone and soft sarcomas.

83 Molecular Profiling of Primary and Secondary Bone Lymphomas: Frequent Mutations in EZH2 and other Epigenetic Genes Implicate Germinal-Center B-cell Origin

Sebastiaan Somers[1], Ruben de Groen[1], Ronald van Eijk[1], Tom van Wezel[2], Erik de Winter[2], Hendrik Veelken[2], Patty Jansen[2], Inge I.H.Briaire-de Bruijn[1], Judith Bovee[1], Joost Vermaat[1], Arjen Cleven[2]
[1]Leiden University Medical Center, Leiden, Netherlands, [2]LUMC, Leiden, Netherlands

Disclosures: Sebastiaan Somers: None; Ruben de Groen: None; Ronald van Eijk: None; Tom van Wezel: None; Erik de Winter: None; Hendrik Veelken: None; Patty Jansen: None; Inge I.H.Briaire-de Bruijn: None; Judith Bovee: None; Joost Vermaat: None; Arjen Cleven: None

Background: Diffuse large B-Cell Lymphoma's (DLBCL) with only bone localizations are rare and account for <1% of all DLBCLs. Primary bone lymphoma (PBL) is defined as single bone lesions without or with locoregional lymphadenopathies (Ann Arbor stages IE and IIE), whereas secondary bone lymphoma (SBL) is defined as disseminated disease with single or multiple bone lesions (stage III/IV). To our knowledge molecular profiling of this specific entity has not been performed extensively yet. This study aims to unravel the mutational constitution of this rare DLBCL subtype.

Design: Fresh frozen bone material was available for 15 patients diagnosed between 2003 and 2018. DNA was extracted by using a kit for genomic DNA (Wizard kit, Promega). A validated targeted Next Generation Sequencing (NGS) panel of 52 lymphoma-relevant genes was developed based on an extensive literature study including recent whole exome sequencing studies. Sequencing was performed at the Ion Torrent S5. These findings were correlated with clinicopathologic characteristics.

Results: In this cohort a total of 8 PBLs and 7 SBLs were included. Mutations were identified in 32 genes, of which the majority was involved in the epigenetic regulation. High mutation frequencies were found in the following genes: *EZH2*(46,7%), *KMT2D* (33,3%), *PIM1* (33,3%), *CREBBP* (20,0%), *KLHL6* (20,0%), *BCL2* (20,0%) and *TNFRSF14* (13,3%), indicating a Germinal Center B-cell (GCB) origin. Low frequency of mutations was found for genes related to the non-GCB phenotype, such as *MYD88* (6,7%) and *CD79B* (6,7%). *EZH2* mutations were more frequently observed in PBL (62.5%) compared to SBL (25%). *KLHL6* mutations were more common in SBL (37,5%) compared to PBL (0%).

Conclusions: Despite small PBL and SBL patient numbers, this study demonstrates a mutational profile with frequently mutated genes involved in epigenetic regulation, implicating a GCB origin according to GCB profiles found in other gene expression studies. Given the high mutation frequencies, EZH2 might be a possible target for novel therapeutic strategies in PBL/SBL patients. Whether mutations in *KLHL6,* known as a tumor suppressor, play a role in the clinically more disseminated SBL patients needs further investigation.

84 EWSR1 Rearranged Small Round Blue Cell Tumors with Variant Fusion Transcripts are Distinct from Ewing Sarcoma and Myoepithelial Tumors

David Suster[1], Melissa Krystel-Whittemore[1], Martin Taylor[2], Valentina Nardi[1], Ivan Chebib[3], Gunnlaugur Petur Nielsen[1], Vikram Deshpande[1]
[1]Massachusetts General Hospital, Boston, MA, [2]Boston, MA, [3]Massachusetts General Hospital, Harvard Medical School, Boston, MA

Disclosures: David Suster: None; Melissa Krystel-Whittemore: None; Martin Taylor: None; Valentina Nardi: None; Ivan Chebib: None; Gunnlaugur Petur Nielsen: None; Vikram Deshpande: None

Background: Tumors previously considered part of the Ewing sarcoma family have recently been shown to harbor various distinct genetic rearrangements including *BCOR*- and *CIC*- fusion transcripts. These non-ETS small round cell tumors (SRCT) with variant translocations have unique immunohistochemical profiles and clinical courses compared to conventional Ewing sarcoma. Here-in we describe 4 *EWSR1*-translocated SRCT with variant non-ETS fusion partners.

Design: Four malignant SRCT with *EWSR1* rearrangement by fluorescence in-situ hybridization were identified. Non-ETS variant fusion partners were determined using next generation sequencing with anchored multiplex polymerase chain reaction for targeted fusion transcript detection. Their morphologic, immunohistochemical, and clinical features were evaluated.

Results: There were 2 males and 2 females aged 31 to 57 years. Of the four cases, two were located within bone and two were in soft tissue. Histologically, the tumors were composed of a monotonous population of predominantly small round blue cells (2 cases) or spindled to ovoid shaped cells (2 cases). The tumors displayed predominantly high mitotic activity (up to 93 mitoses/10 HPF), necrosis, and all cases showed a dense hyalinized/fibrotic background stroma. Tumors with variant fusion transcripts but with clear evidence of myoepithelial differentiation were excluded from the study. By immunohistochemistry the tumors showed a polyphenotypic profile (See table 1). Fluorescence in-situ hybridization performed on 4/4 cases showed an *EWSR1* rearrangement. Next generation sequencing identified four non-ETS fusion transcripts including: *EWSR1-PATZ1* (2 cases), *EWSR1-ZNF444* (1 case), and *EWSR1-PBX3* (1 case). Two patients developed widely metastatic disease at 6 years (Case 1) and 6 years (Case 2) and two patients were free of recurrence or disease 3-6 months status post resection (Cases 3 and 4).

Table 1: Patient Characteristics

Case #	Sex	Age	Location	Cell morph	Fusion Product	Epithelial IHC	Myoepithelial IHC	Melanocytic IHC	Rhabdo IHC	CD99 and other IHC	Vascular IHC	Diagnosis before fusion testing
1	M	57	Distal Tibia	Oval-Spindle	*EWSR1-PBX3*	EMA+, Ker-	SMA+	S100-, HMB45-	MuscAct+	CD99-	ERG-	Malignant Myoepithelioma
2	F	31	Peritoneal soft tissue	Oval-Spindle	*EWSR1-PATZ1*	EMA-, Ker-	SMA-	S100+, SOX10+, HMB45-	Desm+, Myog+, MyoD1+, Caldes+	CD99+, GFAP+, WT-1+	CD34+	HG Sarcoma with EWSR1 rearrangment
3	F	53	Pelvic side wall	Round	*EWSR1-PATZ1*	MNF116-, Ker-, EMA-	SMA+	S100+, SOX10+, HMB45-, MITF-	Desm+, MyoD1+, Myog+	CD99+, GFAP+, MDM2-, BCOR-	ERG+, CD34+, CD31+	HG sarcoma with rhabdomyomatous differentiation
4	M	44	Flank mass	Round	*EWSR1-ZNF444*	EMA+, CAM5.2-	SMA+	S100+	Desm+, MyoD1+, Myog-	CD99+, Synap+, BCOR-	FLI1-, CD34-	HG sarcoma with EWSR1 rearrangement

IHC = immunohistochemistry, Ker = keratin AE1/AE3, MusAct = muscle actin, Desm = desmin, Myog = myogenin, Synap = synaptophysin, Caldes = caldesmon, HG = high grade.

Conclusions: The morphologic features, polyphenotypic character and *EWSR1*-non-ETS fusion transcripts support the distinction of these undifferentiated round to spindle cell neoplasms from Ewing sarcoma as well as from conventional myoepithelial tumors. While some tumors displayed genetics previously described in myoepithelial lesions the cases in this study failed to show any morphological evidence of myoepithelial differentiation. We suggest classifying these tumors as fusion-specific SRCT due to their non-ETS fusions and varied immunohistochemical profiles.

85 Novel Recurrent PHF1-TFE3 Fusions in a Subset of Ossifying Fibromyxoid Tumors

Albert Suurmeijer[1], Wangzhao Song[1], Yun-Shao Sung[2], Lei Zhang[2], David Swanson[3], Christopher Fletcher[4], Brendan Dickson[5], Cristina Antonescu[2]

[1]University Medical Center Groningen, Groningen, Netherlands, [2]Memorial Sloan Kettering Cancer Center, New York, NY, [3]Mount Sinai Hospital, Toronto, ON, [4]Brigham and Women's Hospital, Boston, MA, [5]Mount Sinai Health System, Toronto, ON

Disclosures: Albert Suurmeijer: None; Wangzhao Song: None; Yun-Shao Sung: None; Lei Zhang: None; David Swanson: None; Christopher Fletcher: None; Brendan Dickson: None; Cristina Antonescu: None

Background: Ossifying fibromyxoid tumor (OFMT) is an uncommon mesenchymal neoplasm of uncertain differentiation and intermediate biologic behavior. Although diagnostic criteria for classic OFMTs have been established, which often include an incomplete peripheral shell of bone, immunoreactivity for S100 and *EPC-PHF1* fusions, the diagnosis of atypical or malignant tumors remains challenging.

Design:

We searched our files for OFMT with either unknown genetic abnormalities or tumors with PHF1 rearrangements, but lacking a known gene partner. A combined molecular approach, including targeted RNA Seq and fluorescence in situ hybridization (FISH) was used to identify fusion candidates. Tumors were examined for worrisome histologic features and all cases were tested by IHC for TFE3, desmin, and S100. Clinical follow-up was retrieved where available.

Results: We identified 5 OFMTs with PHF1-TFE3 fusions in 3 males and 2 females, median age 64 years (range 62-70 years). One OFMT originated in the scapula, 4 occurred in the deep soft tissues (gluteal muscle, thigh, abdominal wall and cervical paraspinal). Median tumor size was 10 cm (range 5.2-19 cm). All tumors had morphological features compatible with OFMT. In 2 cases only needle biopsies were available. The 3 resected tumors showed an increased mitotic activity (2-6 mitoses in 2mm2). All 5 tumors showed diffuse nuclear staining for TFE3. Desmin was positive in three cases, whereas none showed S100 expression. The PHF1-TFE3 fusions were detected by RNA-Seq in 3 cases and further confirmed by FISH. In the remaining 2 cases, PHF1 and TFE3 gene rearrangements were detected by FISH alone, using both break apart and fusion assays. Follow-up was available in all but one recent case. Three patients developed lung metastases or regional metastases (2 at presentation, one after 2 years). Of the 4 patients with follow-up one died of disease one year after diagnosis, while the remaining 3 are alive with disease six months, two years, and ten years after clinical presentation.

Conclusions: We report novel recurrent PHF1-TFE3 fusions in a subset of OFMT with aggressive behavior, including local recurrences and distant metastases. Although morphologically the tumors had features in keeping with OFMT, none showed areas of ossification, and

all were negative for S100 protein. Our results add OFMT to the list of tumors driven by TFE3 oncogenic activation through recurrent gene fusions, and TFE3 immunoreactivity can be used as a screening tool for this genetic abnormality.

86 Fibro-Osseous Pseudotumor of Digits and Myositis Ossificans Show Consistent COL1A1-USP6 Rearrangement: A Clinicopathological and Genetic Study of 27 Cases

Marian Svajdler[1], Michael Michal[2], Petr Martinek[1], Zdenek Kinkor[3], Michal Michal[1], Peter Szepe[4], Roman Mezencev[5], Peter Švajdler[6]
[1]Biopticka Laborator SRO, Plzen, Czech Republic, [2]Charles University and Bioptic Laboratory Ltd. Pilsen, Plzen, Czech Republic, [3]Biopticka Laborator, Plzen, Czech Republic, [4]University Hospital Martin, Martin, Slovakia, [5]School of Biological Sciences, Georgia Institute of Technology, Atlanta, GA, [6]University Hospital of Safarik in Kosice, Kosice, Slovakia

Disclosures: Marian Svajdler: None; Michael Michal: None; Petr Martinek: None; Zdenek Kinkor: None; Michal Michal: None; Peter Szepe: None; Roman Mezencev: None; Peter Švajdler: None

Background: Myositis ossificans (MO) and fibro-osseous pseudotumor of digits (FOPD) are localized, self-limiting bone-producing pseudosarcomatous lesions.Traditionally, MO and FOPD were thought to be of non-neoplastic origin, recently however, *USP6* rearrangement was reported as a consistent genetic finding in MO and FOPD, thus expanding the spectrum of clonal "transient" neoplasms harboring *USP6* translocation.*COL1A1* was described as a fusion partner of *USP6* in a subset of MO cases, but the fusion partners of *USP6* in FOPDs have not been reported to date.

Design: We analyzed a series of MO and FOPD cases using next generation sequencing (NGS) to find out whether FOPD cases will show the same genetic change as MO.

Results: The study group consisted of 15 MO and 12 FOPD cases (15 M: 12 F). For MO cases, the median age was 35 years (range 6 – 62 years), and the median age of FOPTD cases was 32 years (range 5 – 64 years). 16 cases were seen in consultation and the tentative diagnosis was provided by the submitting pathologist for 10 cases. In 7 cases, the correct diagnosis was suggested and second preferred diagnosis was proposed in 3 of the 7 cases, including Nora's lesion, extraskeletal osteosarcoma (OSa), and parosteal OSa. Two incorrect diagnoses comprised giant cell tumor of soft tissue and OSa. The rest of the cases was sent to "rule out sarcoma".
Histologically, remarkable morphological overlap between both lesions was documented. Using NGS, 5 of 7 (71.4%) MO cases and 4 of 5 (80%) FOPD cases, which could be analyzed, showed *COL1A1-USP6* fusion. With the exception of one case with breakpoints in *COL1A1* exon 1 and *USP6* exon 3, all fusion transcripts detected were represented by *COL1A1* exon 1 fused to *USP6* exon 1 or 2.

Conclusions: Considering MO and FOPD together as a single entity, 75% of the analyzed cases were positive for *COL1A1-USP6* fusion. In the appropriate clinical and histological context, the confirmation of the *USP6* rearrangement may be useful in establishing the correct diagnosis of MO or FOPD, avoiding overdiagnosis of sarcoma.

87 Grade of Dedifferentiated Liposarcomas Correlates with Survival

Timothy Tay[1], Aye Aye Thike[1], Jiancheng Hong[2], Mohamad Farid[2], Kesavan Sittampalam[1]
[1]Singapore General Hospital, Singapore, Singapore, [2]National Cancer Centre Singapore, Singapore, Singapore

Disclosures: Timothy Tay: None; Aye Aye Thike: None; Jiancheng Hong: None; Mohamad Farid: None; Kesavan Sittampalam: None

Background: Dedifferentiated liposarcomas (DL) range from low grade spindle cell proliferations to high grade pleomorphic sarcomas. Although both low- and high-grade tumors can show marked disparity in morphology, the prevailing thought is that they share the same aggressive behaviour. Some studies, however, suggest that low grade DL with mitotic activity of <5 per 10 high power fields (hpf) do not behave as badly as DL and propose classifying these tumors as cellular variant of well differentiated liposarcoma (CWDL). We investigate if this is true in our cohort.

Design: The primary resections of WDL and DL from patients at a tertiary cancer centre over a 10 year period were reviewed histologically. DL with mitotic activity of <5 per 10 hpf were classified as CWDL while the other DL were graded according to the FNCLCC system. Clinicopathologic parameters including survival data were recorded. Statistical analysis was then performed.

Results: The primary resections of well- and de-differentiated liposarcomas from 88 patients were reviewed. Duration of follow up ranged from 0.3 to 128.6 months (mean 41.4, median 39.7). Size ranged from 2 to 40 cm (mean 17.6, median 17.0). Forty-three tumors (48.9%) were retroperitoneal while 45 tumours (51.1%) were from the extremities. Among the 88 tumors, 45 tumors (51.1%) were DL of which 14 (31.1%) were classified as CWDL, 11 (24.4%) were grade 2 DL and 19 (44.4%) were grade 3 DL. Disease specific-death occurred in 16 patients with DL. Of the 16 patients, 3 (18.7%) had CWDL, 1 (6.3%) had grade 2 DL and 12 (75.0%) had grade 3 DL. Higher tumor grade was associated with shorter overall survival on Kaplan-Meier analysis (p=0.006) which was confirmed by multivariate analysis (p=0.046, HR=4.37, 95% CI: 1.03, 18.47). A lower mitotic count (0-9 per 10 high power fields) and necrosis of <50% also had better overall survival (p=0.015 and p=0.005 respectively) but not on multivariate analysis. Thirteen patients developed metastasis, of which 2 (15.4%) had

CWDL, 3 (23.1%) had grade 2 DL and 8 (61.5%) had grade 3 DL. The two patients with CWDL developed higher grade DL on local recurrence before developing metastasis.

Conclusions: The grade of DL correlates with overall survival indicating that not all DL show the same degree of aggressive behaviour. DL with mitotic activity of <5 per 10 hpf shows a better prognosis than FNCLCC grade 2 and 3 DL and may be considered as FNCLCC grade 1 equivalent tumors or as CWDL.

88 Comprehensive Genomic Profiling of Kaposi Sarcoma

Julie Tse[1], Laurie Gay[2], Jeffrey Ross[3], Vincent Miller[3], Garrett Frampton[4], J. Keith Killian[3]
[1]Boston, MA, [2]Cambridge, MA, [3]Foundation Medicine, Cambridge, MA, [4]Foundation Medicine, Somerville, MA

Disclosures: Julie Tse: *Employee*, Foundation Medicine, Inc.; Laurie Gay: *Employee*, Foundation Medicine, Inc.; Vincent Miller: *Employee*, Foundation Medicine, Inc.; *Advisory Board Member*, Revolution Medicines

Background: The molecular features of Kaposi sarcoma (KS), a malignant vascular neoplasm, have not been widely characterized. We performed a preliminary comprehensive genomic profiling (CGP) study to compare KS in the two subtypes most common in the U.S.: classic and AIDS-related.

Design: 14 cases of histopathologically confirmed KS underwent hybrid capture-based CGP, including RNA-seq for 265 genes in a subset of cases. Tumor mutational burden (TMB, mutations per megabase) was calculated from 1.1MB of sequenced DNA and microsatellite stability (MSI) was determined on the basis of 114 homopolymeric loci. The results were analyzed for all classes of genomic alterations (GA), including base substitutions, insertions and deletions, rearrangements, and copy number alterations (CNA).

Results: All patients were male, with a median age of 43 years (range 24 to 92). HIV status was known in 10 patients: 8 positive (all under age 65) and 2 negative (both over age 65). None were transplant recipients. Based on HIV status, cases were divided into AIDS-related (n=8), classic (n=2), and unspecified (n=4) (Table 1). Classic KS patients were oldest. Primary tumor site included skin (n=12), stomach (n=1), and unknown (n=1). HHV8 immunostain was positive in all 10 cases studied.

The mean histopathologic fraction of tumor nuclei (%TN) was 32% (range 10 – 80) and the mean depth of coverage was 639 reads. Known or likely pathogenic GA were detected in 64% cases. Activating mutations in *KRAS* and inactivating mutations in *TP53* were the most common pathogenic GA (14% each). Others included activating mutations in *NRAS* and inactivating mutations in *CDKN2A*, *NOTCH1*, and *PIK3R1*. CNA (loss of *CDKN2A* and *CDKN2B*) were detected in one case. One case harbored gain of chromosomes 3 and 5. All cases had low TMB (mean 1.4 mut/Mb, range 0 – 5.7), and cases with MSI testing were microsatellite stable (n=9). Gene rearrangements were not detected. HHV8 viral DNA was detected in all cases regardless of subtype, tumor purity, and/or absence of GA load.

	AIDS-related	Classic	Unspecified
Number of Cases (n=14)	8	4	2
Median age (range) in years	43 (24-64)	83 (74-92)	41 (24-71)
Known or likely pathogenic GA	*KRAS* *TP53* *PTPN6* *ASXL1* *TLL2* *PRDM1*	*KRAS* *NRAS* *CDKN2A* *TP53* *NOTCH1* *PIK3R1* *TET2* *CDKN2A loss* *CDKN2B loss* *Chr. 3 gain* *Chr. 5 gain*	*CD36* *HNF1A*
MSI-High	0%	0%	0%
Mean TMB (mut/Mb)	1.4	3.7	0.4
Median TMB (mut/Mb)	1.2	3.7	0
TMB>20 mut/Mb	0%	0%	0%
HHV8 virus detected by IHC	5/5	1/1	4/4
HHV8 virus detected by CGP	8/8	2/2	4/4

Conclusions: KS specimens have a relatively low %TN due to admixed stromal cells; however, sequencing at high depth of coverage can detect GA. KS harbors a mutational profile with few GA, low TMB, MSS, and HHV8 viral DNA. The detection of low TMB is consistent with other virally driven neoplasms, such as the subset of Merkel cell carcinoma harboring polyomavirus. Furthermore, whether classic KS may harbor a higher TMB than AIDS-related KS warrants additional study.

89 EWSR1-NFATC2 Translocation Associated Sarcoma: A Clinicopathological Case Series of a Rare Bone/Soft Tissue Neoplasm

Grace Wang[1], Dafydd Thomas[2], Jessica Davis[3], Tony Ng[4], Andrew Horvai[5], Soo-Jin Cho[5], Rajiv Patel[1], Paul Harms[1], Bryan Betz[6], Jonathan Mchugh[7], David Lucas[8]

[1]University of Michigan, Ann Arbor, MI, [2]University of Michigan Hospitals, Ann Arbor, MI, [3]Oregon Health & Science University, Portland, OR, [4]University of British Columbia, Vancouver, BC, [5]University of California, San Francisco, San Francisco, CA, [6]University of Michigan Medical School, Ann Arbor, MI, [7]University of Michigan Health System, Ann Arbor, MI, [8]Michigan Medicine, Ann Arbor, MI

Disclosures: Grace Wang: None; Dafydd Thomas: None; Jessica Davis: None; Andrew Horvai: None; Soo-Jin Cho: None; Rajiv Patel: None; Paul Harms: None

Background: In recent years, a novel group of small round cell tumors harboring a *EWSR1-NFATC2* translocation with partial immunomorphologic overlap with Ewing sarcoma has been sporadically reported. To our knowledge, there has not been a case series devoted to describing detailed clinicopathologic and immunohistochemical characteristics of this unique group of sarcomas.

Design: Six cases of *EWSR1-NFATC2* sarcoma were identified using reverse transcription polymerase chain reaction (RT-PCR) and fluorescence in situ hybridization (FISH) methods. Immunohistochemical and clinical data is obtained from each patient's electronic medical record.

Results: All six tumors arose in adults and ranged from 2.2 cm to 8.9 cm. Three tumors were primary bone sarcomas of the radius, while the other three were primary soft tissue sarcomas. The tumors were locally destructive. With the exception of one case, the tumors had poor responses to neoadjuvant or adjuvant chemotherapy. All patients underwent primary resection. Demographic, clinical, and outcome data are tabulated below. All six tumors demonstrated *EWSR1-NFATC2* fusion transcript by RT-PCR and/or FISH, as well as amplification of the rearranged *EWSR1* gene by FISH. The tumors showed distinctive histomorphology consisting of monomorphic small round-to-epithelioid cells in anastomosing cords with low nuclear pleomorphism, fine chromatin, scant cytoplasm and abundant myxohyaline to collagenous stroma. Metastatic tumors from two patients showed histologic progression to undifferentiated sarcomas characterized by highly pleomorphic round and spindle cells arranged in sheets and fascicles with frequent mitoses and extensive geographic necrosis. Immunohistochemical staining for CD99 was present in all six tumors and ranged from patchily weak to diffusely strong membranous staining. One tumor had focal cytokeratin staining, while three had patchy EMA staining. All tumors were negative for S100, synaptophysin and desmin. A broader, more comprehensive immunohistochemical panel is underway.

CASE	Age/Sex	Primary site	Local recurrence	Metastasis	Outcome	Follow-up (mo)
1	42/M	Right radius	Yes	Soft tissue, bone	DOD	93
2	67/M	Left radius	No	No	AWOD	14
3	59/M	Peri-clavicular soft tissue	Yes	No	AWOD	144
4	24/F	Gastroc-nemius muscle	No	No	AWOD	23
5	42/M	Right radius	No	Lung	AWD	16
6	32/M	Peri-clavicular soft tissue	No	No	AWOD	24

Conclusions: In sum, *EWSR1-NFATC2* sarcoma is a novel translocation-associated sarcoma with a highly recurrent *EWSR1* fusion amplification that, to our knowledge, has never been reported in other *EWSR1* associated sarcomas. The sarcoma exhibits distinctive histopathologic features, presents as either a primary bone or soft tissue tumor, with predilection for the radius and demonstrates locally aggressive clinical behavior with potential for histologic progression and metastasis.

90 EZH2 Expression in Rhabdomyosarcoma: A Potential Biomarker and Therapeutic Target

Qian Wang[1], Kate Shapiro[2], Yong Lu[2], Kenneth Shroyer[2], Sonya Hwang[2]
[1]Stony Brook, NY, [2]Stony Brook Medicine, Stony Brook, NY

Disclosures: Sonya Hwang: None

Background: Rhabdomyosarcoma (RMS) is the most common soft tissue sarcoma in children under 15 years of age and one of most common soft tissue sarcomas of adolescents and young adults. Prognosis is variable, with survival rates ranging from 95% to 15%, depending on the patient's age, tumor subtype, and other factors. Enhancer of zeste homolog 2 (EZH2) is a histone methyl transferase that represses gene transcription via methylation of Lysine-27 of Histone 3 (H3K27). Its overexpression and prognostic role in different tumor types has been widely investigated. Some studies have found overexpression of EZH2 in rhabdomyosarcoma cell lines and primary tumors when compared to benign skeletal muscle. EZH2 has also been reported to play an important role in maintaining cell proliferation during development and tumorigenesis. In this study, we compare the expression of EZH2 with its downstream product, tri-methylated H3K27, and proliferation marker Ki-67.

Design: We included seven cases of benign skeletal muscle and 18 cases of rhabdomyosarcoma from our institution's archives, including alveolar (5), embryonal (8), unclassified (1), spindle cell (2), and pleomorphic (1) subtypes. One case was a metastatic tumor, unclassified (same patient as the unclassified primary tumor). Immunostains for EZH2, H3K27, and Ki-67 were performed using standard techniques on formalin-fixed paraffin-embedded tissue blocks. Based on a scoring system used in prior studies, the immunostains were evaluated for the presence of nuclear staining, staining intensity (0 negative, 1 weak, 2 strong), and percentage of positive cells.

Results: Strong and diffuse EZH2 staining was observed in all primary and recurrent RMS tumors, but not in metastatic tumor or benign skeletal muscle. Ki-67 expression was similar to that of EZH2; strong and diffuse in tumor cells, but negative or only focally positive in benign tissue. H3K27 expression was strong and diffuse in tumor cells, similar to that of EZH2. However, although EZH2 was not expressed in benign skeletal muscle, strong and diffuse H3K27 expression was retained.

Conclusions: EZH2 is highly expressed in rhabdomyosarcoma and may function independently of H3K27, based on different expression patterns in benign muscle. EZH2 expression was lost in one metastatic lesion, in contrast to the primary tumor, suggesting involvement by another pathway. Our results suggest that EZH2 may be a useful biomarker and potential therapeutic target for rhabdomyosarcoma.

91 Three Novel Genetic Aberrations Involving PLAG1 Gene Leading to Lipoblastoma in Three Different Patients: High Level Amplification, Partial Deletion, And Intrachromosomal Complex Rearrangement Of 8q

Guoliang Wang[1], Jacqueline Batanian[2]
[1]University of Missouri, Columbia, MO, [2]SLU, St. Louis, MO

Disclosures: Guoliang Wang: None; Jacqueline Batanian: *Primary Investigator*, None

Background: Lipoblastoma is a rare benign neoplasm with overlapping histology with other lipomatous tumors. Several genetic aberrations have been reported in lipoblastomas including genetic fusion *PLAG1*-partner, interchromosomal complex rearrangements involving 8q and low level of amplification due to multiple copies of chromosome 8.

Design: In this study, cytogenetical methods including karyotype, array Comparative Genomic Hybridization (Array CGH) and fluorescence in situ hybridization (FISH) were used to investigate three cases of lipoblastoma.

Results: Novel genetic aberrations involving *PLAG1* gene were identified in all three cases (Table 1). Case 1: A high level of *PLAG1* amplification up to 50 copies identified in a 4 year-old girl with recurrence of a right flank mass originally diagnosed as lipoma (Figure 1). Case 2: A partial deletion of *PLAG1* FISH probe showing the 3' signal but not the 5' segment of *PLAG1* in a 17 month- old boy with a retroperitoneal mass. The partial deletion was confirmed by array-CGH which revealed the flanking junction breakpoints are involving the 3'*PLAG1* and 5' *HAS2* genes (Figure 1). Case 3: An insertion of 2q31 into 8q11.2 with an inversion of 8q12 with 8q24 and a translocation of 8q24 with 12q24.1 leading to separation of *PLAG1* FISH probe in a 5 year-old girl with a left back mass (Figure 2).

Table 1. Clinical and cytogenetical data for three lipoblastomas

Case	Age/Sex	Location	Size	Karyotype	FISH	Array CGH
1	4y/F	Right axilla/ right flank	7cm	ND	*PLAG1* amplification (~50 copies)	Normal
2	17m/M	Retroperitoneal	15cm	ND	*PLAG1*partial Deletion	8q12.1q24.13 deletion
3	5y/F	Left back	4.5cm	46,XX,ins(8;2)(q11.2;q31)t(8;2;12)(q24;q31;q24.1)[10]	*PLAG1*separation	Normal

Figure 1 - 91

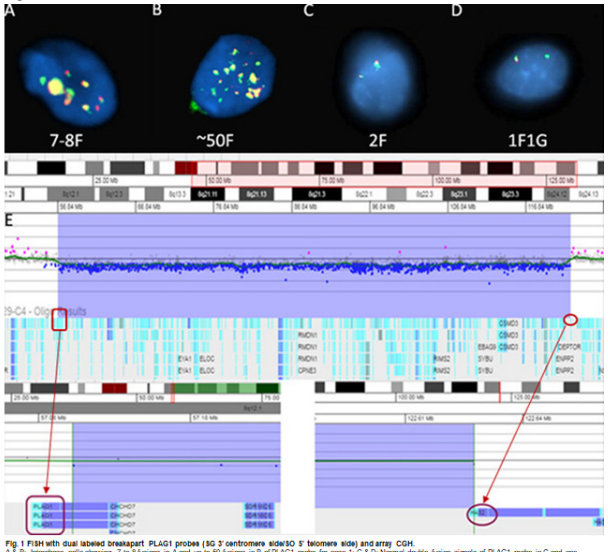

Fig. 1 FISH with dual labeled breakapart PLAG1 probes (5G 3' centromere side/3O 5' telomere side) and array CGH. A & B: Interphase cells showing 7 to 8 fusions in A and up to 50 fusions in B of PLAG1 probe for case 1; C & D: Normal double fusion signals of PLAG1 probe in C and one normal fusion PLAG1 signal and one 3' centromere signal (5G) in D for case 2; E: Array CGH of case 2 revealing a large interstitial deletion of 6q12.1-q24.13 of 65.76 Mb with the junction breakpoints involving PLAG1 and HAS2 genes (highlighted with red rectangle and ovoid shape, respectively).

Figure 2 - 91

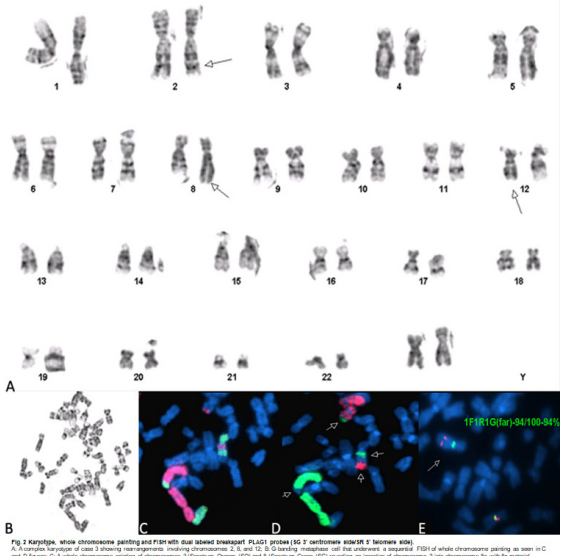

Fig. 2 Karyotype, whole chromosome painting and FISH with dual labeled breakapart PLAG1 probes (5G 3' centromere side/5R 5' telomere side). A: A complex karyotype of case 3 showing rearrangements involving chromosomes 2, 8, and 12. B: G-banding metaphase cell that underwent a sequential FISH of whole chromosome painting as seen in C and D figures. C: A whole chromosome painting of chromosomes 2 (Spectrum Orange (SO) and 8 (Spectrum Green (SG) revealing an insertion of chromosome 2 into chromosome 8q with 8q material translocated onto 2q. D: A whole chromosome painting of chromosomes 2 (SG) and 12 (SO) showing a translocation of 12q into 8q, and 2q to 12q with 2q inserted into 8q. E: Metaphase FISH revealing one normal PLAG1 fusion signal and one separation signal remaining on the long arm of chromosome 8.

Conclusions: In this series of 3 cases of lipoblastoma, we, for the first time, identified a high level amplification of *PLAG1* up to 50 copies, a partial deletion of PLAG1 gene by FISH resulted in *PLAG1-HAS2* gene fusion by array-CGH and a complex translocation involving 8q, 2q and 12q being a new partner. Our novel cytogenetics findings further confirm the importance of *PLAG1* and expand the mechanisms of *PLAG1* transcriptional up-regulation in lipoblastoma pathogenesis.

92 Differential Vascularity in Genetic and Non-hereditary Heterotopic Ossification

Alisha Ware[1], Niambi Brewer[2], Eileen Shore[3], Aaron James[4]
[1]Baltimore, MD, [2]University of Pennsylvania, Philadelphia, PA, [3]University of Pennsylvania Perelman School of Medicine, Philadelphia, PA, [4]Johns Hopkins University School of Medicine, Baltimore, MD

Disclosures: Alisha Ware: None; Aaron James: None

Background: Non-hereditary heterotopic ossification (NHHO) is a common reactive complication of surgery and trauma that causes bone formation in muscle and soft tissues. Progressive osseous heteroplasia (POH) and fibrodysplasia ossificans progressiva (FOP) are rare genetic causes of HO. POH, caused by *GNAS* mutations, involves intramembranous ossification of the skin that progresses to involve the deeper connective tissues. FOP, caused by *ACVR1* mutations, generally spares the skin and causes inflammatory lesions that progress to endochondral ossification of muscle and connective tissues. Previously, we characterized the vascular patterning of NHHO, and demonstrated that dynamic temporal vascular changes accompany maturation of the forming heterotopic bone (Cocks, Hum Pathol 2017). Here, we detail the vascular patterning associated with genetic versus non-hereditary HO.

Design: Vascular histomorphometric analysis was performed on patient samples from POH (n=6), FOP (n=3), and NHHO (n=5). 43-47 random images per diagnostic category were analyzed. Endpoints for analysis included blood vessel (BV) number, area, density, size, and wall thickness. Each image was sub-categorized by phase of HO, including the presence of pre-HO nodular fasciitis (NF)-like areas, early HO woven bone, or more mature lamellar bone containing foci.

Results: Conserved temporal dynamic changes in vascularity were seen across all HO lesions. Immature NF-like areas had the highest blood vessel (BV) number ($p=0.018$), while the more mature foci of lamellar bone had the highest BV area ($p=0.02$). Distinct differences in the degree of vascularity were seen between genetic versus NHHO. In areas of woven bone, POH had the largest BV size, the highest BV area, and highest BV wall thickness when compared to FOP and NHHO ($p<0.01$), while FOP had the highest number of BV ($p<0.001$). With maturation of HO into lamellar bone, these differences in vascularity by diagnostic category were less pronounced.

Conclusions: Both genetic and non-hereditary heterotopic ossification disorders show temporospatial variation in vascularity, suggesting an intimate relationship between osteogenesis and vasculogenesis in these entities. Both POH and FOP show a relative enrichment in vascularity during their evolution in comparison to non-hereditary HO. These findings suggest that angiogenic pathways are potential therapeutic targets in both genetic and non-hereditary forms of heterotopic ossification.

93 Systematic Analysis of GATA3 Expression in 530 Primary Mesenchymal Neoplasms

Christina Wei[1], Greg Charville[2], Gregory Bean[2], Megan Troxell[3], Kimberly Allison[2], Matt Van De Rijn[3], Robert West[4]
[1]Stanford University Medical Center, Palo Alto, CA, [2]Stanford University School of Medicine, Stanford, CA, [3]Stanford University Medical Center, Stanford, CA, [4]Stanford University, Stanford, CA

Disclosures: Christina Wei: None; Greg Charville: None; Gregory Bean: None; Megan Troxell: None; Kimberly Allison: None; Matt Van De Rijn: None; Robert West: None

Background: GATA3 is a transcription factor involved in the development of mammary, salivary, urothelial and hematopoietic tissues. Evidence of its expression by immunohistochemistry (IHC) is used to support the association with aforementioned tissue origins. Occasionally, poorly differentiated mesenchymal-like neoplasms can arise in breast, head and neck and genitourinary sites, especially in the setting of recurrence or post-radiation therapy. Distinguishing de novo primary sarcoma from a metaplastic transformation of the original carcinoma is challenging. However, frequency of GATA3 expression in primary mesenchymal neoplasms is poorly understood. In this study, we systematically evaluated the frequency of GATA3 expression in 530 primary mesenchymal neoplasms.

Design: Multiple tissue microarrays (TMA) were constructed using archived formalin-fixed, paraffin embedded clinical specimens diagnosed and collected from nine medical institutions using the Tissue Arrayer. The slides were stained using a standard clinical protocol (Leica Bond 3 automated IHC) employing a GATA3 monoclonal antibody (clone L50-823), with built-in placental tissue in the TMA serving as positive control. Nuclear staining of GATA3 was evaluated and scored using semi-quantitative five-tiered scale: 0=negative, 1=focal weak staining (<=20%), 2=weak staining (>20%), 3= focal moderate to strong staining (<=20%), and 4=moderate to strong (>20%).

Results: 530 cases of primary benign and malignant mesenchymal neoplasms and their GATA3 expression characteristics are summarized in FIGURE 1. GATA3 positivity is seen more frequently in malignant and high risk neoplasms compared to benign (30/434 versus 0/96). Tumors with anti-GATA3 immunoreactivity include MPNST (16.7%), leiomyosarcoma (8%), undifferentiated pleomorphic sarcoma (4%), malignant and high risk GIST (3.6%) and embryonal rhabdomyosarcoma (2.4%). The reactivity ranges from weak to diffuse strong positive (FIGURE 2).

Figure 1 - 93

TABLE 1. Expression of GATA3 in 530 primary mesenchymal neoplasms in various organ systems

Primary soft tissue neoplasm	Number of Positive/Total Cases	Mean Semiquantative Score in Positive Cases (0-4)*
Embryonal Rhabdomyosarcoma (total)	2/81	4 ± 0
Abdomen/retroperitoneum/pelvis	1/14	
Orbital	1/8	
Extremities	0/15	
Genitourinary (testis, prostate, vagina, bladder)	0/16	
Head and neck	0/24	
Thoracic	0/4	
Fibromatosis	0/43	0
Gastrointestinal stromal tumor (total)	3/102	
Malignant/high risk	3/84	
Intermediate/low risk	0/18	
Uterine leiomyoma (total)	0/17	0
Leiomyosarcoma (total)	12/150	2.0 ± 1.3
Uterus	8/80	
Retroperitoneum/pelvis	2/20	
Gastrointestinal	0/11	
Genitourinary	0/6	
Extremity/chest wall	2/29	
Head and neck/thoracic	0/4	
Peripheral nerve sheath tumor, benign	0/11	0
Peripheral nerve sheath tumor, malignant	12/72	3.1 ± 1.3
Solitary fibrous tumors	0/7	0
Synovial sarcoma	0/22	0
Undifferentiated pleomorphic sarcoma	1/25	4

*Semi-quantitative five-tiered scale: 0 = negative, 1 = focal and weak staining (≤ 20%), 2 = weak staining (>20%), 3 = moderate to strong staining (≤ 20%), and 4 = moderate to strong (> 20%).

Figure 2 - 93

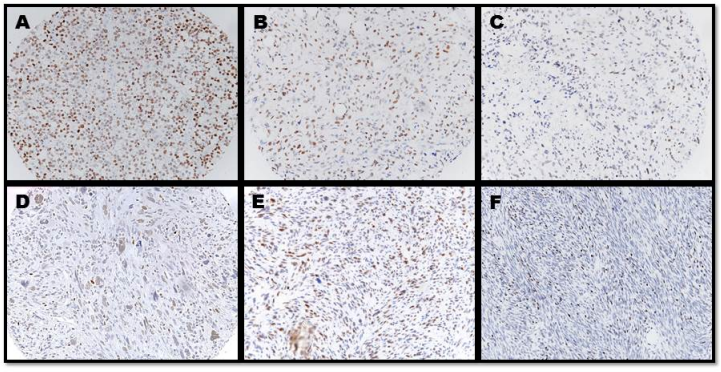

Figures 1: GATA3 expression can be observed in a subset of primary sarcoma in various organ systems. A) Embryonal rhabdomyosarcoma in the abdomen; B) Leiomyosarcoma in the chest wall; C) Leiomyosarcoma in the kidney; 4) Undifferentiated pleomorphic sarcoma in the leg; 5) Malignant peripheral nerve sheath tumor in the extremity; 6) Malignant gastrointestinal stromal tumor in the small intestine. (200X)

Conclusions: Our results demonstrate that GATA3 expression can be found in primary malignant mesenchymal neoplasms, including rare cases with diffuse strong immunoreactivity. This may be a potential diagnostic pitfall in the interpretation of GATA3 in the context of spindle cell neoplasms. In this series, GATA3 expression is observed in higher-grade neoplasms, such as in MPNST and malignant/high risk GIST.

94 Diagnostic utility of pan-TRK immunohistochemistry in inflammatory myofibroblastic tumor

Hidetaka Yamamoto[1], Yui Nozaki[1], Kenichi Kohashi[1], Yoshinao Oda[2]
[1]Kyushu University, Fukuoka, Japan, [2]Fukuoka, Japan

Disclosures: Hidetaka Yamamoto: None; Yui Nozaki: None; Kenichi Kohashi: None; Yoshinao Oda: None

Background: Inflammatory myofibroblastic tumor (IMT) is a spindle cell neoplasm of intermediate malignancy, and the diagnosis is often challenging due to the morphological overlap with reactive lesion or other spindle cell tumors. More than half of IMTs have *ALK* gene rearrangement, and minor subset have *ROS1, NTRK3* or *RET* gene rearrangement. Recently, pan-TRK antibody against NTRK1, 2 and 3 has been developed. Here, we assessed the potential diagnostic utility of pan-TRK immunohistochemistry for IMT.

Design: We examined 40 cases of IMT using immunohistochemistry (IHC) with a rabbit monoclonal pan-TRK antibody. Gene rearrangement was confirmed by fluorescence in situ hybridization (FISH) and/or reverse transcription-polymerase chain reaction (RT-PCR).

Results: Forty IMTs were classified as *ALK* (n=29), *ROS1* (n=2), *NTRK3* (n=2), *RET* (n=0) and "quadruple-negative" (n=7) genotype determined by molecular analyses. Both *ETV6-NTRK3* fusion-positive cases showed nuclear and cytoplasmic staining for pan-TRK in the vast majority of tumor cells. None of *ALK, ROS1* or quadruple-negative type IMTs showed nuclear staining for pan-TRK; however, about one-third of them showed focal and weak cytoplasmic staining. One exceptional case of *RANBP2-ALK* positive epithelioid inflammatory myofibroblastic sarcoma, an aggressive variant of IMT, showed diffuse and moderate cytoplasmic staining for pan-TRK. Other *ETV6-NTRK3* positive tumors such as infantile fibrosarcoma (n=3) and salivary secretory carcinoma (n=23) were also showed nuclear and cytoplasmic staining for pan-TRK.

Conclusions: These results suggest that pan-TRK IHC with nuclear and cytoplasmic staining pattern may be useful to identify *ETV6-NTRK3* positive IMT and may be helpful in selecting patients for TRK-targated therapy.

95 Prognostic impact of the MDM2/HMGA2 ratio and clinicopathological factors in well-differentiated and dedifferentiated liposarcoma

Kyoko Yamashita[1], Kenichi Kohashi[2], Yuichi Yamada[2], Shinya Akatsuka[3], Yoshinao Oda[4]
[1]The Cancer Institute of Japanese Foundation for Cancer Research, Koto-ku, Japan, [2]Kyushu University, Fukuoka, Japan, [3]Nagoya University Graduate School of Medicine, Nagoya, Japan, [4]Fukuoka, Japan

Disclosures: Kyoko Yamashita: None; Kenichi Kohashi: None; Yuichi Yamada: None; Shinya Akatsuka: None; Yoshinao Oda: None

Background: Well-differentiated/dedifferentited liposarcoma (WD/DDLPS) is the most common soft tissue sarcoma, and DDLPS is generally recognized to be less aggressive than undifferentiated pleomorphic sarcoma, although a small part of the patients suffer from distant metastasis leading to poor prognosis. The purpose of this study is to clarify the clinicopathological and genetic factors related to the distant metastasis and poor prognosis in DDLPS.

Design: Clinicopathological factors were examined in 45 DDLPS cases and 6 WDLPS cases, while 32 DDLPS cases and 5 WDLPS cases were analyzed by custom CGH array. This array was designed to densely cover gene regions in the areas known to be frequently amplified in WD/DDLPS (1q21-24, 6q23-24, 12q13-15, 12q23-24, 19q13, and JUN) with a median probe spacing of 590-829 bp at exons and 2.5kb in non-exonic regions. In statistical analyses, the simple Cox model and the log-rank test were used for continuous and categorical variables, respectively ($P<0.05$).

Results: Nine cases showed distant metastases leading to poor prognosis (die of disease or follow-up ended in terminal state), and 8 cases of them were analyzed by the custom CGH array. We detected 17 genes whose amplification (log ratio>2) was related to metastasis and poor prognosis, and 6 genes whose amplification was associated with good prognosis (continuously disease free more than 6 years). MDM2 was included in the former and HMGA2 was in the latter, and the MDM2/HMGA2 ratio of amplification or gain level was significantly related to both overall survival (OS) ($P= 0.028$) and metastasis-free survival (MFS) ($P= 0.041$). Amplification or gain of MDM2 was detected in all cases, while those of HMGA2 was not detected in 3 cases, one of which had distant metastasis and poor prognosis with minimal genomic changes. Among the clinicopathological factors, histological tumor grade was most strongly related to OS ($P= 0.0018$), and degree of inflammatory cell infiltration (none to mild vs severe) and immunoreactivity for MDM2 (weak and focal vs moderate vs strong and diffuse) also tended to be related to OS ($P=0.0718$ and $P=0.0636$, respectively). However, myogenic differentiation estimated by immunoreactivity for aSMA and desmin seemed not to be related to both OS ($P=0.96$ and 0.91, respectively) and MFS ($P=0.42$ and 0.83, respectively).

Conclusions: We showed that high MDM2/HMGA2 ratio of amplification or gain level was significantly associated with both distant metastasis and poor life outcomes in WD/DDLPS.

96 Nonlinear Microscopy: Intraoperative Analysis of Fresh Bony Tissue

Tadayuki Yoshitake[1], James G. Fujimoto[1], Lucas Cahill[2], Seymour Rosen[3], Ashley Ward[3]
[1]Massachusetts Institute of Technology, Cambridge, MA, [2]MIT-Harvard, Cambridge, MA, [3]Beth Israel Deaconess Medical Center, Boston, MA

Disclosures: Tadayuki Yoshitake: None; James G. Fujimoto: None; Lucas Cahill: None; Seymour Rosen: None; Ashley Ward: None

Background: Intraoperative histological evaluation of bone has not been considered possible because of the nature of the tissue. Nonlinear microscopy (NLM) is a versatile laser based imaging technique that enables visualization of tissue similarly to conventional optical microscopy and has been used to examine breast tissues (Cahill et al., 2018). NLM can image freshly excised, intact tissue without the need for physical sectioning and seemed a possible methodology to examine intraoperative bone specimens.

Design: Bone and adjacent soft tissue were stained with fluorescent nuclear (acridine orange) and stromal/cytoplasmic (sulforhodamine) dyes for 2 minutes, rinsed with saline for ~30 seconds, and placed onto a glass window of a specimen holder for NLM imaging. NLM's optical sectioning enables visualization of a thin layer of tissue structure similar to physical sectioning with a cryotome or microtome. Manipulation of the NLM focus depth enables examination of multiple levels within tissue up to ~100 um analogous to serial sectioning. Furthermore, imaging depth can reach up to several mm in sparse tissue regions such as trabecular bone structure. Magnifications range from 5X to 20X and are interchangeable while imaging. The NLM fluorescent signal is displayed with an adjustable H&E equivalent. Individual images can be viewed in real-time like a conventional optical microscope, or can be mosaicked to assemble large montages like a slide scanner. The specimen holder was constructed to hold large intact specimens similar to whole slide imaging as well as small fragments of tissue such as needle biopsies and has ports to add saline and formalin. Formalin fixation does not disturb NLM imaging and afterwards the tissue can be processed as usual, without impairment of ordinary staining.

Results: 10 femoral heads and 4 knee joint specimens obtained during replacement procedures were transected and sagittal sections made and examined by NLM. The basophilic matrix and chondrocytes of articular cartilage were easily assessed. Trabecular bone was recognized, and its three-dimensional construct of the network were visualized up to several mm in depth. Endosteal tissue and synovium were recognized. The marrow elements, adipose and hematopoietic elements could be assessed. Megakaryocytes could be well defined and granulopoeisis was distinguished by the intense granule staining.

Figure 1 - 96

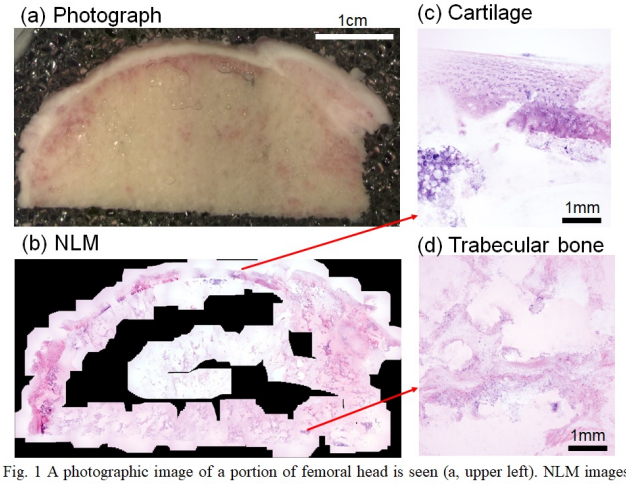

Fig. 1 A photographic image of a portion of femoral head is seen (a, upper left). NLM images were taken of the articular surface and within more central portions of the femoral head. The captured images during real-time evaluation were "stitched" together using a computer program (b, lower left) to show the correspondence with the photograph (a). Higher power images of cartilage (c, upper right) and trabecular bone (d, lower right) are shown.

Figure 2 - 96

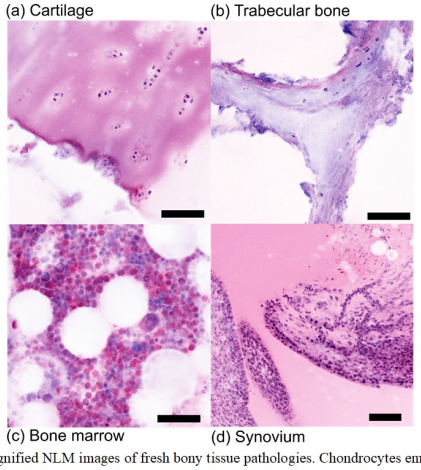

Fig. 2 Magnified NLM images of fresh bony tissue pathologies. Chondrocytes embedded in an acellular hyaline matrix are seen in hyaline cartilage (a, top left). Bone trabeculae containing osteocyte nuclei and lamellae are visible (b, upper right). Megakaryocytes, immature granulocytes and erythrocyte precursors are seen representing mature trilineage hematopoiesis (c, bottom left). Synovium is visualized as villous projections lined by cuboidal epithelium with underlying fibrous tissue containing chronic inflammatory cells and stromal cells (d, bottom right). Scale bars: a 100 um, b 100 um, c 50 um, d 200 um.

Conclusions: The ability to examine fresh bone and adjacent tissues rapidly presents a new paradigm in intraoperative tissue study.

97 Subarticular Pseudo-Abscesses Are Associated with Lymphoplasmacytic Synovitis

Lingxin Zhang[1], Edward DiCarlo[1]
[1]Hospital for Special Surgery, New York, NY

Disclosures: Lingxin Zhang: None; Edward DiCarlo: None

Background: Inflammatory pseudo-abscesses, previously reported as sterile osteomyelitis (O'Connell, 1999), are collections of neutrophils in the subarticular bone in the absence of documented infection. Rheumatoid arthritis (RA) and other inflammatory arthropathies (IA) may have clinical presentations that are not easily distinguished from septic arthritis (SA). This is confounded by the known presence of high numbers of neutrophils in most cases of IA joint effusions. We present histological evidence that these neutrophil collections are associated with synovial inflammation of the type seen in IA.

Design: A retrospective review of the pathology records for cases that had neutrophilic subarticular inflammatory collections reported by the senior author between 1997 and 2015 was performed. Patient demographics, clinical features, and pathologic findings in the synovium and subchondral bone were analyzed.

Results: 161 surgical specimens (140 from large joints and 21 from small joints) were found in 147 patients. The median age was 65 years (12-87 years) and 78% were female. At the time of surgery, 80 patients had a known history of some form of IA (95% RA). Subsequently, 13 more patients were found to have IA or clinical suspicion of IA; 54 patients were not followed in the database.

Microscopically, the articular surface typically showed focal complete loss of the cartilage with sclerosis of the exposed superficial bone – secondary osteoarthritis. The cases, as part of the selection criteria, had subarticular / subchondral cystic regions that contained fibrin, neutrophils, and macrophages (Fig. 1, 10x). In addition, inflammatory synovial pannus was present in 20% of the cases. In 92% of specimens with synovium (155 of 161), the synovium showed hyperplasia of the lining layer with inflammation composed of lymphocytes, plasma cells, and exudative neutrophils without necrosis or granulation tissue (Fig. 2, 40x). Bi-nucleate plasma cells and Russell bodies were common.

Figure 1 - 97

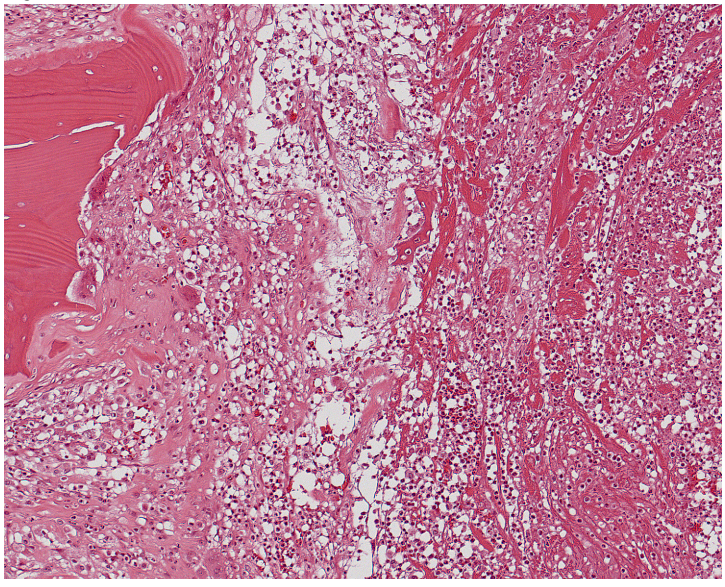

Figure 2 - 97

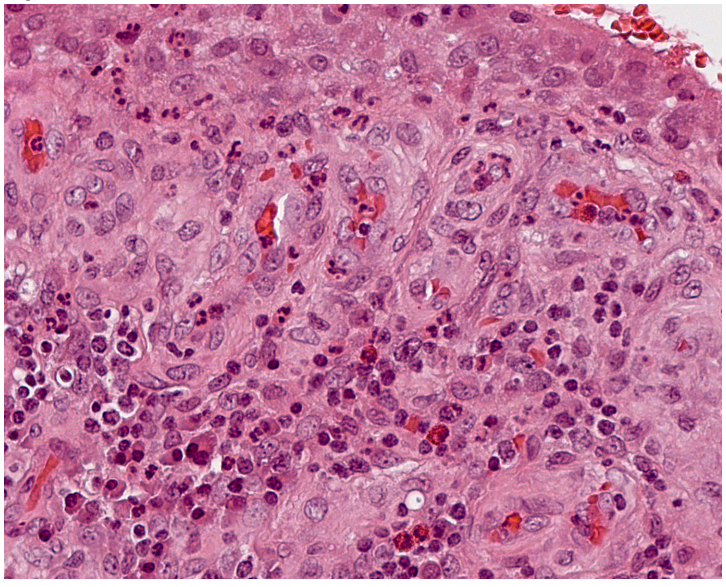

Conclusions: This retrospective study is of cases that had subarticular inflammatory foci with a prominent neutrophilic component. The large majority of these cases also had synovial lymphoplasmacytic inflammation. This type of synovial inflammation is a common finding in IA. Therefore the presence of these foci may be seen within the inflammatory spectrum of IA. In the absence of documented infection, this finding is best interpreted as a mimic of infection - a "pseudo-abscess" - rather than an indication of prior or current infection.

98 Dedifferentiated Gastrointestinal Stromal Tumor: Morphologic Characterization of 16 Cases

Longmei Zhao[1], Wei-Lien Billy Wang[2], Andrew Horvai[3], Jason Hornick[4], Leona Doyle[5], Rhonda Yantiss[6], Abbas Agaimy[7], Brian Rubin[8]

[1]Cleveland Clinic Foundation, Cleveland, OH, [2]The University of Texas MD Anderson Cancer Center, Houston, TX, [3]University of California, San Francisco, San Francisco, CA, [4]Brigham and Women's Hospital, Harvard Medical School, Boston, MA,[5]Brigham and Women's Hospital, Boston, MA, [6]Weill Cornell Medical College, New York, NY, [7]Erlangen, Germany, [8]Cleveland Clinic, Cleveland, OH

Disclosures: Longmei Zhao: None; Wei-Lien Billy Wang: None; Andrew Horvai: None; Jason Hornick: None; Leona Doyle: None; Rhonda Yantiss: None; Abbas Agaimy: None; Brian Rubin: None

Background: Gastrointestinal stromal tumors (GISTs) are the most common mesenchymal tumors of the gastrointestinal tract. However, significant diagnostic challenges remain with regard to dedifferentiated GIST, showing a GIST showing transition from morphologically and immunohistochemically typical GIST to an anaplastic sarcomatous neoplasm that lacks KIT and/or DOG1 expression. Here we describe the largest series to date of dedifferentiated GIST.

Design: The pathology files of 6 different institutions were searched for cases of dedifferentiated GIST. Routine hematoxylin and eosin slides, and available immunohistochemical stains were re-reviewed to confirm the diagnosis. Clinicopathologic features were retrospectively reviewed. Treatment and clinical history were obtained from patient files and contributing physicians.

Results: Sixteen cases were identified. There were 8 men and 8 women, with age ranging from 27 to 81 years (mean, 62.9 y). Primary tumors were located in the stomach in 10 cases, followed by small bowel in 5 cases and unknown primary location in 1 case. Primary tumor size ranged from 6.5 to 26.0 cm (mean 15.3 cm). Four patients had metastasis at diagnosis. In 5 patients, dedifferentiation occurred in the setting of imatinib treatment, whereas the remaining 11 arose de novo (Table 1). The dedifferentiated component had an anaplastic/pleomorphic appearance with high mitotic activity (mean 30 per 5 mm2) and necrosis (13/16), including 4 cases with heterologous rhabdomyosarcomatous differentiation expressing myogenin (1/4) and/or MYOD1 (4/4), and showed complete loss or dramatically decreased KIT and/or DOG1 (16/16) expression (Figs. 1 & 2 and Table 1).

Case	Age/Sex	Location	Size (cm)	State at Presentation	Metastases	Recurrent	Preoperative Imatinib Therapy	Histologic Type	Necrosis	MF/5 mm^2	Atypical Mitosis	Malignant Giant Cells
1	74/F	Stomach	8.0	Liver mets	Liver	Yes	Yes	Anaplastic/rhabdoid	Extensive	5	Yes	Yes
2	64/M	Small bowel	11.0	Primary	Peritoneal	Yes	No	Epithelioid	Extensive	55	Yes	Yes
3	73/F	Stomach	12.5	Primary	No	Yes	No	Anaplastic	Extensive	7	Yes	Yes
4	51/M	Small bowel	15.0	Primary	Peritoneal	Yes	No	Spindle	No	46	Yes	Yes
5	81/F	Unknown	25.0	Peritoneal mets	Peritoneal	Yes	No	Spindle	Extensive	55	Yes	Yes
6	78/M	Small bowel	6.5	LN mets	LN	NA	No	Anaplastic	Extensive	28	Yes	Yes
7	43/F	Stomach	10.5	Primary	Liver	No	No	Anaplastic	Focal	28	Yes	Yes
8	46/M	Small bowel	10.0	Lung mets	Lung, liver, pancreas	Yes	No	Anaplastic	Extensive	20	Yes	Yes
9	63/F	Stomach	17.5	Peritoneal mets	Peritoneal	NA	No	Epithelioid	Yes	5	No	No
10	75/M	Stomach	16.0	Primary	Peritoneal	Yes	No	Anaplastic	No	94	Yes	No
11	57/F	Small bowel	22.0	Primary	Unknown	Yes	No	Anaplastic	Focal	25	Yes	Yes
12	78/M	Stomach	11.0	Primary	Peritoneal	Yes	Yes	Anaplastic	Present	5	No	Yes
13	67/M	Stomach	12.5	Peritoneal and omentum mets	Peritoneal, omentum	NA	Yes	Anaplastic/rhabdoid	Present	20	Yes	Yes
14	27/F	Stomach	26.0	Primary	No	Yes	Yes	Anaplastic	Focal	5	Yes	Yes
15	67/ F	Stomach	19.0	Primary	No	No	Yes	Anaplastic/rhabdoid	Present	55	Yes	Yes
16	NA/M	Stomach	23.0	Primary	No	NA	NA	Anaplastic/rhabdoid	No	25	Yes	No

Table 1. Clinical and histopathologic features of dedifferentiated GIST. F indicates female; M, male; LN, lymph nodes; NA, not applicable. Necrosis: Focal <10%, present 10-50%, extensive >50%.

Figure 1 - 98

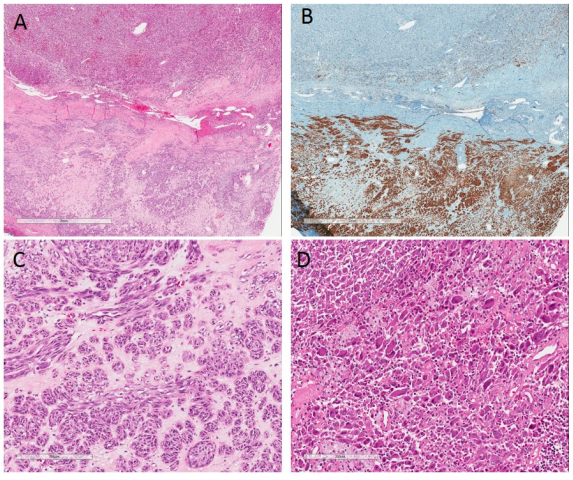

Figure 1. Dedifferentiated GIST showing a conventional spindle cell component (A and C), which is strongly positive for KIT (B, lower panel), in abrupt transition to a pleomorphic, anaplastic area (A and D), which is negative for KIT (B; upper panel).

Figure 2 - 98

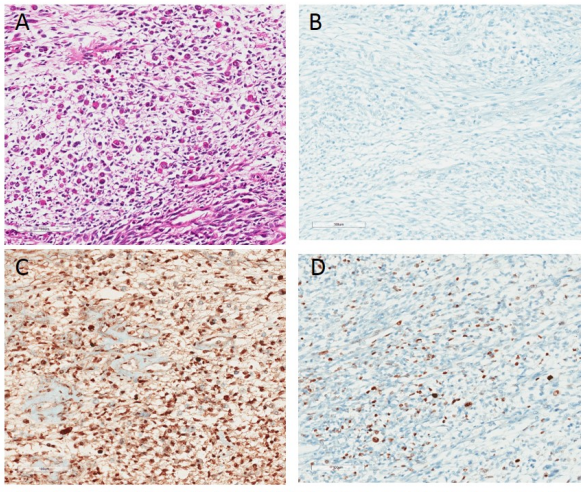

Figure 2. Dedifferentiated GIST showing rhabdomyosarcomatous differentiation (A), which is negative for CD117 (B), and strongly positive for MYOD-1 (C) and myogenin (D).

Conclusions: Dedifferentiated GIST may occur either de novo or after imatinib treatment. A key to arriving at the accurate diagnosis of dedifferentiated GIST is the recognition of a well-differentiated conventional component with transition to an anaplastic component accompanied by complete loss of, or a dramatic decrease in KIT and/or DOG1 expression. Molecular profiling may be a helpful adjunct in limited biopsy material if GIST is suspected clinically.

99 Comprehensive genomic profiling of the primary craniofacial osteosarcomas

Guo Zhu[1], Chuanyong Lu[2], Khedoudja Nafa[3], Michael Klein[4], Sinchun Hwang[3], Lu Wang[5], Meera Hameed[3]
[1]Cooper University Hospital, Camden, NJ, [2]Montefiore Medical Center, Bronx, NY, [3]Memorial Sloan Kettering Cancer Center, New York, NY, [4]The Hospital for Special Surgery, New York, NY, [5]St Jude Children's Research Hospital, Memphis, TN

Disclosures: Guo Zhu: None; Chuanyong Lu: None; Khedoudja Nafa: None; Michael Klein: None; Sinchun Hwang: None; Lu Wang: None; Meera Hameed: None

Background: Craniofacial osteosarcomas (CFOS) are uncommon comprising about 6-7% of all osteosarcomas. They usually present in adulthood and have favorable prognosis compared to conventional osteosarcomas. It is unclear whether CFOS are genetically similar to conventional osteosarcoma.

Design: Forty cases with confirmed diagnosis of CFOS were included for clinicopathologic and survival analysis. Thirty-four cases of non-radiation associated CFOS with follow-up data were selected for survival analysis. Sixteen cases of high-grade CFOS were subject to MSK-IMPACT targeted Next-Generation Sequencing and SNP array analyses. These clinical findings were previously presented, however, not published.

Results: Thirty-four cases (15F, 19M) included in survival analysis with ages ranging from 9 to 78 years. Sixteen tumors were in maxilla, 12 in mandible, 6 at skull base, nasoethmoid complex or other locations. Twenty-eight tumors were high-grade and 6 were low-grade. The predominant histological subtypes of high-grade are osteoblastic in 8, chondroblastic in 6, fibroblastic in 5, and not specified in 9 cases.

NGS analysis revealed marked chromosomal instability with a high number of chromosomal amplifications and deletions. The number of non-synonymous mutations (SNP or small in/del) ranged from 1 to 10 per case. The most frequently mutated gene is *TP53* (68%) with both missense and truncating mutations and often accompanied by loss of heterozygosity. *CDKN2A/2B* homozygous deletion is the second most common occurring in 31% of cases. Other genetic alterations include *PTEN* inactivation (4), *RB1* inactivation (3), *TERT* amplification and promoter hotspot mutation (3) and *APC* missense mutation (2). The frequent copy number alterations include 4p16.2 (including *FGFR3* and *NSD2*) deletion (4), 19p13.12 (including *NOTCH3* and *BRD4*) amplification (3), 19q12 (including *CCNE1*) amplification (2), 19q13 (including *AKT2* amplification (3), 8q21.24 (including *MYC*) amplification (3). No clear association was found between genetic alterations and histologic variants for most cases. *GNAS* R201 mutation, which co-mutated with *TP53* and *APC* was found in two cases where osteosarcoma arose in a background of fibrous dysplasia.

Conclusions: CFOS are heterogeneous and share some of the frequently mutated genes with conventional osteosarcoma such as *TP53, CDKN2A/2B, RB1* and *PTEN*. A subset of CFOS arise from preexisting fibrous dysplasia and carry *GNAS R201* mutation with additional abnormalities.